Canadian Technical Report of
Fisheries and Aquatic Sciences

Technical reports contain scientific and technical information that contributes to existing knowledge but which is not normally appropriate for primary literature. Technical reports are directed primarily toward a worldwide audience and have an international distribution. No restriction is placed on subject matter and the series reflects the broad interests and policies of the Department of Fisheries and Oceans, namely, fisheries and aquatic sciences.

Technical reports may be cited as full publications. The correct citation appears above the abstract of each report. Each report is abstracted in *Aquatic Sciences and Fisheries Abstracts* and indexed in the Department's annual index to scientific and technical publications.

Numbers 1-456 in this series were issued as Technical Reports of the Fisheries Research Board of Canada. Numbers 457-714 were issued as Department of the Environment, Fisheries and Marine Service, Research and Development Directorate Technical Reports. Numbers 715-924 were issued as Department of Fisheries and the Environment, Fisheries and Marine Service Technical Reports. The current series name was changed with report number 925.

Technical reports are produced regionally but are numbered nationally. Requests for individual reports will be filled by the issuing establishment listed on the front cover and title page. Out-of-stock reports will be supplied for a fee by commercial agents.

Rapport technique canadien des
sciences halieutiques et aquatiques

Les rapports techniques contiennent des renseignements scientifiques et techniques qui constituent une contribution aux connaissances actuelles, mais qui ne sont pas normalement appropriés pour la publication dans un journal scientifique. Les rapports techniques sont destinés essentiellement à un public international et ils sont distribués à cet échelon. Il n'y a aucune restriction quant au sujet; de fait, la série reflète la vaste gamme des intérêts et des politiques du ministère des Pêches et des Océans, c'est-à-dire les sciences halieutiques et aquatiques.

Les rapports techniques peuvent être cités comme des publications complètes. Le titre exact parait au-dessus du résumé de chaque rapport. Les rapports techniques sont résumé dans la revue *Résumés des sciences aquatiques et halieutiques*, et ils sont classés dans l'index annual des publications scientifiques et techniques du Ministère.

Les numéros 1 à 456 de cette série ont été publiés à titre de rapports techniques de l'Office des recherches sur les pêcheries du Canada. Les numéros 457 à 714 sont parus à titre de rapports techniques de la Direction générale de la recherche et du développement, Service des pêches et de la mer, ministère de l'Environnement. Les numéros 715 à 924 ont été publiés à titre de rapports techniques du Service des pêches et de la mer, ministère des Pêches et de l'Environnement. Le nom actuel de la série a été établi lors de la parution du numéro 925.

Les rapports techniques sont produits à l'échelon régional, mais numérotés à l'échelon national. Les demandes de rapports seront satisfaites par l'établissement auteur dont le nom figure sur la couverture et la page du titre. Les rapports épuisés seront fournis contre rétribution par des agents commerciaux.

101-03472/

Canadian Technical Report of
Fisheries and Aquatic Sciences 2347

March 2001

Physical Oceanography of Tracadie Bay, PEI: Analysis of Sea Level, Current, Wind and Drifter Data

by

M. Dowd, F. H. Page, R. Losier, P. McCurdy, and G. Bugden[1]

Fisheries and Oceans Canada
Ocean Sciences Division,
Biological Station
531 Brandy Cove Road, St. Andrews, NB, E5B 2L9, Canada

[1]Fisheries and Oceans, Ocean Sciences Division, Bedford Institute of Oceanography, Dartmouth, NS

This is the two hundred and forty-first Technical Report of
The Biological Station, St. Andrews, NB

© Her Majesty the Queen in Right of Canada, 2001

Cat. No. Fs 97-6/2347E ISSN 0706-6457

Correct citation for this publication:

Dowd, M., F. H. Page, R. Losier, P. McCurdy, and G. Bugden. 2001. Physical oceanography of Tracadie Bay, PEI: analysis of sea level, current, wind and drifter data. Can. Tech. Rep. Fish. Aquat. Sci. 2347: iii + 77 p.

ABSTRACT

Dowd, M., F. Page, R. Losier, P. McCurdy, and G. Bugden. 2001. Physical oceanography of Tracadie Bay, PEI: analysis of sea level, current, wind and drifter data. Can. Tech. Rep. Fish. Aquat. Sci. 2347: iii + 77 p.

This report examines physical oceanographic data collected in Tracadie Bay, Prince Edward Island (PEI), Canada during 1997-99. This effort was part of the DFO Strategic Science Initiative entitled "Coastal Oceanography for Sustainable Aquaculture Development." The purpose of this report is to present that portion of the Tracadie Bay data set that relates to the barotropic circulation of the bay. These data include: sea level anomalies, currents (from both moored current meters as well as transect data from a boat-mounted ADCP), drifter deployments and wind observations from a meteorological station. The study outlines some basic analyses of these data in order to provide for a physical characterization of the bay from the perspective of its barotropic circulation. Both time and frequency domain descriptions of the sea level, wind and current data are presented. Spatial patterns in the currents in the bay are also considered using an under-ice current meter array, transect data from an ADCP and drifter trajectories.

RÉSUMÉ

Dowd, M., F. Page, R. Losier, P. McCurdy, and G. Bugden. 2001. Physical oceanography of Tracadie Bay, PEI: analysis of sea level, current, wind and drifter data. Can. Tech. Rep. Fish. Aquat. Sci. 2347: iii + 77 p.

Ce rapport fait l'examen des données océanographiques physiques recueillies dans la baie de Tracadie, à l'Île-du-Prince-Édouard, au Canada, de 1997 à 1999. Il s'agit de travaux s'inscrivant dans le cadre de l'initiative stratégique du MPO en matière de sciences intitulée « Océanographie côtière pour le développement durable de l'aquaculture » (COSAD). Le rapport a pour objet de présenter la portion de l'ensemble de données pour la baie de Tracadie qui concerne la circulation barotrope de la baie. On y retrouve donc des données sur les anomalies du niveau de la mer, les courants (recueillies à partir de courantomètres à l'ancre et obtenues le long d'un transect grâce à un profileur monté sur un bateau) et des observations notées au moyen de bouées dérivantes ainsi que des observations sur les vents faites dans une station météo. L'étude décrit certaines analyses de base faites de ces données afin de caractériser la baie sur le plan physique, du point de vue de sa circulation barotrope. On y donne des représentations en temps et en fréquences du niveau de la mer, des vents et des courants. Sont également pris en compte des modèles spatiaux des courants dans la baie grâce à des courantomètres distribués sous la glace, des données obtenues le long d'un transect grâce à un profileur et par les trajectoires de bouées dérivantes.

INTRODUCTION

A DFO strategic Science initiative entitled "Coastal Oceanography for Sustainable Aquaculture Development," or COSAD, was started in 1996 to help address issues of carrying capacity of finfish and shellfish aquaculture. It adopted the perspective that progress towards these objectives could be made by describing, understanding and modelling of the physical oceanography of some typical inshore environments used for aquaculture. Its objectives were: *i*) to develop an understanding of the physical oceanography of typical coastal environments in Atlantic Canada by gathering empirical data on the hydrography, current patterns and meteorology within these environments, and to develop high resolution three-dimensional finite element circulation models for these environments; *ii*) to use the empirical observations and circulation models to estimate the transport pathways, flux and exchange rates of water and suspended materials between and within shellfish and aquaculture sites; and *iii*) use these estimates in conjunction with information on shellfish and finfish needs to help understand the carrying capacities of the study areas. In this study, our focus is a subset of the oceanographic information collected in Tracadie Bay, PEI for the purpose of a measurement-based characterization of the sea level and current regime of the bay.

Tracadie Bay is a shallow, nearly enclosed tidal lagoon located on the north shore of PEI, Canada (Fig. 1). Its general oceanographic characteristics are shared by a number of bays on the north shore of PEI and the Gulf coast of New Brunswick. Tracadie Bay is notable for its extensive shellfish aquaculture development focusing on the blue mussel (*Mytilus* spp.). The overall Tracadie Bay system is made up of Tracadie Bay proper as well as the adjoining Winter Bay (Fig. 2). Tracadie Bay is connected to the Gulf of St. Lawrence by a narrow opening through a barrier beach sand dune development. The immediately adjacent shoreline region of the Gulf of St. Lawrence is a dynamic environment characterized by an extensive surf zone with associated beach hydrodynamics (e.g. longshore currents) and sediment transport. The main channel into the bay branches into two channels separated by intertidal flats. Tracadie Bay is connected to Winter Bay through a relatively narrow constriction. Some branching channels are found at the head of Winter Bay, but there is no significant freshwater input (in terms of generating dynamically important density, or pressure, gradients). The Tracadie Bay system is ice covered in the winter months.

Digitized bathymetry of Tracadie Bay was obtained from the Canadian Hydrographic Service. A contour plot of these data is given in Fig. 2. The geometry of the bay may be characterized as follows. Tracadie Bay has a mean (low water) depth of 3 m and a maximum depth of 6 m. The surface area of the bay at low tide is 14 km^2. The intertidal zone comprises some 4 km^2, and is concentrated adjacent to the entire shoreline, in addition to some tidal flats near the mouth of the bay (Fig. 2). The low tide volume of the bay is estimated at $37(10^6)$ m^3 and the tidal prism ranges from $4\text{-}12(10^6)$ m^3 and is due to semi-diurnal and diurnal tides.

The purpose of this study is twofold: (*i*) to present sea level, current, wind and drifter data collected during the Tracadie Bay phase of the COSAD project from 1997-99; and (*ii*) to carry out a preliminary statistical analysis of the above data in order to obtain a physical characterization of Tracadie Bay from the perspective of its barotropic circulation. The report is structured as follows. Section 2 provides an analysis of a set of sea level anomaly time series. Section 3 examines the current meter records with an emphasis on a description of the spectral properties of these data. Wind data, and an analysis of the wind-driven circulation, are presented in Section 4. In Section 5, spatial patterns in the circulation field are examined using a current meter array, ADCP transects and drifter data. A brief summary follows in Section 6. Appendices A through E contain plots of the current, wind and drifter data.

SEA LEVEL

Sea level is an important dynamic variable related to both the circulation and flushing of coastal embayments. Sea surface height anomalies can be derived from recorded time series of pressure from instruments moored on the sea floor. If we neglect atmospheric pressure variations and assume a constant density for seawater, vertical integration of the hydrostatic equation indicates that pressure increases by 1 decibar for every 1 m of water depth. For Tracadie Bay, this proves to be a good approximation. In this section, we examine bottom pressure anomalies from an array of pressure gauges in order to characterize the tidal regime of Tracadie Bay, as well as to infer the phase and amplitude changes associated with the propagation of the tidal wave in the bay.

Bottom pressure data was collected from three sites in Tracadie Bay in June-August 1999 using Vemco Minilog TDR recorders (see Fig. 3 for locations). These instruments had a resolution of 10

cm in depth with an advertised error of 3% in absolute depth (it is thought that the majority of this error is due to temperature effects on the internal pressure sensor). The sampling interval was set to record pressure at 5-min intervals in order to ensure that any small phase differences between the sites were recorded. The deployment locations corresponded to: (*i*) an outside site at a bell buoy offshore of the mouth of Bay (designated Buoy), (*ii*) a site in the middle of Tracadie Bay (designated TB), and (*iii*) a site at the head of Winter Bay (designated WB). The depths of these bottom-moored instruments were approximately 15 m, 4 m and 2 m, respectively. This observing array was designed to record sea level in each of the three broad regions of the study area.

Note that while we have measured bottom pressure, we are reporting the results as sea level anomalies. This is not strictly correct since no correction has been made for the inverse barometer effect in converting pressure to sea level. Atmospheric pressure variations cause sea level to change by about 1 cm for a 1 millibar change in atmospheric pressure (Gill 1982, section 9.9). These effects are relatively small and associated mainly with low frequency synoptic weather patterns.

A time series of the sea level derived from the detrended pressure anomalies are shown in Fig. 4. These were detrended by removing a 3rd order polynomial from the records. The sea level shows oscillations associated with the diurnal and semi-diurnal components of the tide, as well as modulations in the envelope of tidal height due to the interaction ('beating') of the tidal constituents. The series is noisy and has a blocky appearance due to the finite (10-cm) sensor resolution and the relatively low tidal amplitude signal. Overall, sea level amplitude variation is generally less than 1 m. The WB and TB sea level fluctuations have a slightly lower overall amplitude than that recorded outside the bay at the Buoy.

CORRELATION ANALYSIS

Temporal variations in the recorded sea level time series were examined by calculating sample auto- and cross-correlation functions. Sample auto-correlations for the three locations are shown in Fig. 5. All three records show a strong periodicity associated with multiples of a 1-d time lag, as expected in a series dominated by the diurnal tide. The Buoy, and to a lesser extent the TB, series also show the influence of the semi-diurnal tide at lags having odd multiples of a 1/2-d period (even multiples are absorbed into the diurnal peaks). If we focus on lags of 2 h or less, an interesting phenomenon is evident in all three records: the auto-correlation at zero lag shows an abrupt increase over its adjacent values (lag0>0). This type of behavior is found in auto-regressive models that are observed with additional random noise and can provide a measure of the signal-to-noise ratio in the recorded pressure series.

The sample cross-correlation function was also determined for all pair-wise combinations of the three pressure records: TB/WB, TB/Buoy, and WB/Buoy. These are shown in Fig. 6. A diurnal periodicity, similar to that of the auto-correlation function, is seen in all three records. The main feature of interest in the cross-correlation functions is the presence of a maximum at non-zero lags. This is interpreted as an offset (a phase or time lag) between the two series being correlated. Such an offset is strongly evident in the cross-correlations of WB/Buoy and TB/Buoy, indicating that the Buoy sea level leads both TB and WB sea level by ~1.67 h. In contrast, the rise and fall of WB and TB sea level is nearly synchronous.

SPECTRAL ANALYSIS

The frequency domain properties of the sea level time series were examined through calculation of auto- and cross-spectra (e.g. Priestley 1981). This spectral analysis was based on calculating the raw (auto- and cross-) periodograms, and a Parzen window was used to improve consistency of the spectral estimator (Priestley 1981, section 6.2). Standard quantities derived from the cross-spectra were calculated, including the coherency, phase and gain spectra. Cross-spectral analysis was undertaken for each of the pairwise combinations: TB/WB, TB/Buoy, and WB/Buoy.

The auto-spectra of the three time series are shown in Fig. 7. Note that these are in variance preserving form (i.e., the area under any portion of the curve directly reflects the variance, or energy, in that region). The auto-spectra all show both daily and twice-daily peaks in power with periods of 24.45 h and 12.39 h, respectively. The spectra indicate that energy in the diurnal band dominates over energy in the semi-diurnal band. The semi-diurnal energy is attenuated as one moves from the outside regions landward into Winter Bay. The diurnal energy shows a similar, but weaker, pattern of attenuation. These frequency-dependent effects are likely due to bottom friction.

Cross-spectral analysis of the WB and TB time series (Fig. 8) show near perfect coherency in the diurnal and semi-diurnal bands (>0.99). The phase spectra confirm that the two records are in-phase (<0.05 radians) in these spectral bands, i.e. sea level rises and falls almost simultaneously. The gain spectrum shows that the tidal energy in WB is less than that found in TB, indicating an overall decrease in the sea level (gain levels of 0.89 and 0.79 for diurnal and semidiurnal bands, respectively).

Cross-spectral analyses of the Buoy record with both TB and WB time series show distinct differences in the diurnal and semi-diurnal bands. Comparison of the Buoy and TB records (Fig. 9) indicates that the diurnal tide has a phase lag of about 31° (2.1 h), with the Buoy leading TB. The diurnal tidal energy is not attenuated between these sites, as evidenced from the near identical auto-spectra, as well as the gain value of 0.99. In contrast, the tidal energy in the semi-diurnal band in TB is attenuated relative to the Buoy (gain of 0.83), and it has a phase lag approaching 41° (1.4 h). For the Buoy versus WB analysis (Fig. 9), we see a similar pattern. The phase lags for the diurnal and semi-diurnal bands are 29° and 42°, respectively. The gain spectra indicate that the diurnal tidal energy in WB is about 88% of that of the Buoy, whilst the semidiurnal component has only 66% of its energy.

HARMONIC ANALYSIS

Harmonic analysis was used to isolate portions of the record associated with the variability at particular, identifiable tidal frequencies, i.e. line spectra (Godin 1972). The preceding analysis indicates a mixed diurnal and semi-diurnal tide in Tracadie Bay. Harmonic analysis was carried out using the techniques of Godin (1972) as implemented by Foreman (1977). Results from these analyses are shown in Table 1, including the major tidal constituents and their amplitude and Greenwich phase. The analysis indicates that the dominant tidal constituents are K_1 (diurnal, declination luni-solar), O_1 (diurnal, principal lunar) and M_2 (semi-diurnal, principal lunar). It is noted that the constituents S_2, N_1, and Q_1 also play a minor role in all three records. This analysis confirms the decrease in tidal amplitude and the change in phase as one moves from the Gulf of St. Lawrence into Tracadie Bay.

A harmonic regression of the sea level anomaly time series was also implemented using the dominant tidal frequencies K_1, O_1, and M_2 as explanatory variables. The rationale for this was to retain the original sampling variability and allow for full control over further tidal analysis and any subsequent de-tiding procedure. Table 1 shows the coefficient of determination R^2 and indicates that the harmonic regression explains between 76-78% of the total variance. The residual variance remains mainly in high frequency fluctuations, but also includes some sea level variations associated with other minor tidal constituents that were neglected in the analysis.

CURRENTS

During the period 1997-99, a total of 28 current meter deployments were made in Tracadie Bay. The InterOcean Systems S4 electromagnetic current meters recorded 5-min vector averages of the horizontal current at a sampling interval of either 15 or 30 min. The current meter deployments may be grouped into two broad categories: (*i*) currents from channel areas and (*ii*) currents from interior regions of the bay. Table 2 lists the deployment numbers, their general location and duration. Appendix A provides a complete description of the data recorded in each of the 28 deployments, including deployment dates, location maps, time series plots of the current velocity and progressive vector diagrams.

Current data from channel regions account for 19 of the deployments. This includes the channels connecting Tracadie Bay to the Gulf of St. Lawrence (this has both an east and a west branch, designated "Dunes channel" and "Wharf channel," respectively) and the constriction connecting Tracadie Bay and Winter Bay ("Winter Bay channel"). Currents in these regions tend to be rectilinear and aligned along the channel axis. The flows are generally strong (up to 70 cm s^{-1}) and are dominated by mixed tidal oscillations associated with diurnal and semi-diurnal tidal forcing. Overall, the volume transport is greatest through the Dunes channel, followed by the Winter Bay and Wharf channels. The residual currents in the channels, suggested by the progressive vector diagrams, reflect flood-ebb asymmetries as recorded by a spatially fixed, point measurement of current. These likely have their origin in the tidally varying cross-sectional areas of the channels and the volumetric changes in the enclosed basins (e.g. Friedrichs et al. 1992). This effect is quite pronounced in deployment 62, for example.

In the interior regions, nine current meter deployments were carried out at various sites throughout Tracadie Bay. These records are generally shorter in duration than the channel deployments. These interior deployments may be further split into: (*i*) a set of five under-ice deployments carried out in the winter of 1999 and (*ii*) the remaining four

summer deployments. Overall, the interior flows are generally much weaker than the channels (<15 cm s^{-1}). There is some evidence of tidal periodicity, but the signal is much less regular than found in the channels.

ROTARY SPECTRAL ANALYSIS

Rotary spectra were calculated for the current vector time series. Rotary spectral analysis provides a generalized spectral representation for vector valued time series such as horizontal currents (Gonella 1972; Mooers 1973). Negative frequencies correspond to clockwise rotation of the current vector, while positive frequencies refer to anti-clockwise rotation. For the purposes of this analysis, the current records were grouped according to the following deployment types: (*i*) Wharf channel, (*ii*) Outside channel, (*iii*) Dunes channel, (*iv*) Winter Bay channel, (*v*) Interior under the ice, and (*vi*) Interior in summer.

The rotary spectra for the channel data (Fig. 11 through 14) show no strong preference for either clockwise or anti-clockwise rotating energy. This is not surprising, as the currents are near rectilinear in these areas. Spectral peaks are found corresponding to energy in the diurnal and semi-diurnal bands (with smaller peaks at ~8.3-h period, presumably due to shallow water effects). Although the energy spectra are similar in all three channel regions, the Dunes channel contains significantly more energy than the other areas. Semi-diurnal energy dominates over diurnal energy. This occurs because, while the sea level amplitude associated with the diurnal bands is greater than that of the semi-diurnal band, the shorter period of the semi-diurnal sea level rise leads to relatively stronger currents.

Figures 15 and 16 show the rotary spectra from the interior of Tracadie Bay. These records are generally shorter in duration than the channel records (see Table 2) and contain much less kinetic energy. The winter deployments show an energy distribution centered on the semi-diurnal tidal band (Fig. 15). Deployments 74 and 77 are dominated by clockwise rotating energy, while the other records show little preference in their sense of rotation. The spatial distribution of tidal energy indicates that deployments 75 and 78 (in the upper northeast corner and southern bay, respectively) have relatively little total energy. The rotary spectra of the summer current meter deployments in the interior are shown in Fig. 16. In contrast to the under-ice deployments, the spectra indicate that a significant portion of the energy is found at subtidal frequencies. This low frequency energy shows a tendency to have a preferential sense of rotation for each of the individual records, although this seems to vary between the clockwise and anti-clockwise directions.

HARMONIC ANALYSIS

Harmonic analysis was carried out for the current meter data. This follows essentially the same procedure as for the sea level data and is designed to quantify the variability associated with the particular tidal frequencies that are separable based on the length of the recorded current time series. The main difference from the sea level analysis lies in the fact that the current record is a vector time series and harmonic analysis proceeds by representing the tidal currents associated with a given frequency as a tidal ellipse (Godin 1972). As with the rotary spectra, this is based on a decomposition of the current vector into clockwise and anti-clockwise rotating components. A complete characterization of the tidal ellipse is given by the length of the major axis (A), the length of the minor axis (B), the ellipse orientation (θ) and the Greenwich phase (ϕ) (see Godin 1972; Foreman 1978). These quantities are shown in Table 2 for each of the 28 current meter deployments in Tracadie Bay.

The main features of the harmonic analysis are the following. In the channel data, the currents are near rectilinear and, consequently, the minor axes of the associated current ellipses are close to zero. The ellipse orientation corresponds to the channel axis (but note the 180° ambiguity). The estimated Greenwich phase values for each of the deployment regions show a fair degree of consistency in these areas. (Physically, we expect the phase to be fairly constant for a given deployment region.) For the Dunes channel and the Winter Bay channel, the mean phase values cluster tightly around 76°, 35° and 60° for K_1, O_1, and M_2, respectively. Mean phases in the Wharf channel are 10° and 7° higher for the diurnal constituents and 12° lower for M_2. The interior tidal currents are generally weak. For the interior under-ice data, the deployments are short (~4 d) and K_1 and O_1 are not separable. For these cases, the M_2 Greenwich phase is 73°±29° which, while having a significant spread, is consistent with the channel data. The interior summer data show very weak tidal currents that are characterized by highly variable Greenwich phase values.

A separate harmonic regression was also carried out (similar to the sea level analysis). This included only the dominant constituents K_1, O_1, and M_2 and was based on the original data recorded by the current meter. The coefficient of determination R^2 is

shown in Table 2. For the channel data, the percentage of variance explained by the regression averages 72%. Similarly, for the interior under-ice data there is a mean R^2 of 69%. The residual variance for these cases is largely concentrated in high frequency bands. For the interior summer data the regression shows little explanatory ability, with R^2 values of less than 16%. This is consistent with the rotary spectral analysis, which indicated that the majority of the variance was found at sub-tidal frequencies.

PHASE RELATIONSHIP BETWEEN THE CHANNEL CURRENTS

The harmonic analysis does not allow for a ready inter-comparison of the phase relationships amongst the different regions due to the variability found in the estimated Greenwich phase values. Here we have selected current meter records from the three channel areas that overlap in time. These were analysed to determine if systematic differences in the timing (or phasing) of the currents was present amongst the different locations. There were three deployment periods where the currents records from all three channel areas overlapped for more than 1 mo. These were used as the basis for cross-correlation and cross-spectral analysis. The currents in these regions are near rectilinear and the analysis was simplified by considering only the component of the flow along its principal axis (i.e. using a scalar rather than vector time series).

Summary results from a cross-correlation analysis are shown in the Table 3. The location of the maximum in the sample cross-correlation function indicates whether one time series leads or lags the other. The results in Table 3 shows that the current record from the Wharf channel leads both the Dunes channel and Winter Bay channel by about 15 min. Comparison of the Dunes and Winter Bay channels shows no clear pattern to the time lag.

Cross-spectral analysis allows the phasing information to be expressed as a function of frequency. Summary results for the semi-diurnal frequency band are shown in Table 4. The pattern of the phase lag parallels that of the cross-correlation analysis, with the Wharf channel leading both the Dunes channel and the Winter Bay channel. Phase relationships for currents in the diurnal band are given in Table 5. These do not show a clear a pattern as a result of the greater degree of scatter in the results. The only consistent pattern for the three overlap periods is that the Winter Bay channel leads the Wharf channel in the diurnal frequency band.

WIND-DRIVEN CURRENTS

WIND DATA

During the summers of 1998 and 1999, a meteorological station was deployed in Tracadie Bay. It recorded wind speed and direction, as well as temperature, relative humidity, barometric pressure, and light level. The deployment location on the eastern shoreline is shown in Appendix B. In this section, we focus on the wind data and its link to circulation.

Appendix B shows the wind data collected during 1998 and 1999. Recorded wind speeds range from 0-15 m s^{-1}. Wind rose plots suggest that in 1998 ENE winds appear truncated and in 1999 ESE winds appear low. This bias may be real, or may be an artifact due to shadowing resulting from the shoreline location of the meteorological station.

Rotary spectra of the vector wind series are shown in Fig. 17. For both the 1998 and 1999 records, the wind energy is distributed broadly over the low frequency band. Most of the energy is found at periods greater than 2 d. There is some evidence of an overall clockwise rotational tendency to the wind vector. There is a large peak associated with the synoptic (~6 d) band. We also see small peak at 1-d period associated with diurnal heat and cooling (land-sea breeze). Qualitatively, these rotary spectra resemble those of the current meters from the summer deployments in the interior of the bay (Fig. 16).

WIND DRIVEN CIRCULATION

Relationships between wind and current time series were investigated using cross-correlation and cross-spectral analyses. Except for one case, these analyses showed no clear relationship between the wind and the current. This result was anticipated for the under-ice current records (which are isolated from the effects of surface wind stress) and for the channel data (which are entirely dominated by tidal transport). However, of the three current meter records from the interior of Tracadie Bay with concurrent observed winds (deployments 85, 89 and 90 - note that deployment 91 had no corresponding wind field), only deployment 90 showed any relation to the local wind field. This deployment was located in the southern end of Tracadie Bay (see Appendix A).

Plots of the current records from deployment 90 and corresponding wind field are shown in Fig. 18.

The wind and current data co-vary strongly for both the speed and the v-component of the velocity vectors. This is particularly evident in the low pass filtered (40-h cutoff) wind and current time series. The strong relation between the v-component of the wind and current velocity in this area of weak tidal currents is due to the north-south orientation of the bay and the consequent ability of the wind to generate currents along that axis. The correlations between the vector wind and current series are shown in Fig. 19. The amplitude of the complex valued correlation showed a peak at 0.5 h lag, with the wind leading the current. The corresponding angle between of the current vectors is 39° to the right of the wind. Finally, it is noted that the calculation of rotary cross-spectra did provide additional useful information, due mainly to the short records and the fact that the wind energy is broadly distributed over frequency.

SPATIAL PATTERNS IN CIRCULATION

In this section, spatial patterns in the circulation of Tracadie Bay are examined using the observational data. The data sets considered include: (*i*) a current meter array, (*ii*) transect data from boat-mounted acoustic Doppler current profiler (ADCP), and (*iii*) drifter trajectories. The current meter array provides simultaneous, point measurements of current vector time series distributed amongst different locations in Tracadie Bay. The ADCP provides a time-space series of currents, but can be difficult to interpret since the (tidal) circulation is evolving at the same time it is being sampled. Drifter trajectories yield a time-space series of position that can be crudely linked to the Eulerian currents by differencing of the record. Taken together, the above information allows for some degree of quantification of the circulation patterns of Tracadie Bay. However, a proper assessment would require the data to be dynamically interpolated to obtain synoptic snapshots of the time evolution of the current field (e.g. Dowd and Thompson 1996). Another alternative is a more traditional circulation modelling effort, systematically validated with available *in situ* current data.

SIMULTANEOUS CURRENT METER DEPLOYMENTS

During the period from Feb. 15-19, 1999, five current meters were deployed under the ice in Tracadie Bay (deployments 74-78). These data provide point measurements of the flow in the interior of the bay due purely to tidal forcing (the ice cover isolates the water column from the effects of surface wind stress, but also itself provides frictional drag). Appendix C shows the locations of these five current meters and the predicted tidal height for the 4-d duration of the experiment. Appendix C also contains a time sequence of snapshots of the hourly currents recorded by the instrument array. The time for each panel is referenced to the sea level time series.

The currents for deployment 74 are strongly influenced by the channel connecting Tracadie Bay to the outside and, consequently, respond strongly to changes in the tidal height. Deployment 77 also shows a similar strong control by the flood-ebb cycle. Deployments 75 and 78 are characterized by relatively weak flows. Deployment 75 is located in the northeast corner of the bay and exhibits a northerly flow during strong ebb tides. Deployment 78 is in the southern portion of the bay and its currents follow the flood-ebb cycle, with southward flow during flood and northward flow during ebb.

ADCP TRANSECTS

Observations of the current vector were collected for various transects in Tracadie Bay using a boat-mounted RD Instruments 1200 KHz acoustic Doppler current profiler (ADCP). The ADCP recorded the vertical profile of the horizontal components of the current vector. These were depth-averaged to aid in interpretation of spatial patterns in the barotropic currents. A quality control procedure was used which removed: (*i*) gross positional errors (based on the exceedance of an apparent maximum boat speed of 10 knots) and (*ii*) data points adjacent to temporal gaps in the record where spikes seemed to frequently occur. A low pass smoothing procedure was also carried out on the quality-controlled data (convolution of the data with a three-point smoothing kernel modified to account for the irregularly sampled time series). This sequence of quality control and processing procedures appears to give realistic representation of the depth-mean currents.

During the summers of 1998 and 1999, there were a total of 12 separate periods in which ADCP transects were collected in Tracadie Bay. Appendix D contains information on the deployment periods and shows a graphical representation of the spatial distribution of the depth-mean currents during the deployment periods. For each deployment period, the sea level and wind information is also given to aid in interpretation of the data. The general picture of the circulation that emerges is one of strong currents in the channel areas (especially the Dunes channel) and relatively weak flows in the interior (<10 cm s^{-1}). There is a fair degree of spatial structure evident in

the interior. The head of Tracadie Bay exhibits very weak currents. The central region of the main bay has the strongest currents outside of the channel areas.

DRIFTER DEPLOYMENTS

Drifter deployments were carried out in Tracadie Bay in summer 1998. These Seimac CAST drifters were GPS tracked and deployed without drogues (so that they are influenced by surface currents only in the top meter of the water column). Drifter trajectories from each of the four deployment periods are shown in Appendix E. In all cases, there is little separation in the trajectories of the initial cluster of drifters during the 4- to7-h deployments. In the deployments of July 8/98 and Aug. 18/98, the ebbing tide and the wind act together to influence the displacement to the drifters. In the deployments of July 9/98 and Aug. 20/98, the effect of the ebbing tide is counteracted by wind drift. Clearly, tidal current and wind effects (direct windage and generation of wind driven surface currents) influence the pathways of the observed drifter trajectories.

SUMMARY

In this report, we have presented and analysed a variety of data that were collected in Tracadie Bay, PEI as part of the DFO strategic science initiative "Coastal Oceanography for Sustainable Aquaculture Devlopment." The focus of this study was on producing a basic description of the field observations of sea level, currents, wind and drifters collected during the project. The associated data analyses provided for a characterization of the barotropic circulation in Tracadie Bay.

Sea level (pressure) anomaly data was used to characterize the tidal regime of Tracadie Bay. It was found that Tracadie Bay has a mixed diurnal and semi-diurnal tide with the constituents K_1, O_1, and M_2 playing a dominant role. Analysis of sea level data indicates that the tides within Tracadie Bay lag that of the adjacent Gulf of St. Lawrence by 1-2 h, for both the diurnal and semi-diurnal components. Correspondingly, the tidal amplitude within the bay is reduced as compared to the outside. These frequency dependent effects are due to the restriction of water exchange by the narrow channels that connect Tracadie Bay to the outside (the physics underlying this are reviewed in van de Kreeke 1988, for example). Within the bay itself there is some evidence for a similar pattern in the tides with a time lags of ~15 min between Tracadie Bay and Winter Bay. There is also a small decrease in tidal amplitude that is more pronounced for the semi-diurnal tide as compared to the diurnal tide. Again, this likely results from the constriction between Tracadie Bay proper and Winter Bay. However, there is also speculation that frictional effects associated with intensive suspended longline shellfish culture can lead to modification of the tidal regime (Grant and Bacher 2001).

Analyses of the current data show a general pattern of strong tidal flows in the channel areas and weak flows in the interior of the bay. The channel currents exhibit mixed diurnal and semi-diurnal periodicity, reflecting the dominant K_1, O_1, and M_2 tidal constituents. The majority of the tidal transport occurs through the channel adjacent to the barrier beach (the Dunes channel). The phase relationships in the different channel areas were generally consistent with the sea level analysis.

Under-ice deployments of a current meter array showed weak tidal currents in the interior of the bay, especially in the northeast corner and southern ends of the bay. In the interior of the bay during the summer, kinetic energy in the current records was concentrated at sub-tidal frequencies. It was speculated that these might have their origin in the response of the water column to surface wind stress. However, no significant relationship with wind speed was evident, except for single deployment (#90) at the head of Tracadie Bay. In this case, the component of the wind along the axis of the Bay appears to correlate well with observed currents along that same axis.

Spatial patterns in the circulation were also examined using the under-ice current meter array, ADCP transects and drifter trajectories. These indicated a fair degree of spatial structure in the currents of the bay. Tidal circulation appears to be the dominant factor in both the under-ice array of current meters and in the depth mean currents as recorded by the ADCP. Drifter trajectories were seen to be significantly influenced by both wind effects and tide circulation. Overall, the general tidal circulation pattern inferred from these data indicates that the central region of the bay has relatively strong tidal currents while other regions, particularly the southern end of the bay, have relatively weak currents. There is also some evidence of flood-ebb tidal asymmetry in the observed currents, which gives rise to a (tidal) residual circulation.

ACKNOWLEDGMENTS

This work was funded under a Department of Fisheries and Oceans strategic science initiative entitled "Coastal Oceanography for Sustainable Aquaculture Development." The authors also wish to thank their partners in this effort, including the PEI Department of Fisheries, Aquaculture and Environment and the PEI Mussel Growers Association.

REFERENCES

Dowd, M., and K. R. Thompson. 1996. Extraction of tidal streams from a ship-borne acoustic Doppler current profiler using a statistical-dynamical model. J. Geophys. Res. 101: 8943-8956.

Foreman, M. G. G. 1977. Manual for tidal heights analysis and prediction. Pacific Mar. Sci. Rep. 77-10. Institute of Ocean Sciences, Patrica Bay, Sidney, B.C. 58 p. (1996 revision)

Foreman, M. G. G. 1978. Manual for tidal currents analysis and prediction. Pacific Mar. Sci. Rep. 78-6. Institute of Ocean Sciences, Patrica Bay, Sidney, B.C. 57 p. (1996 revision)

Friedrichs C. T., D. R. Lynch, D. G. Aubrey. 1992. Velocity asymmetries in frictionally dominated tidal embayments: longitudinal and lateral variability, p. 277-312. *In* D. Prandle (ed.) Dynamics and Exchanges in Estuaries and the Coastal Zone. American Geophysical Union. Washington.

Gill, A. E. 1982. Atmosphere-Ocean Dynamics. Academic Press. London. 662 p.

Godin, G. 1972. The Analysis of Tides. University of Toronto Press, Toronto. 264 p.

Gonella, J. 1972. A rotary-component method for analysing meteorological and oceanographic vector time series. Deep Sea Res. 19: 833-846.

Grant, J., and C. Bacher. 2001 . A numerical model of flow inhibition by suspended aquaculture in a Chinese bay. Can. J. Fish. Aquat. Sci. (in press).

Mooers, C. N. K. 1973. A technique for the cross-spectrum analysis of pairs of complex valued time series with emphasis on properties of polarized components and rotational invariants. Deep Sea Res. 20: 1129-1141.

Priestley, M. B. 1981. Spectral Analysis and Time Series. Academic Press. London. 890 p.

Van de Kreeke, J. 1988. Hydrodynamics of tidal inlets. *In* D. G. Aubrey and L. Weishar (eds.) Hydrodynamics and Sediment Dynamics of Tidal Inlets. Springer-Verlag, New York.

Table 1: Summary of a harmonic tidal analyses for the 3 sea level anomaly records. These are based on the dominant tidal constituents K_1, O_1, and M_2. Shown are the amplitude (|A| in meters) and the phase (ϕ in degrees). The last column shown the percentage variation explained by these tidal constituents (R^2) as determined from the harmonic regression.

Location	K_1		O_1		M_2		R^2
	|A|	ϕ	|A|	ϕ	|A|	ϕ	
Buoy	0.207	317	0.1725	280	0.157	280	0.78
Tracadie Bay	0.199	345	0.178	313	0.127	3[illegible]	0.76
Winter Bay	0.175	343	0.146	310	0.103	32[illegible]	0.78

Table 2: Summary of tidal analyses for the current meter deployments. Here, # refers to the deployment number, Δt refers to the duration of the deployment in days. Tidal constituents considered are K_1, O_1, and M_2. Tidal ellipse information is given as follows: length of the major axis A, length of the minor axis B, ellipse orientation θ and Greenwich phase ϕ. The percentage of variation explained by a harmonic regression including K_1, O_1, and M_2 is given by R^2.

#	Δt	K_1				O_1				M_2				R^2
		A	B	θ	ϕ	A	B	θ	ϕ	A	B	θ	ϕ	
Outside														
35	3	18	2	153	127	-	-	-	-	29	0	154	62	0.92
Wharf Channel														
55	42	13	0	180	67	9.4	0	179	36	15	0	180	55	0.67
59	42	10	0	179	92	8	0	180	43	13	0	179	48	0.74
62	43	6	0	6	98	8	0	6	47	14	0	7	43	0.62
Dunes Channel														
56	42	25	0	124	68	17	0	125	36	28	0	124	68	0.82
60	42	21	0	125	85	17	0	123	37	27	0	125	61	0.81
63	43	14	0	124	86	16	0	124	37	27	0	125	64	0.72
66	27	11	0	126	61	17	0	126	39	30	0	126	67	0.72
67	5	20	0	123	114	-	-	-	-	25	0	122	46	0.69
84	14	20	0	14	74	18	0	15	28	23	0	15	47	0.83
88	34	23	0	4	81	17	0	5	33	35	2	2	57	0.80
Winter Bay Channel														
57	40	14	0	173	65	11	0	175	34	17	0	173	63	0.72
61	42	14	0	171	85	13	0	171	32	16	0	170	65	0.78
64	15	9	0	169	92	-	-	-	-	17	0	171	65	0.70
65	40	8	0	1	87	10	1	179	40	16	0	177	57	0.66
82	14	13	0	171	70	-	-	-	-	20	0	171	70	0.82
83	27	15	0	172	70	13	0	170	36	16	0	171	63	0.80
86	35	12	0	170	76	9	0	172	38	19	0	170	56	0.57
87	35	11	0	174	78	9	0	170	32	16	0	170	57	0.55
Interior (Under Ice)														
74	4	2	0	155	121	-	-	-	-	3	0	175	62	0.67
75	4	0	0	133	125	-	-	-	-	1	0	125	46	0.64
76	4	0	0	98	139	-	-	-	-	3	0	76	53	0.62
77	4	2	0	65	157	-	-	-	-	2	0	71	115	0.74
78	4	1	0	108	148	-	-	-	-	1	0	106	90	0.78
Interior (Summer)														
85	26	0	0	83	73	1	0	89	87	0	0	104	39	0.07
89	25	1	0	60	152	1	0	71	69	1	0	68	48	0.11
90	19	0	0	148	143	0	0	103	171	1	0	95	51	0.06
91	34	0	0	64	110	0	0	121	140	0	0	60	36	0.16

Table 3: Time lag in minutes corresponding to the maximum in the cross correlation function. Positive lags indicate that the series in the left-hand column leads the series in the upper row. The three numbers given in each cell refer to the analysis for the three different deployment periods (see text).

	Wharf	Dunes	Winter Bay
Wharf	-	15, 15, 15	15, 15, 15
Dunes	-	-	15, 0, 0
Winter Bay	-	-	-

Table 4: Time lag in minutes for the semi-diurnal components of the current record as derived from cross-spectral analysis. Positive lags indicate that the series in the left-hand column leads the series in the upper row. The three numbers given in each cell refer to the analysis for the three different deployment periods (see text).

	Wharf	Dunes	Winter Bay
Wharf	-	27, 27, 40	17, 33, 27
Dunes	-	-	-10, 5, -12
Winter Bay	-	-	-

Table 5: Time lag in minutes for the diurnal components of the current record as derived from cross-spectral analysis. Positive lags indicate that the series in the left-hand column leads the series in the upper row. The three numbers given in each cell refer to the analysis for the three different deployment periods (see text).

	Wharf	Dunes	Winter Bay
Wharf	-	7, -29, -45	-14, -37, -26
Dunes	-	-	-14, -10, 15
Winter Bay	-	-	-

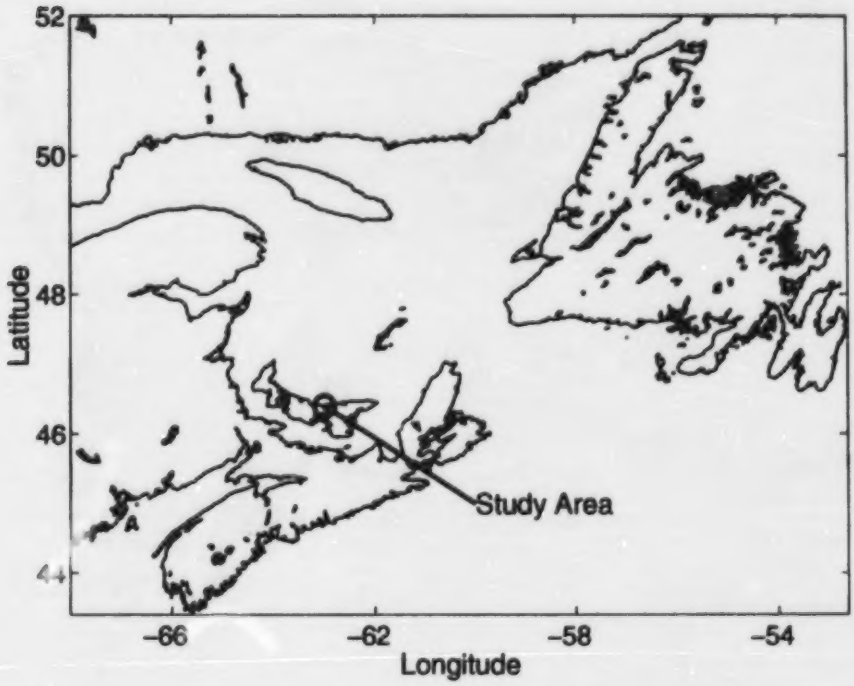

Fig. 1. Location of the study area of Tracadie Bay, P.E.I., Canada.

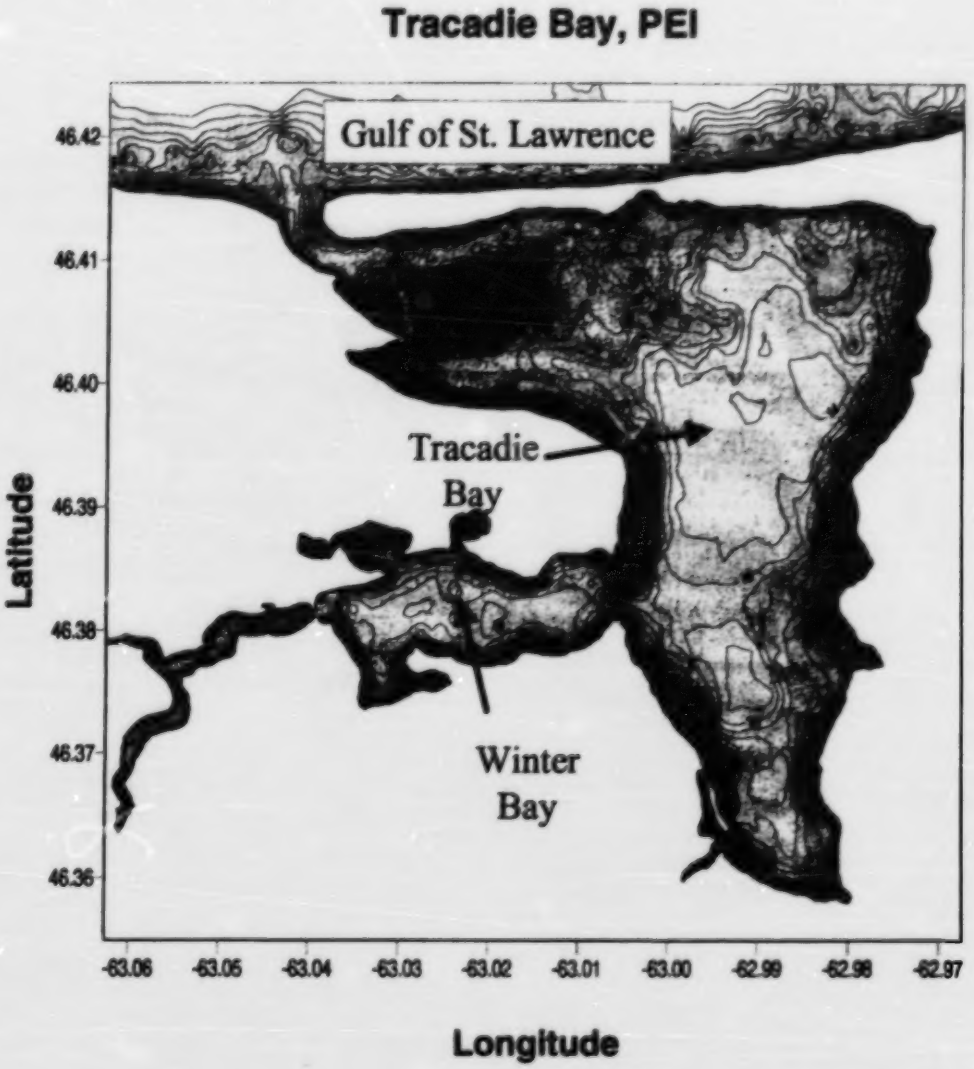

Fig. 2. Map of Tracadie Bay. This contour map of the bathymetry shows the depth in feet relative to mean low water. The lighter gray areas are subtidal (positive depths). The dark gray areas are the inter-tidal zone, which is delineated by the zero contour.

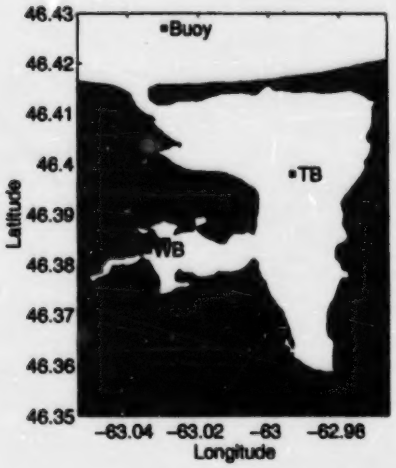

Fig. 3. Map showing the location of the three bottom pressure gauges deployed in summer 1999. The three locations are: (i) outside bell buoy (Buoy), (ii) central Tracadie Bay (TB), and (iii) head of Winter Bay (WB).

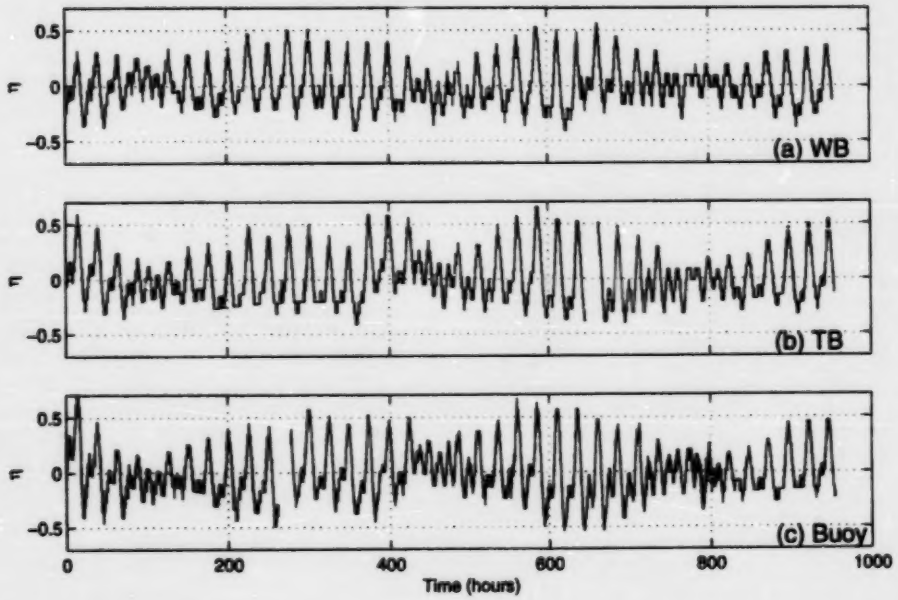

Fig. 4. Sea level anomaly time series. The y-axis shows the sea level (η) in meters derived from the bottom pressure record (i.e. no inverse barometer correction). The x-axis is time in hours starting at July 14, 1999 12:30 GMT.

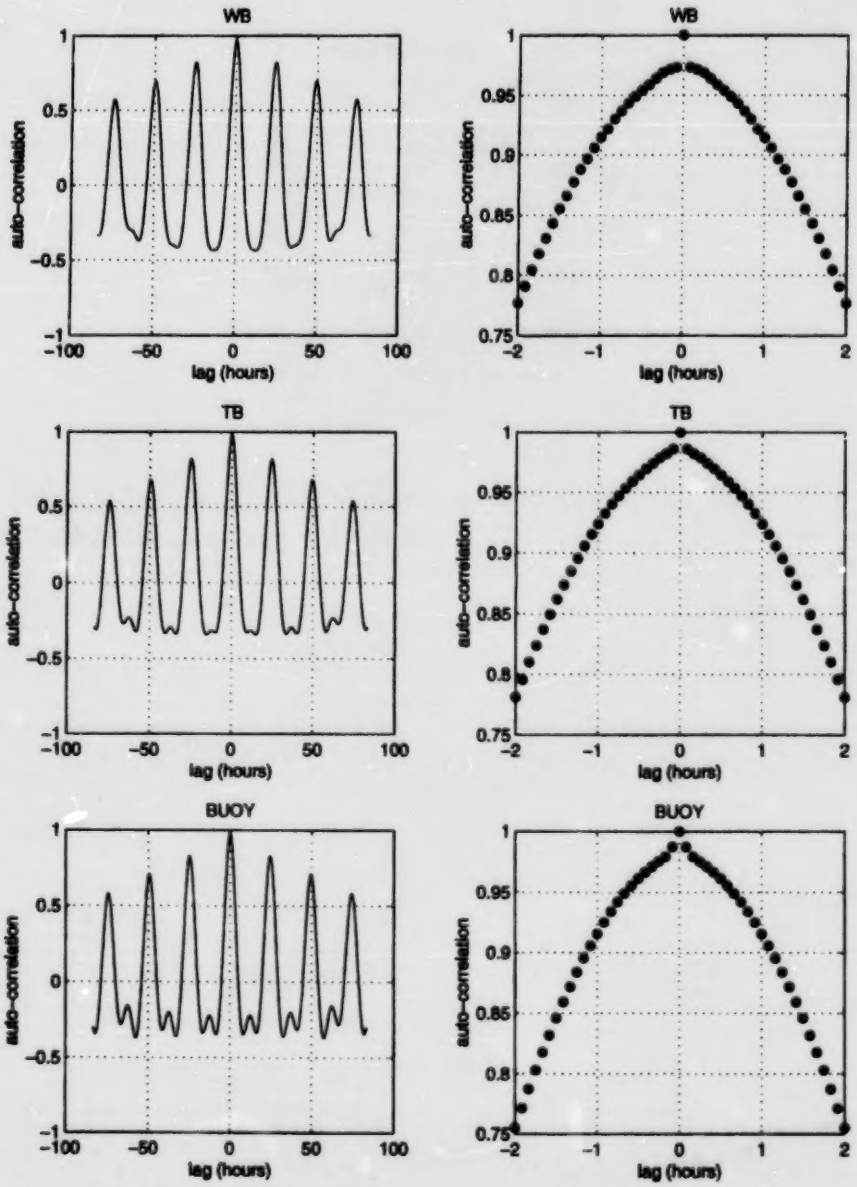

Fig. 5. Sample auto-correlation functions for the 3 sea level time series: Winter Bay (WB), Tracadie Bay (TB) and the outside bell buoy (Buoy). The left panels show the auto-correlation extending out to lags of ±80 h. The right panels show the details near the zero lag region.

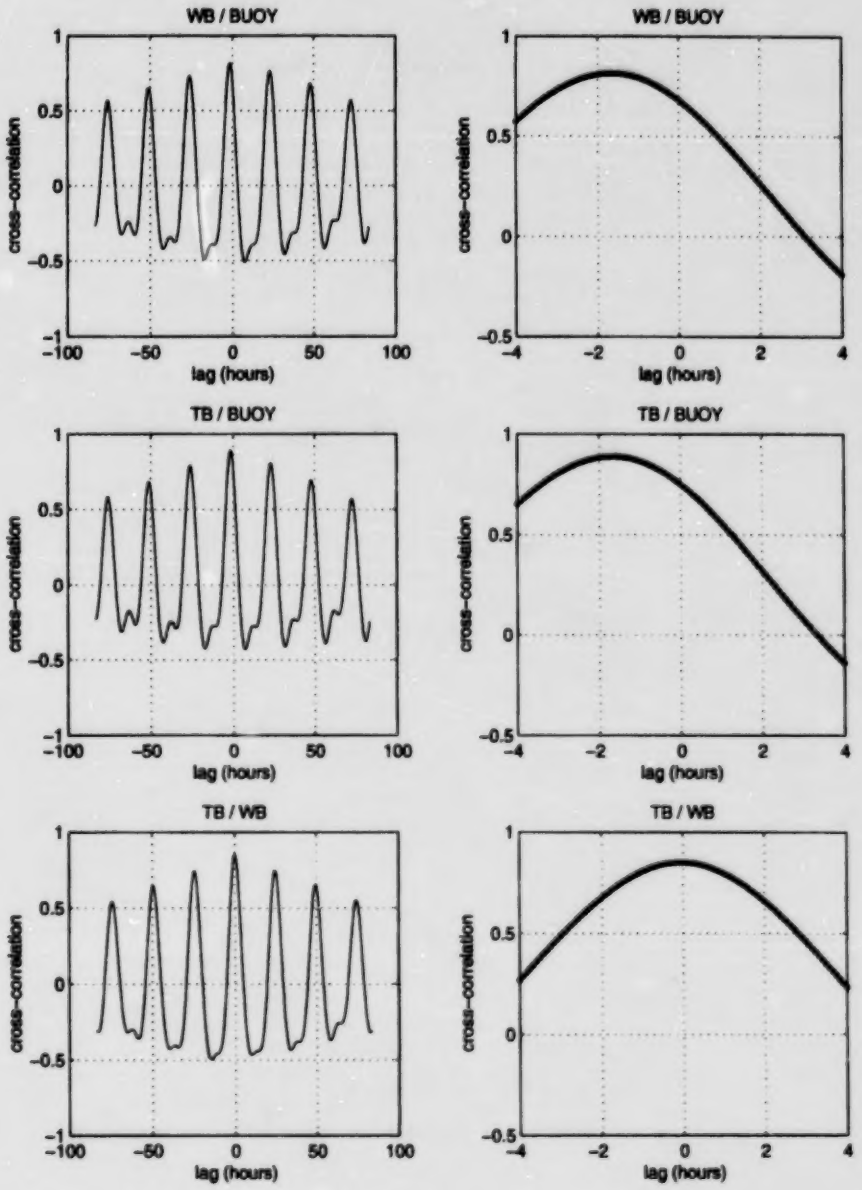

Fig. 6. Sample cross-correlation functions for the pair-wise combinations of the 3 sea level time series from Winter Bay (WB), Tracadie Bay (TB) and the outside bell buoy (Buoy). The left panels show the cross-correlation extending out to lags of ±80 h. The right panels show the details near the zero lag region.

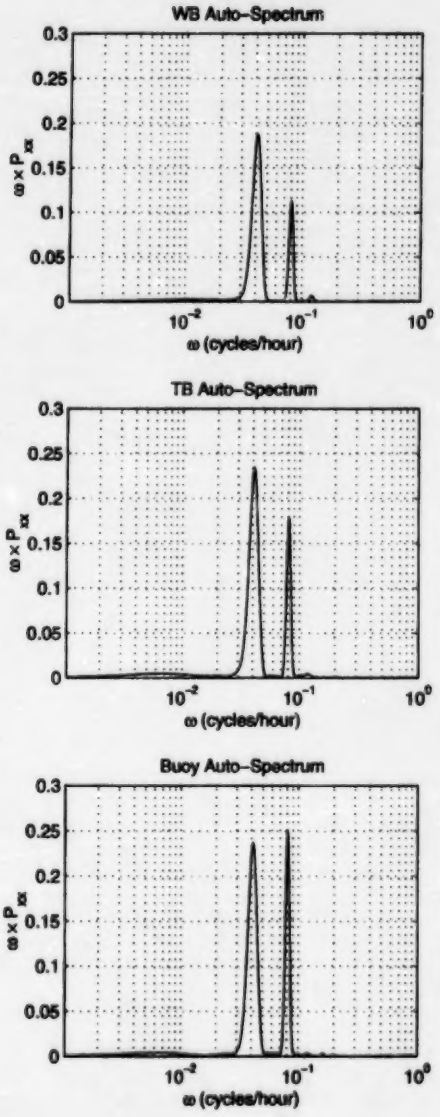

Fig. 7. Variance preserving auto-spectra of the sea level anomaly time series. Here, ω represents the frequency in cycles per hour (cph) and P_{xx} is the power spectral density of the sea level anomaly in units of m^2 cph^{-1}.

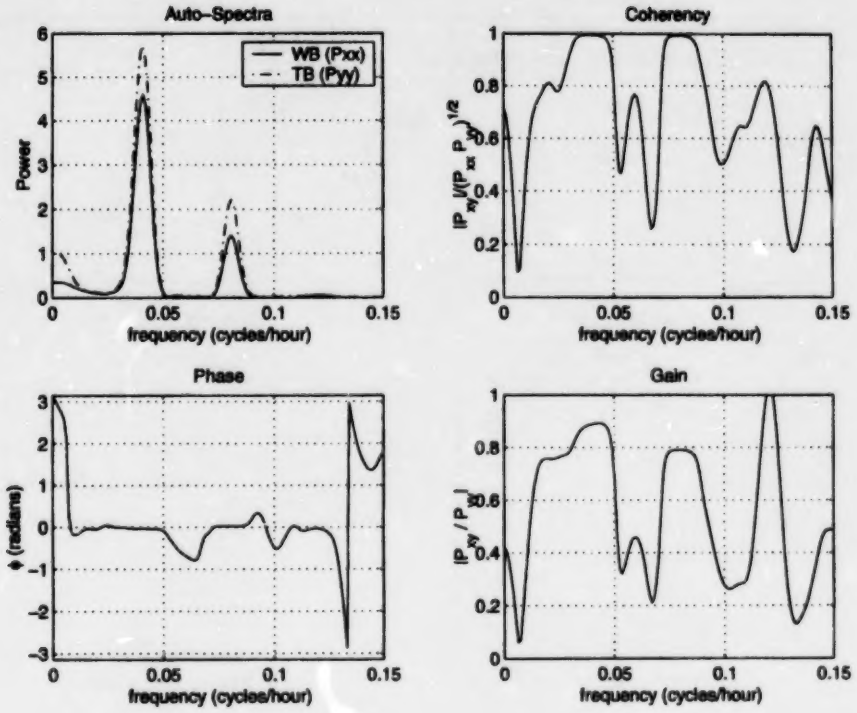

Fig. 8. Results from the cross-spectral analysis of Winter Bay (x) and Tracadie Bay (y) sea level anomaly time series. Shown are the auto-spectra, the coherency spectrum, the phase spectrum and the gain spectrum. Here, P_{xx} and P_{yy} denote the auto-spectra while P_{xy} denotes the cross-spectra, each with units of m^2 cph^{-1}.

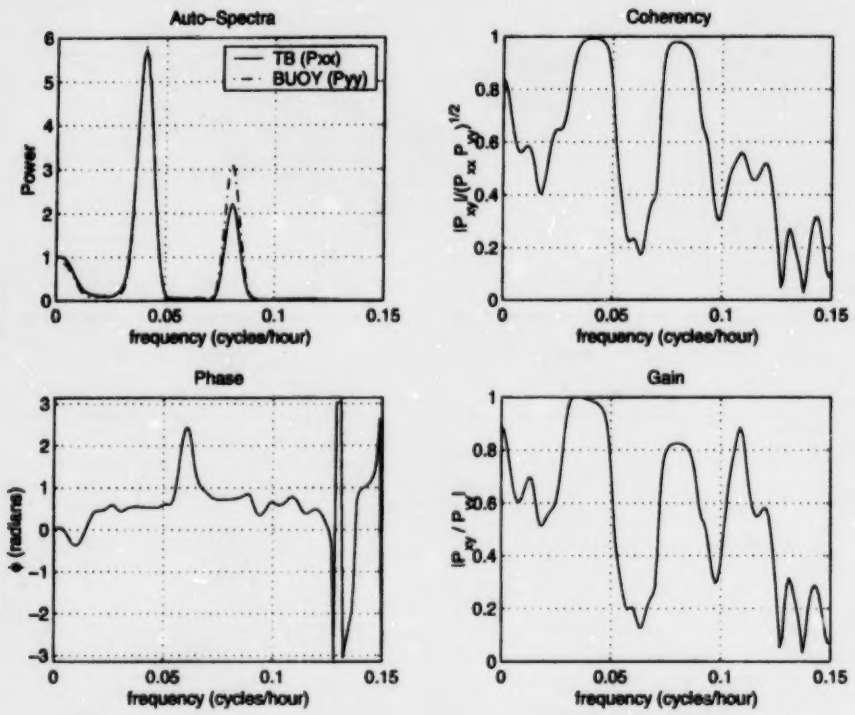

Fig. 9. Results from the cross-spectral analysis of Tracadie Bay (x) and Buoy (y) sea level anomaly time series. Shown are the auto-spectra, the coherency spectrum, the phase spectrum and the gain spectrum. Here, P_{xx} and P_{yy} denote the auto-spectra while P_{xy} denotes the cross-spectra, each with units of m^2 cph^{-1}.

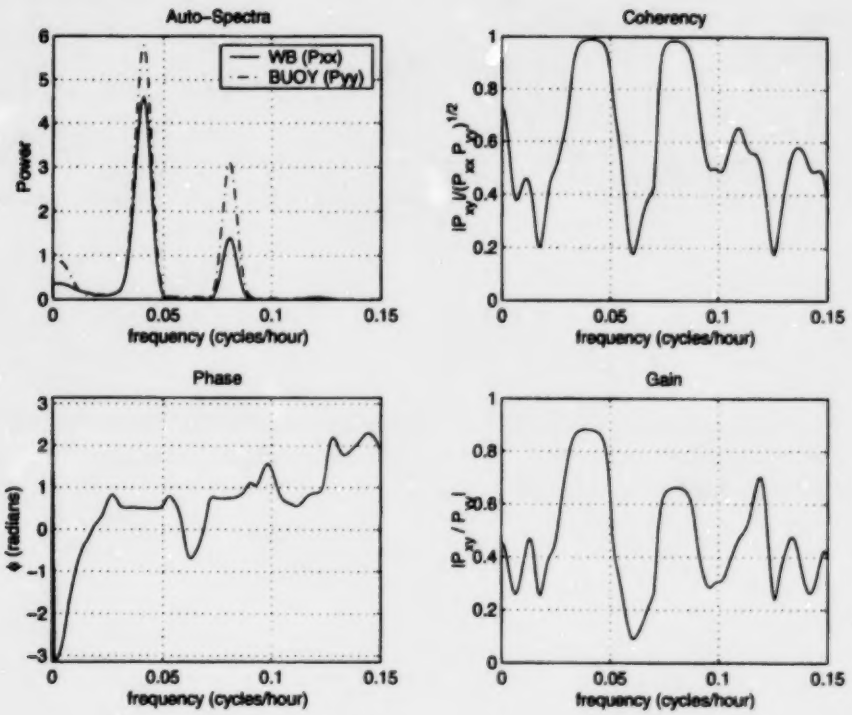

Fig. 10. Results from the cross-spectral analysis of Winter Bay (x) and Buoy (y) sea level anomaly time series. Shown are the auto-spectra, the coherency spectrum, the phase spectrum and the gain spectrum. Here, P_{xx} and P_{yy} denote the auto-spectra while P_{xy} denotes the cross-spectra, each with units of m^2 cph^{-1}.

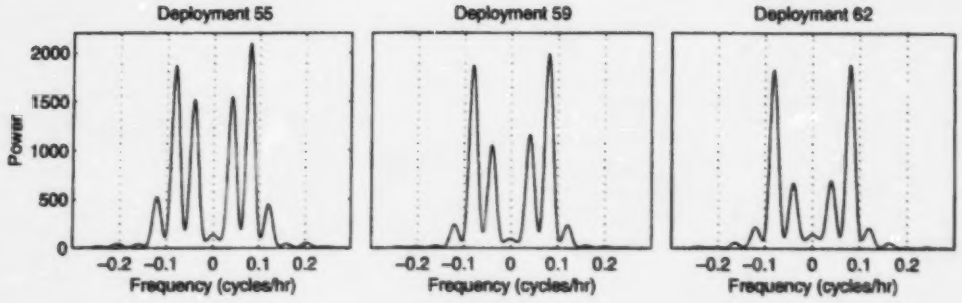

Fig. 11. Rotary spectra for the current time series recorded at the Wharf Channel. Positive (negative) frequencies correspond to anti-clockwise (clockwise) rotating energy. The power spectral density has units $cm^2\ s^{-2}\ cph^{-1}$.

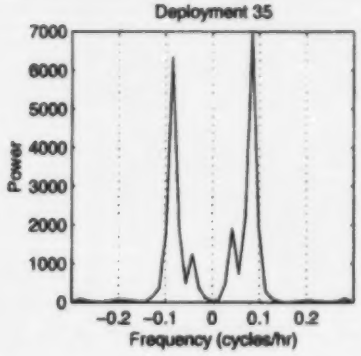

Fig. 12. Rotary spectra for the current time series recorded at the outside channel. Positive (negative) frequencies correspond to anti-clockwise (clockwise) rotating energy. The power spectral density has units $cm^2\ s^{-2}\ cph^{-1}$.

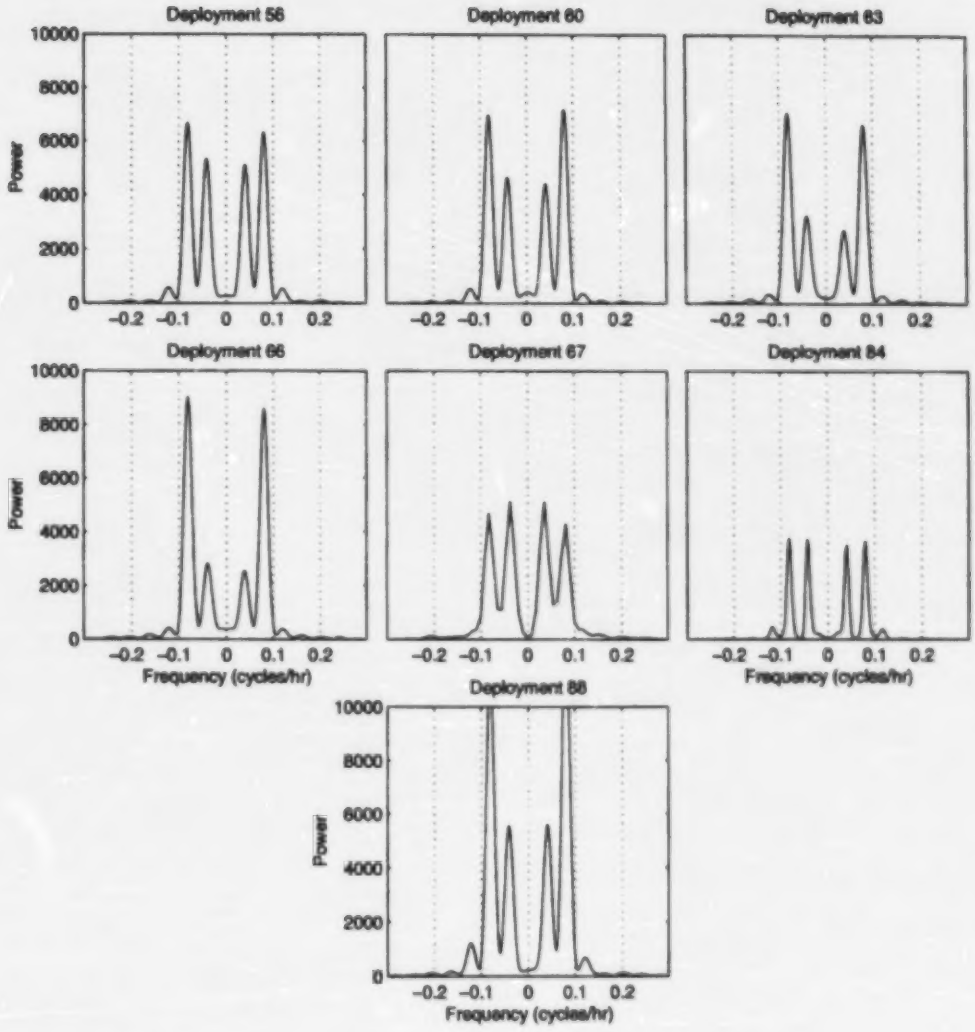

Fig. 13. Rotary spectra for the current time series recorded at the Dunes Channel. Positive (negative) frequencies correspond to anti-clockwise (clockwise) rotating energy. The power spectral density has units $cm^2\ s^{-2}\ cph^{-1}$.

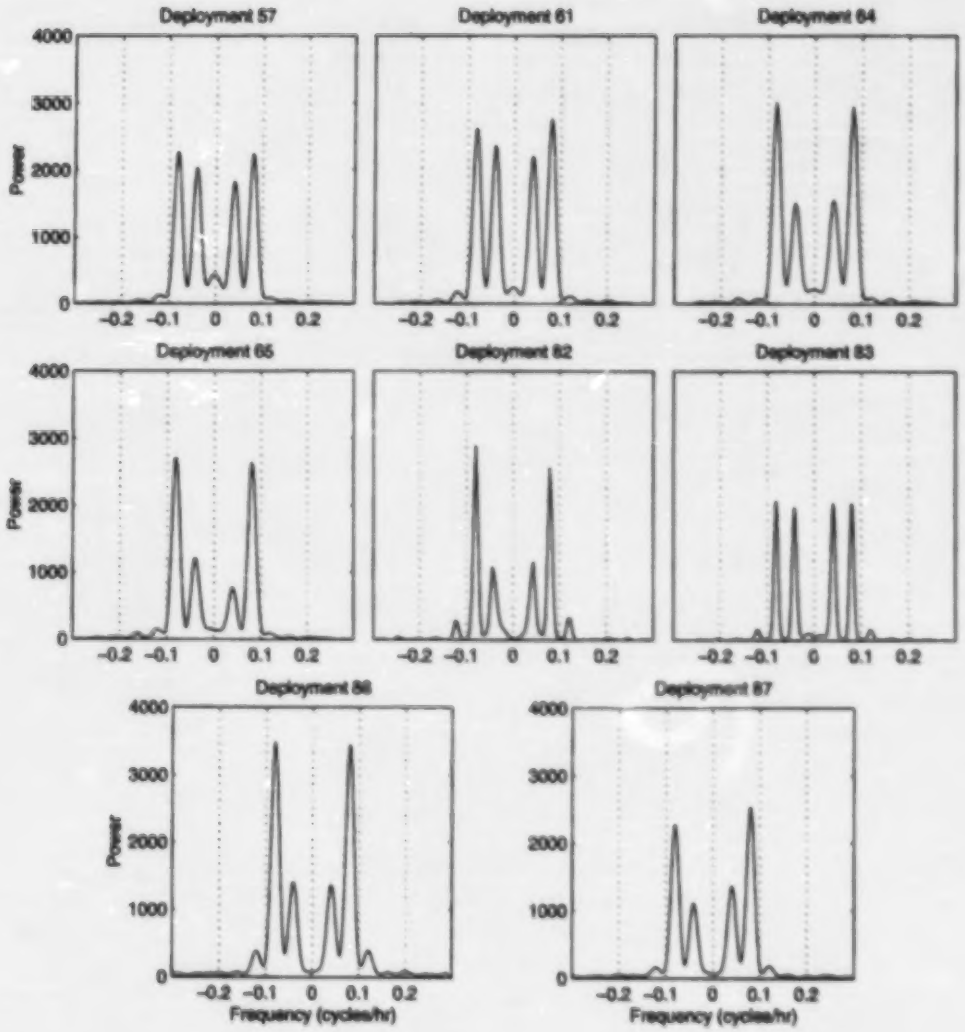

Fig. 14. Rotary spectra for the current time series recorded at the Winter Bay channel. Positive (negative) frequencies correspond to anti-clockwise (clockwise) rotating energy. The power spectral density has units $cm^2\ s^{-2}\ cph^{-1}$.

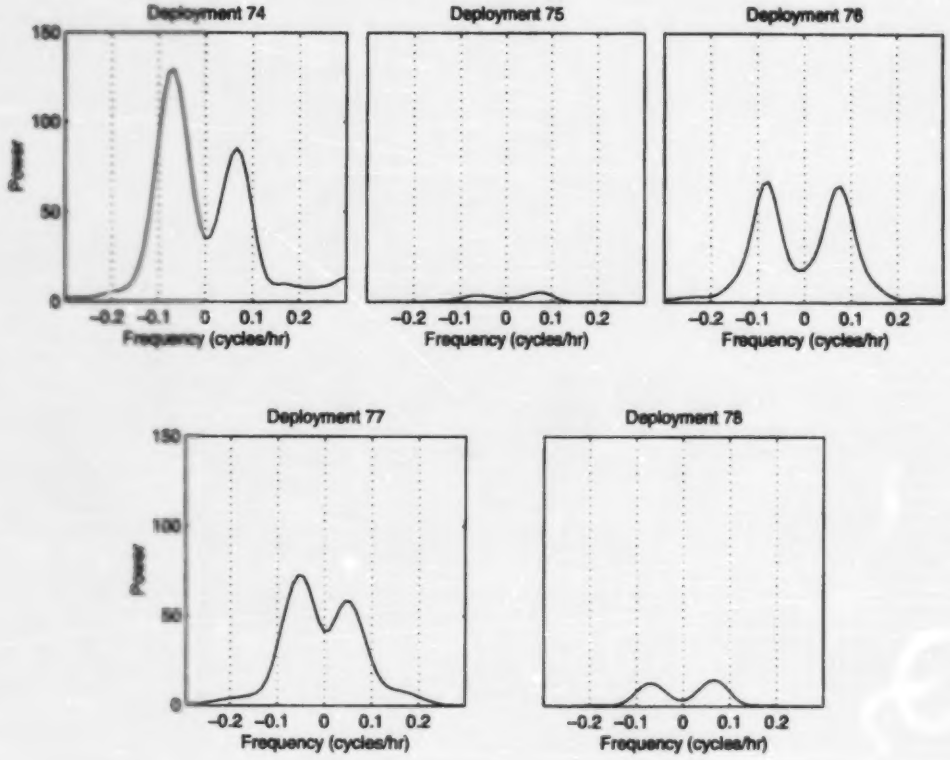

Fig. 15. Rotary spectra for the current time series recorded in the interior under the ice cover. Positive (negative) frequencies correspond to anti-clockwise (clockwise) rotating energy. The power spectral density has units $cm^2\ s^{-2}\ cph^{-1}$.

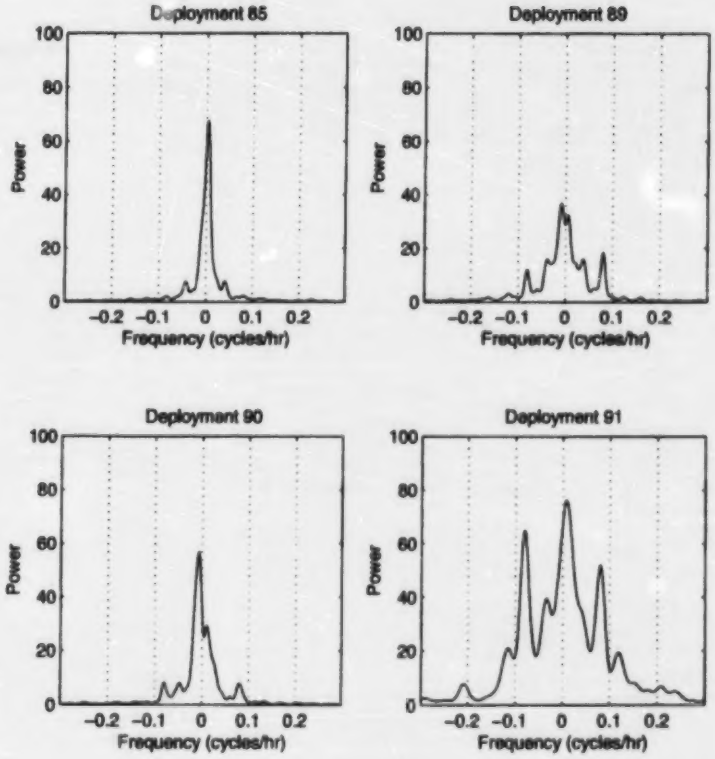

Fig. 16. Rotary spectra for the current time series recorded at the interior bay during the summer. Positive (negative) frequencies correspond to anti-clockwise (clockwise) rotating energy. The power spectral density has units $cm^2\ s^{-2}\ cph^{-1}$.

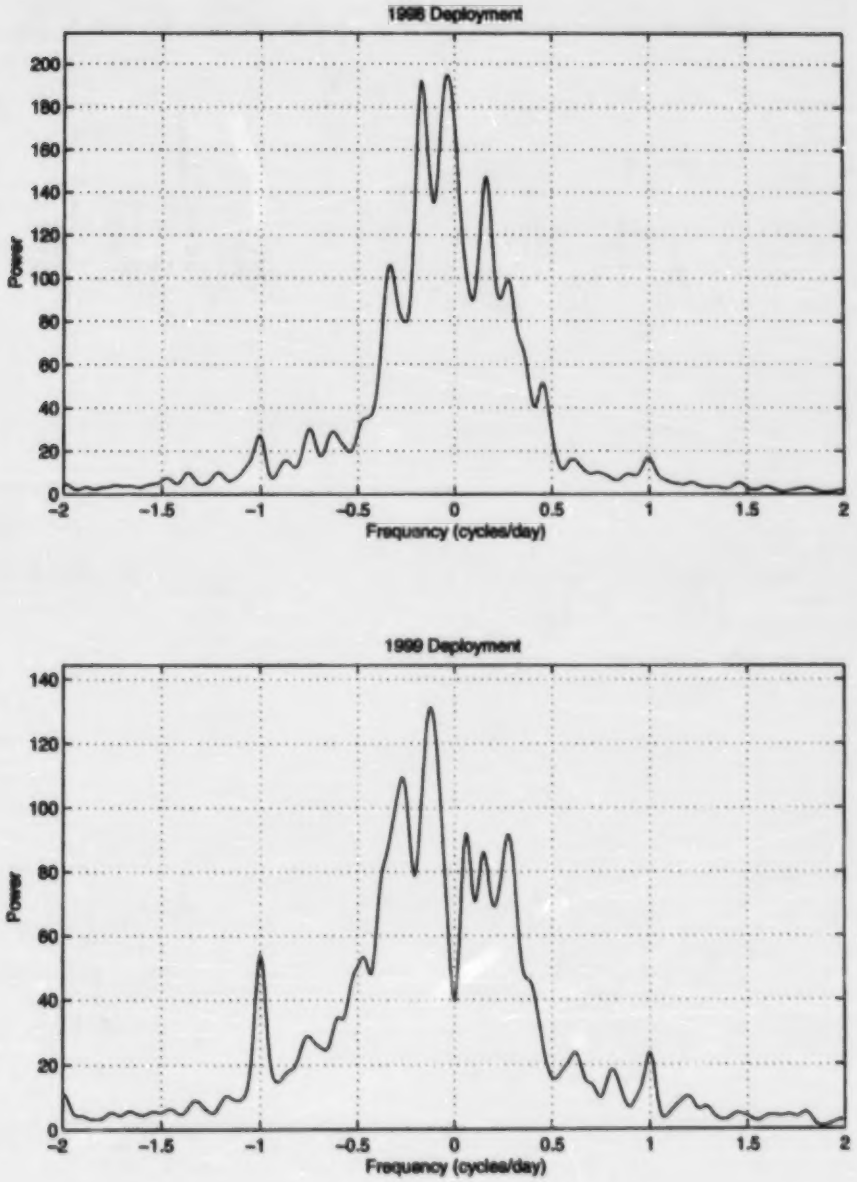

Fig. 17. Rotary spectra for the vector wind data recorded by the meterological station in the summers of 1998 and 1999. Positive (negative) frequencies correspond to anti-clockwise (clockwise) rotating energy. The power spectral density has units $m^2\ s^{-2}\ cpd^{-1}$.

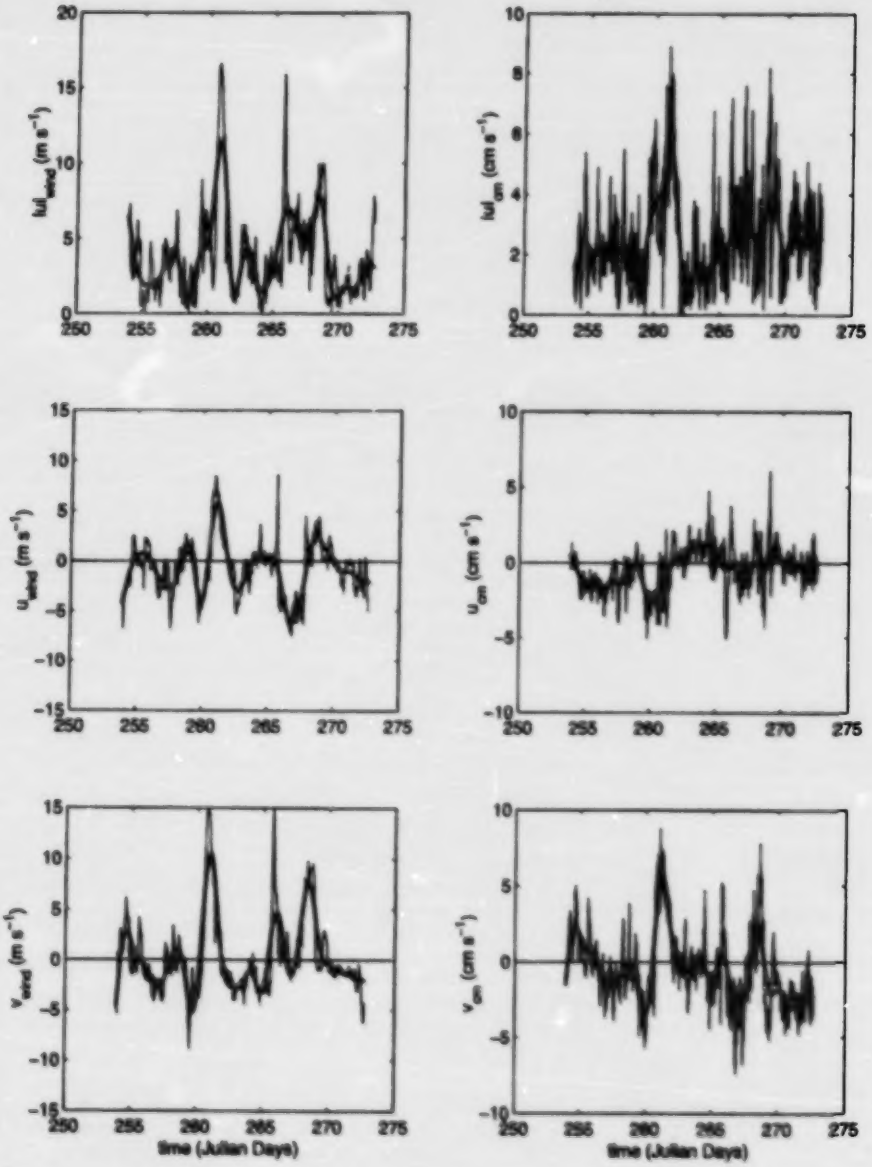

Fig. 18. Current records for deployment 90 and the corresponding wind record for the same period. The left panels correspond to wind data and those on the right show the current data. Upper two panels show speed, the middle two show the u-component of velocity, and lower two panels show the v-component of velocity. The thin solid line represents the recorded series. The thick solid line is the low pass filtered version of the series (with cutoff frequency corresponding to a 40 h period).

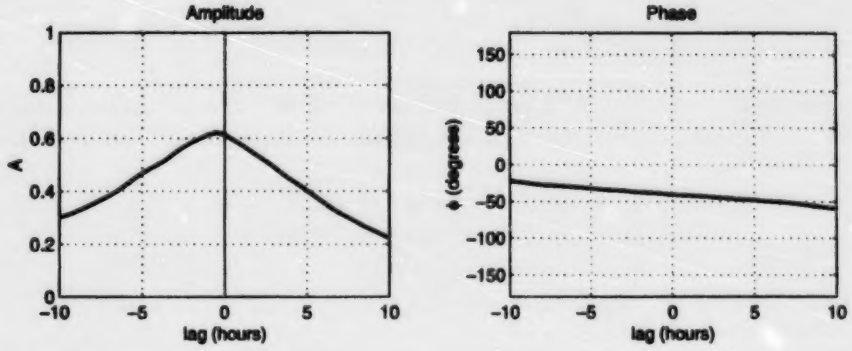

Fig. 19. Correlation between the vector series of wind and current for deployment 90. The left panel shows the amplitude of the complex correlation, while the right panel shows its phase (in degrees).

Appendix A

Current Meter Data

This appendix contains plots of data obtained from the 28 deployments of InterOcean Systems S4 electromagnetic current meters in Tracadie Bay (see text for details).

Figs. A.1 – A.28 each display the following information:

- Map of Tracadie Bay showing the location and date of the current meter deployment,
- East-west (u) component of the current velocity vector,
- North-south (v) component of the current velocity vector,
- Stick plot of the velocity vector time series,
- Rose plot giving the distribution of the speed and direction of the current independent of time,
- Progressive vector diagram showing the (hypothetical) displacement of a particle advected by the recorded velocity time series.

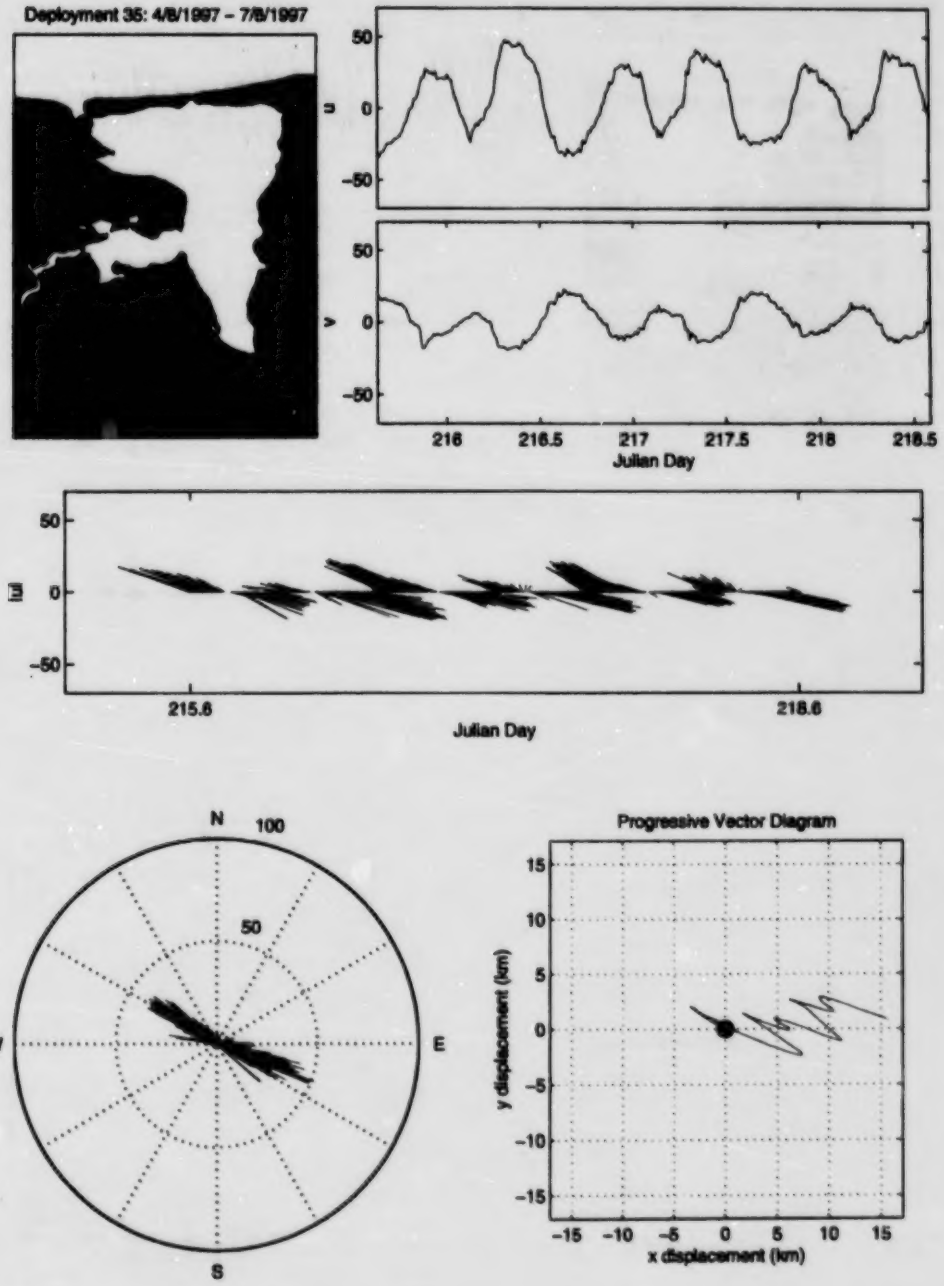

Fig. A.1. Current data for deployment 35.

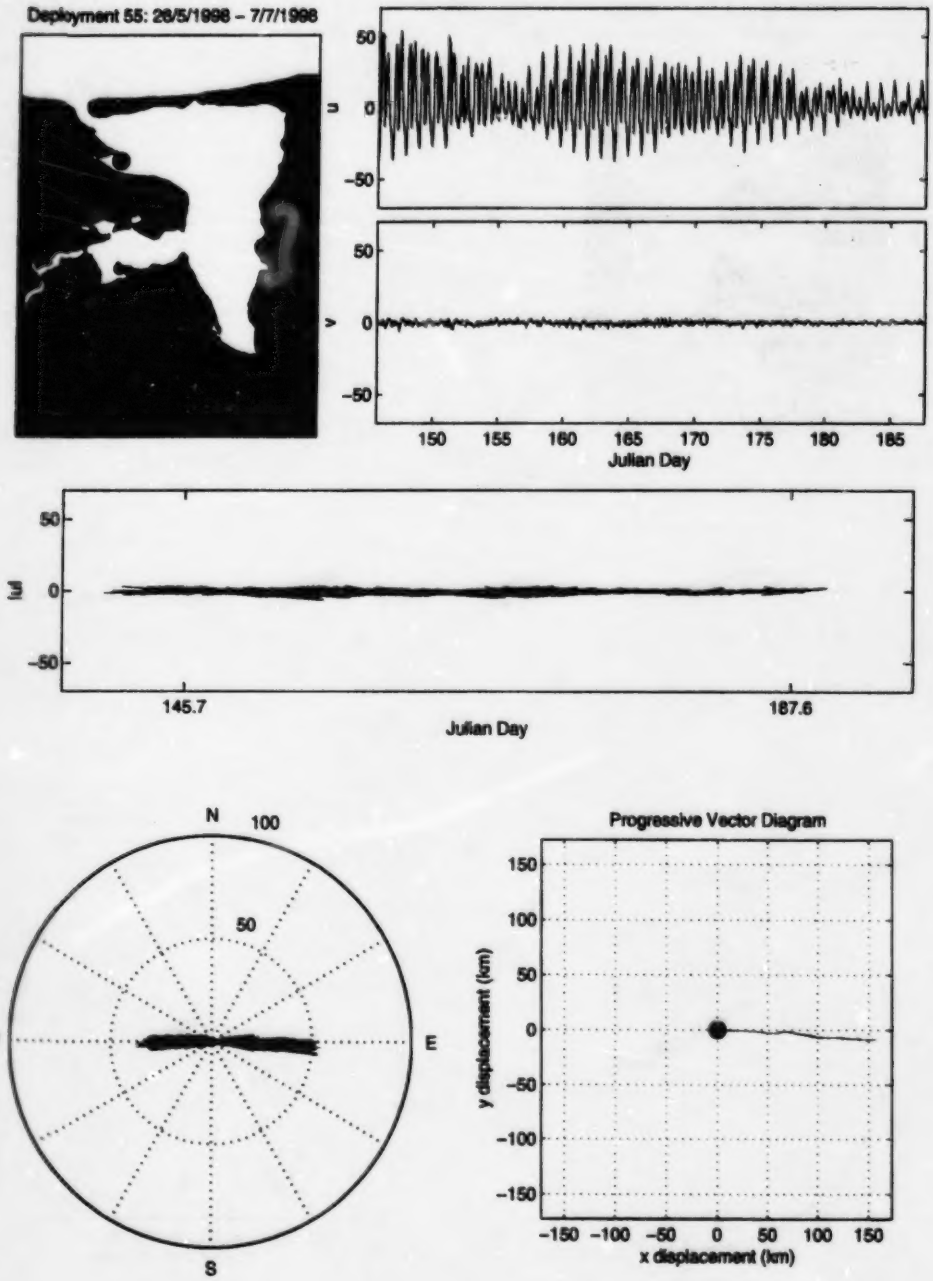

Fig. A.2. Current data for deployment 55.

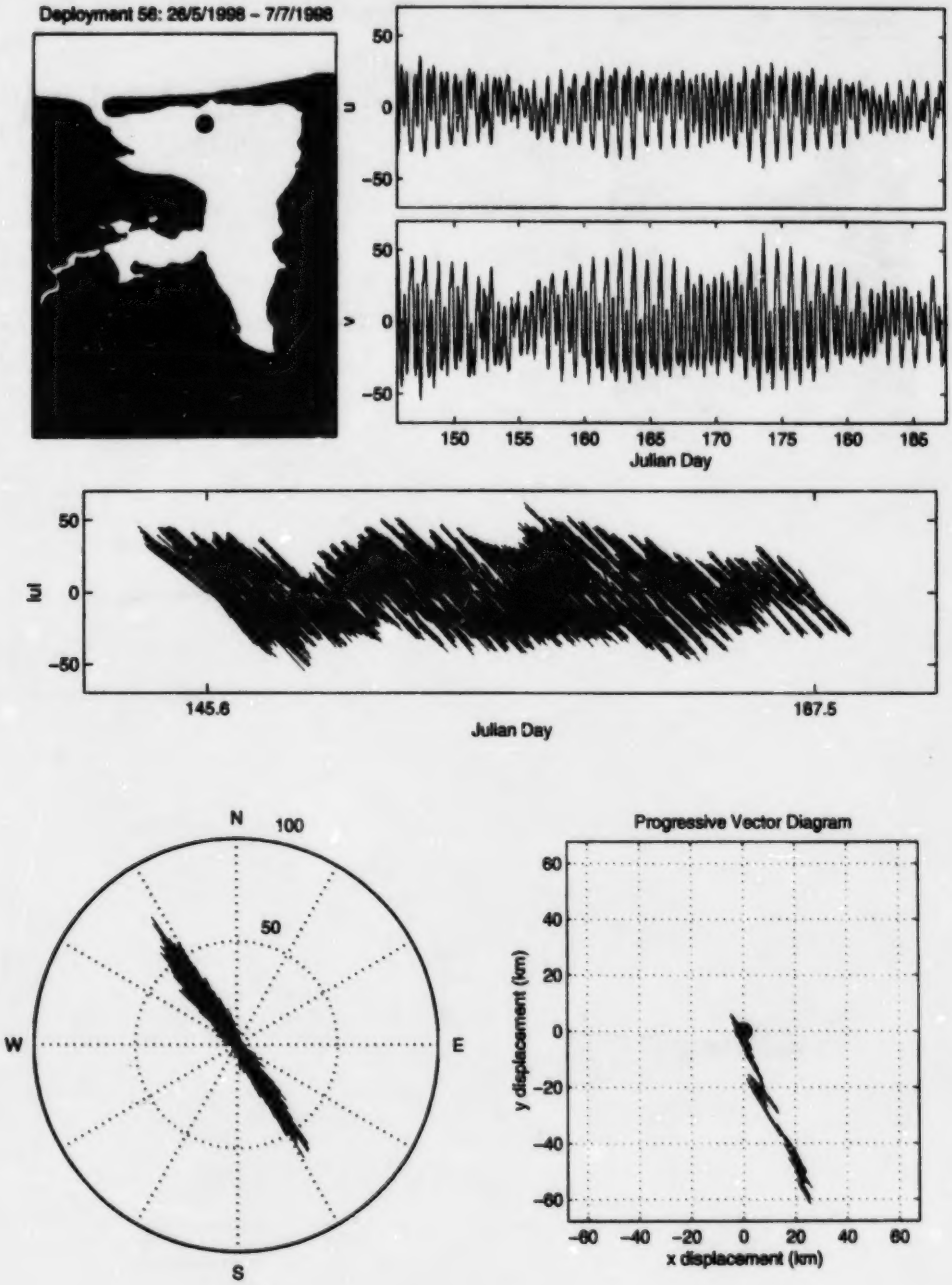

Fig. A.3. Current data for deployment 56.

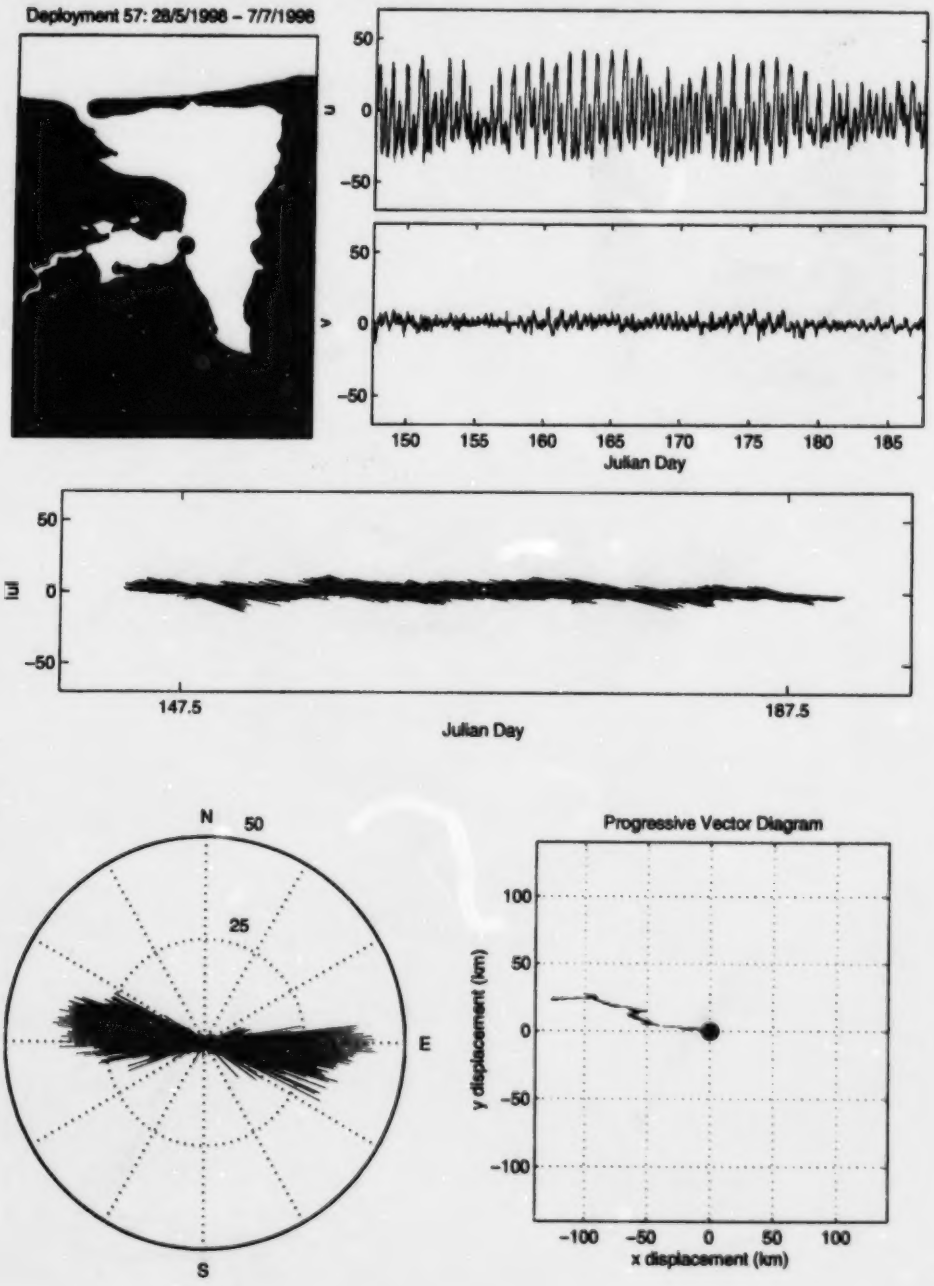

Fig. A.4. Current data for deployment 57.

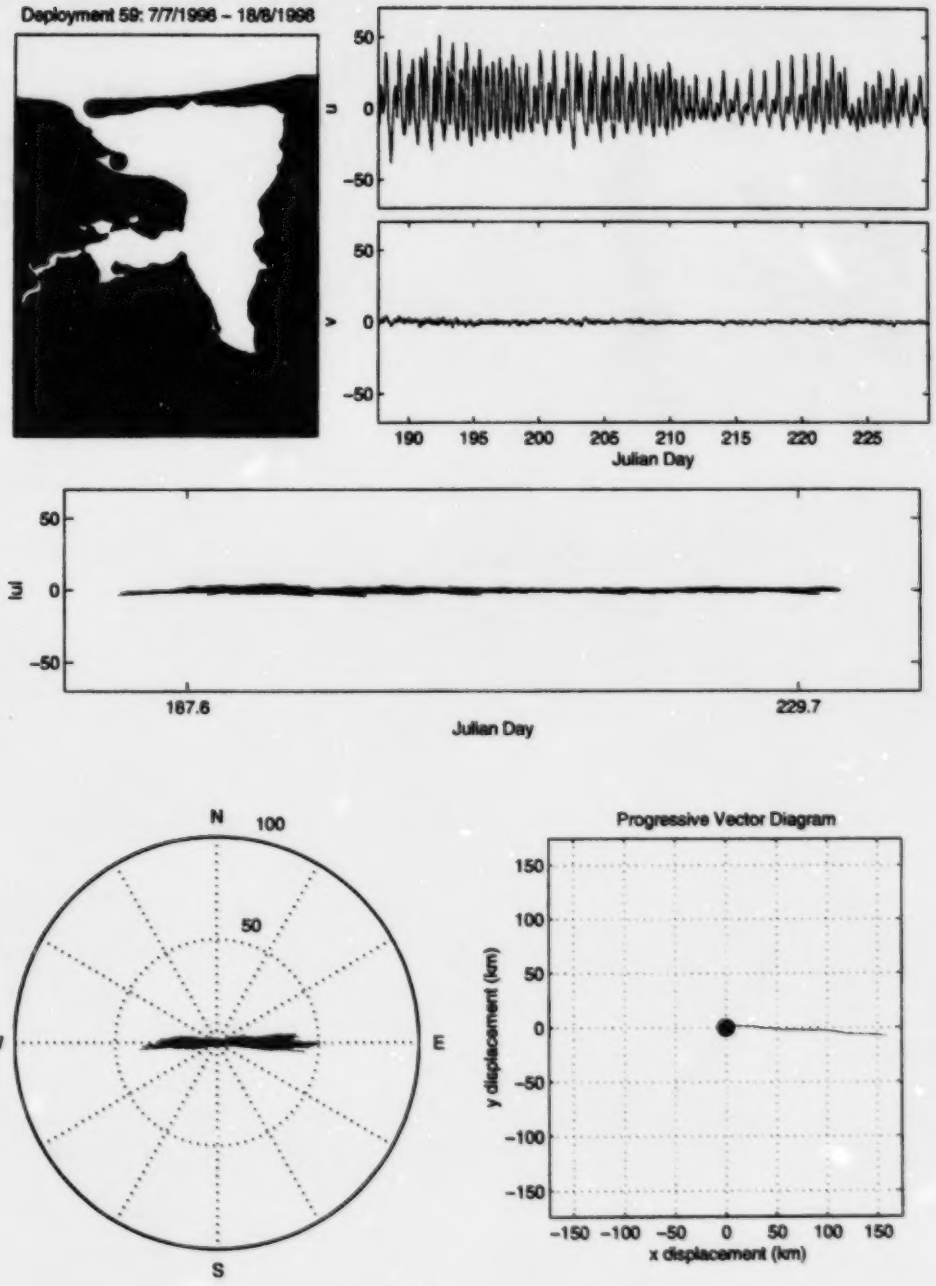

Fig. A.5. Current data for deployment 59.

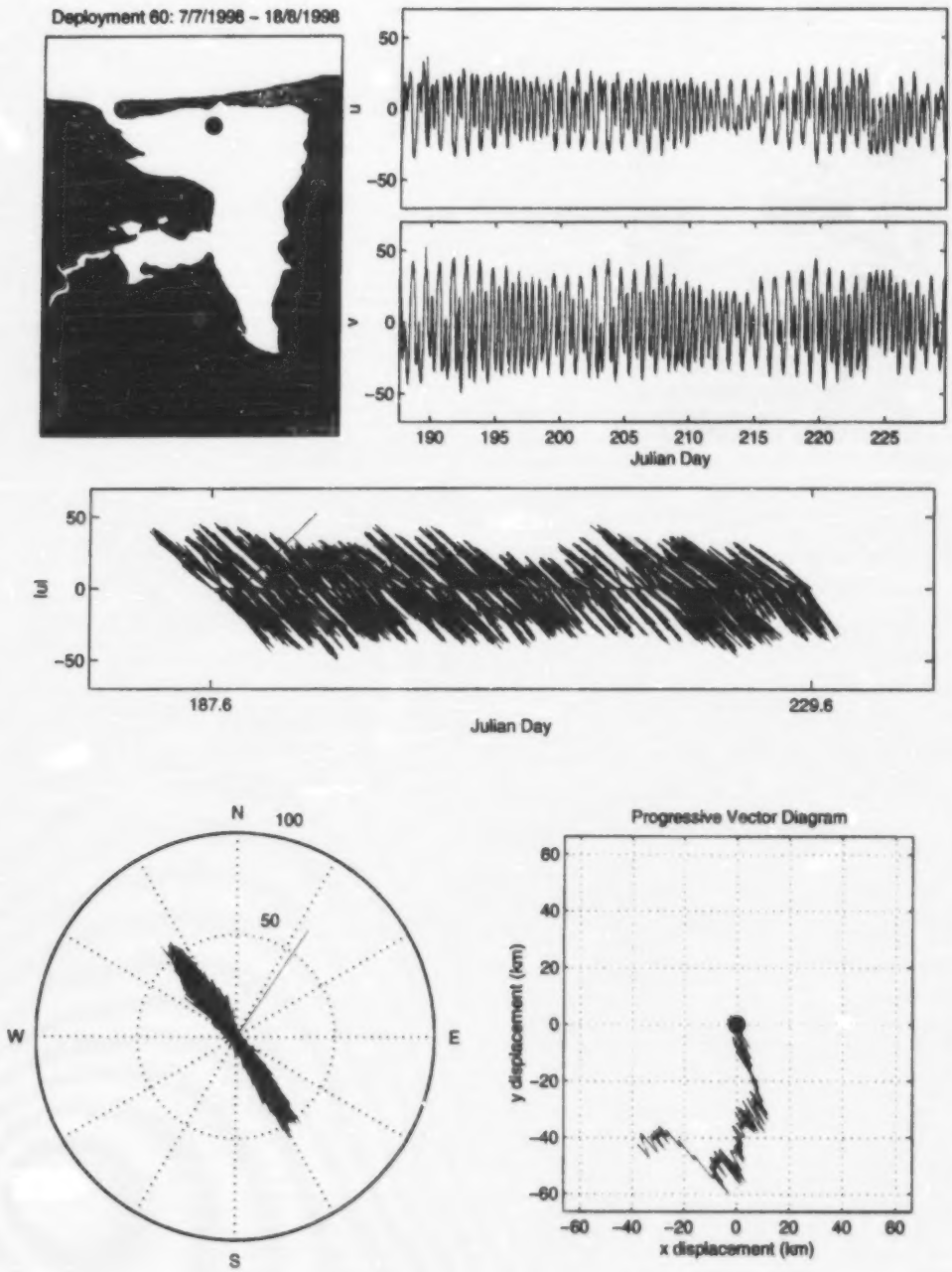

Fig. A.6. Current data for deployment 60.

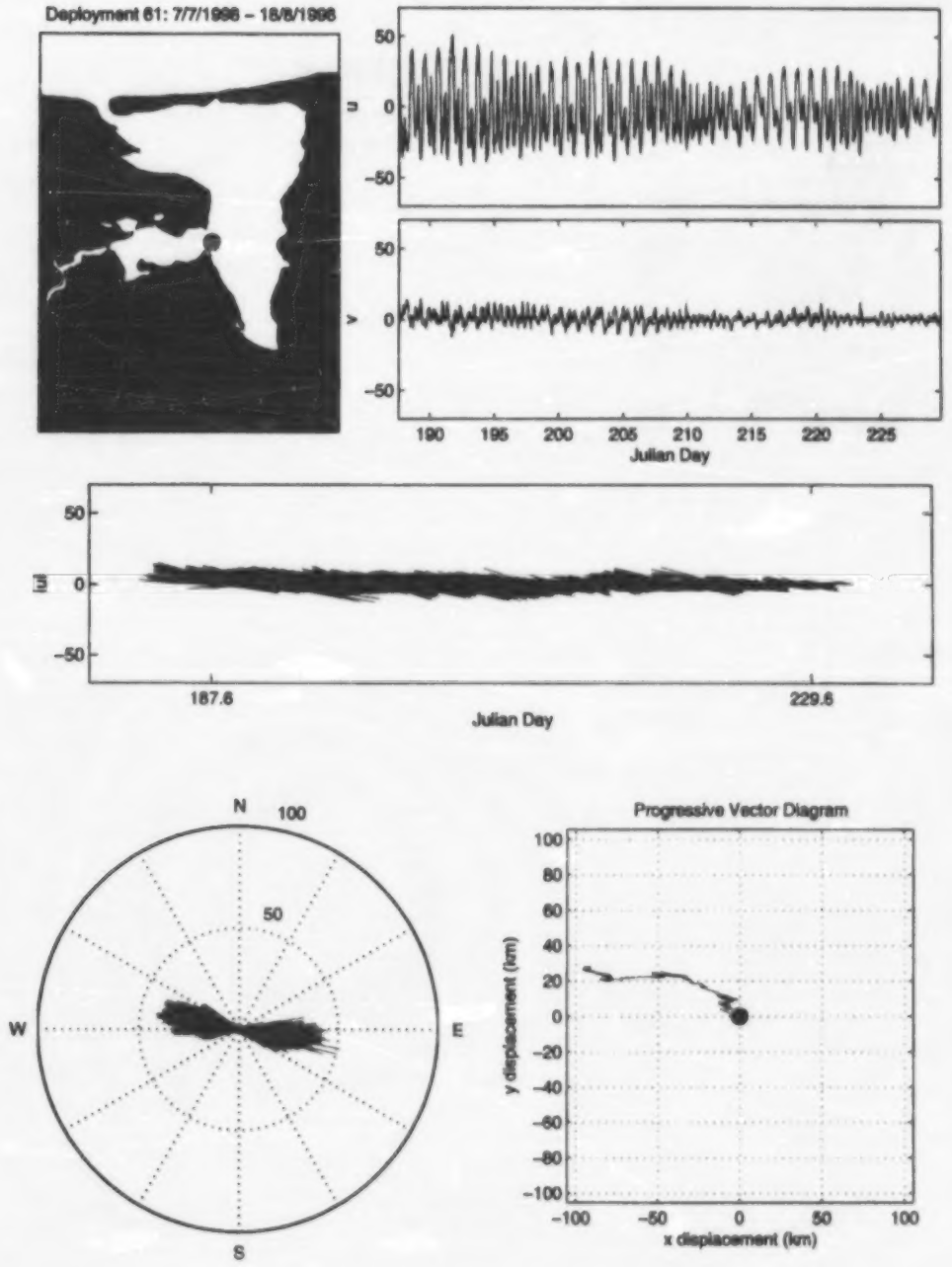

Fig. A.7. Current data for deployment 61.

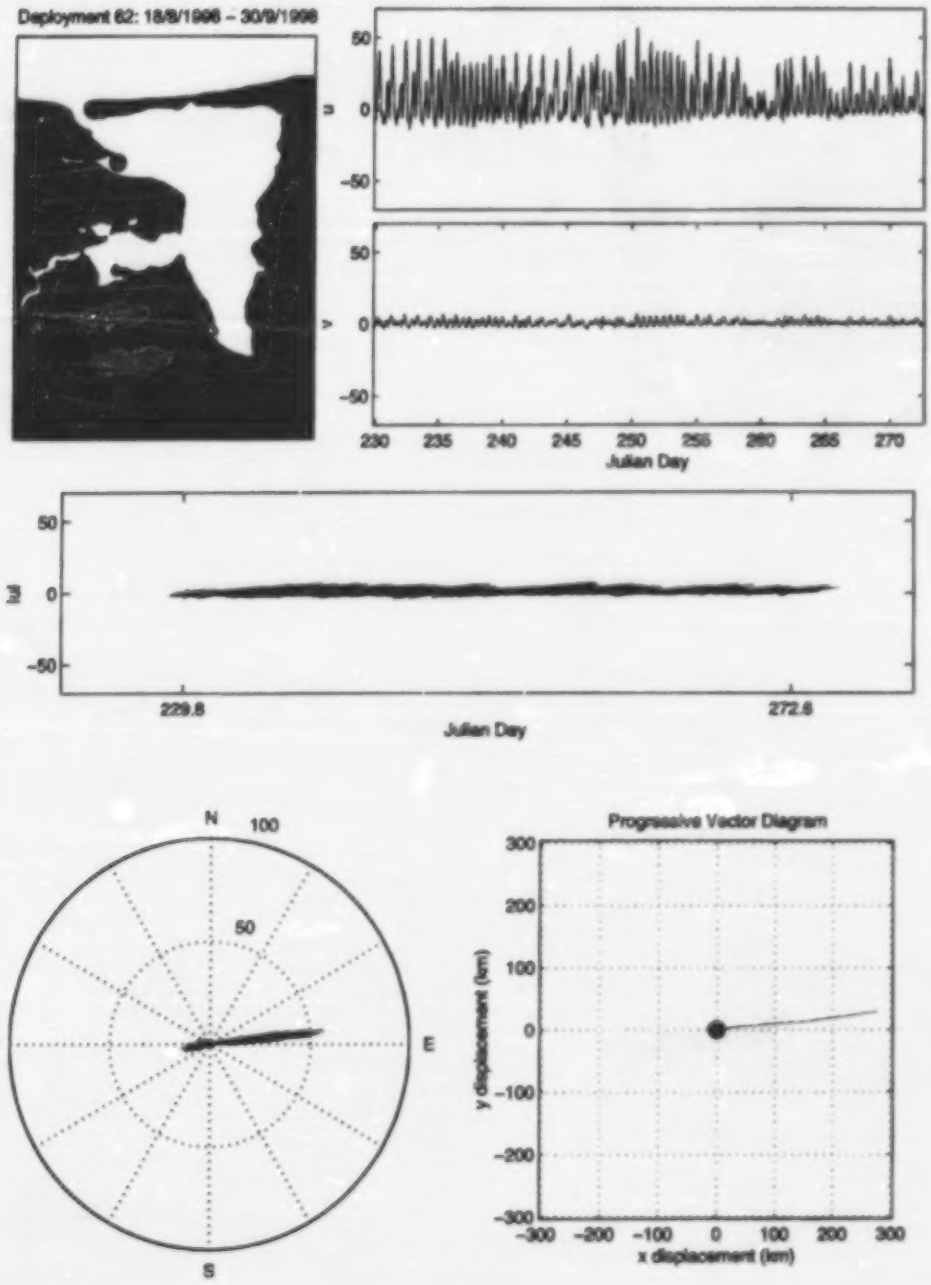

Fig. A.8. Current data for deployment 62.

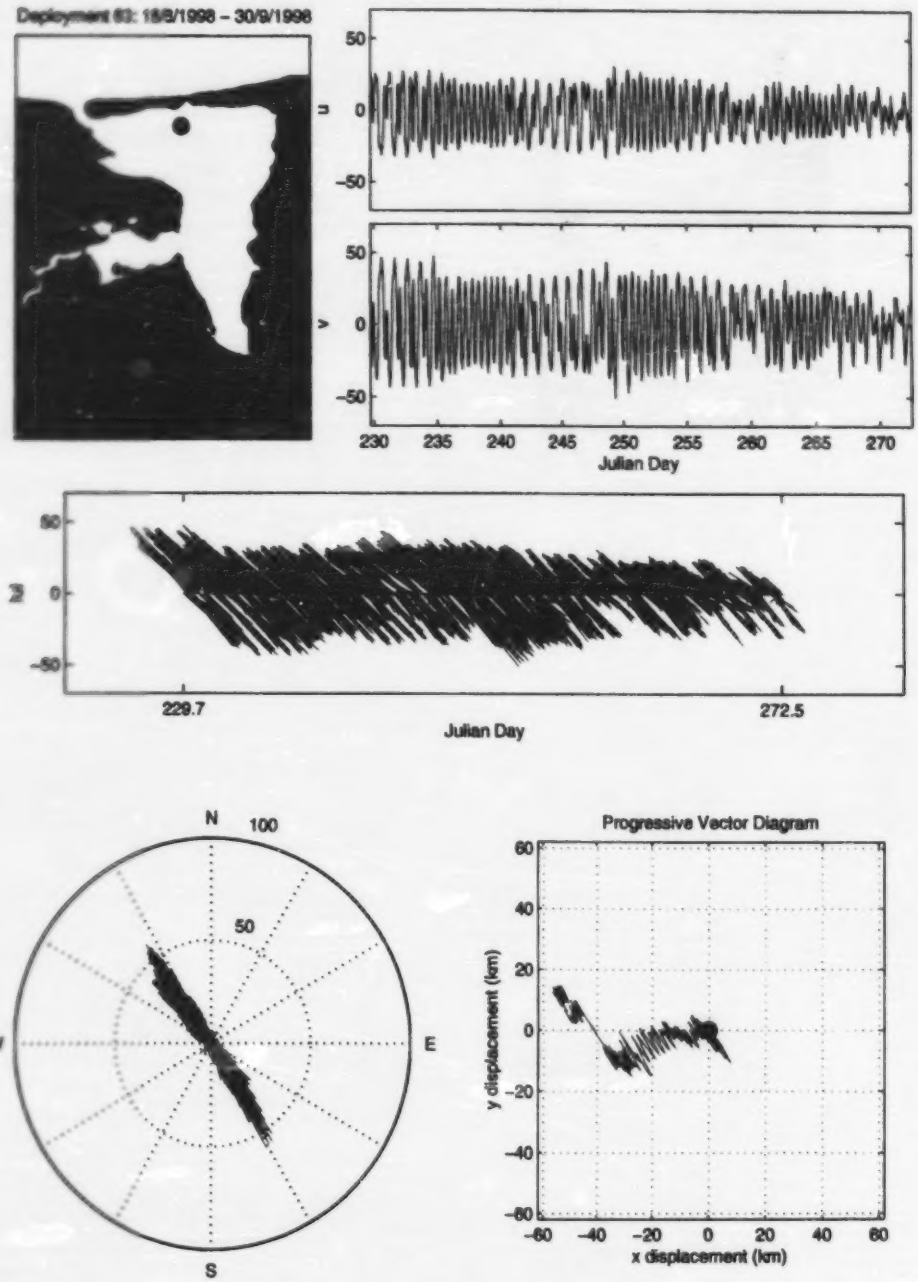

Fig. A.9. Current data for deployment 63.

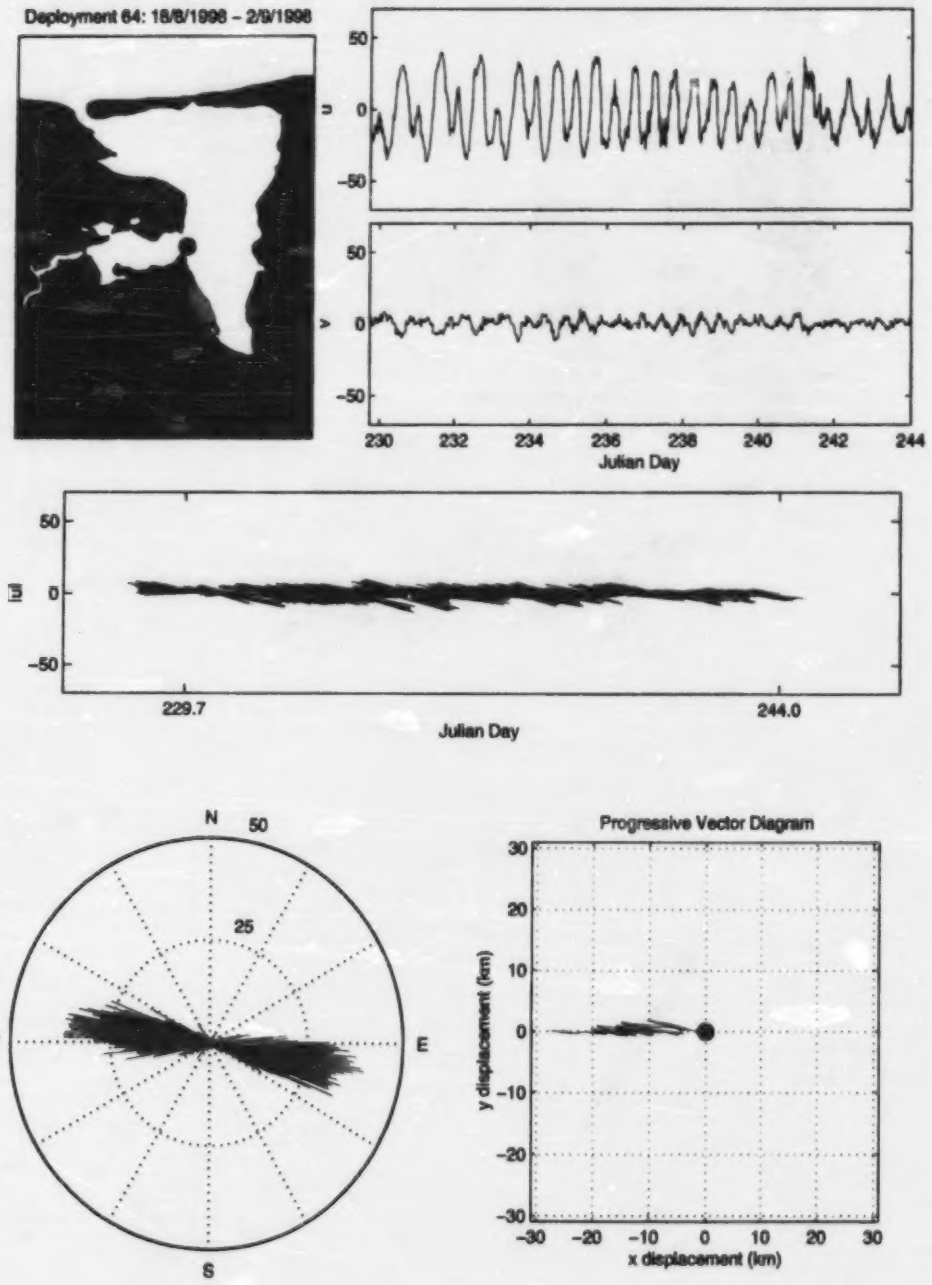

Fig. A.10. Current data for deployment 64.

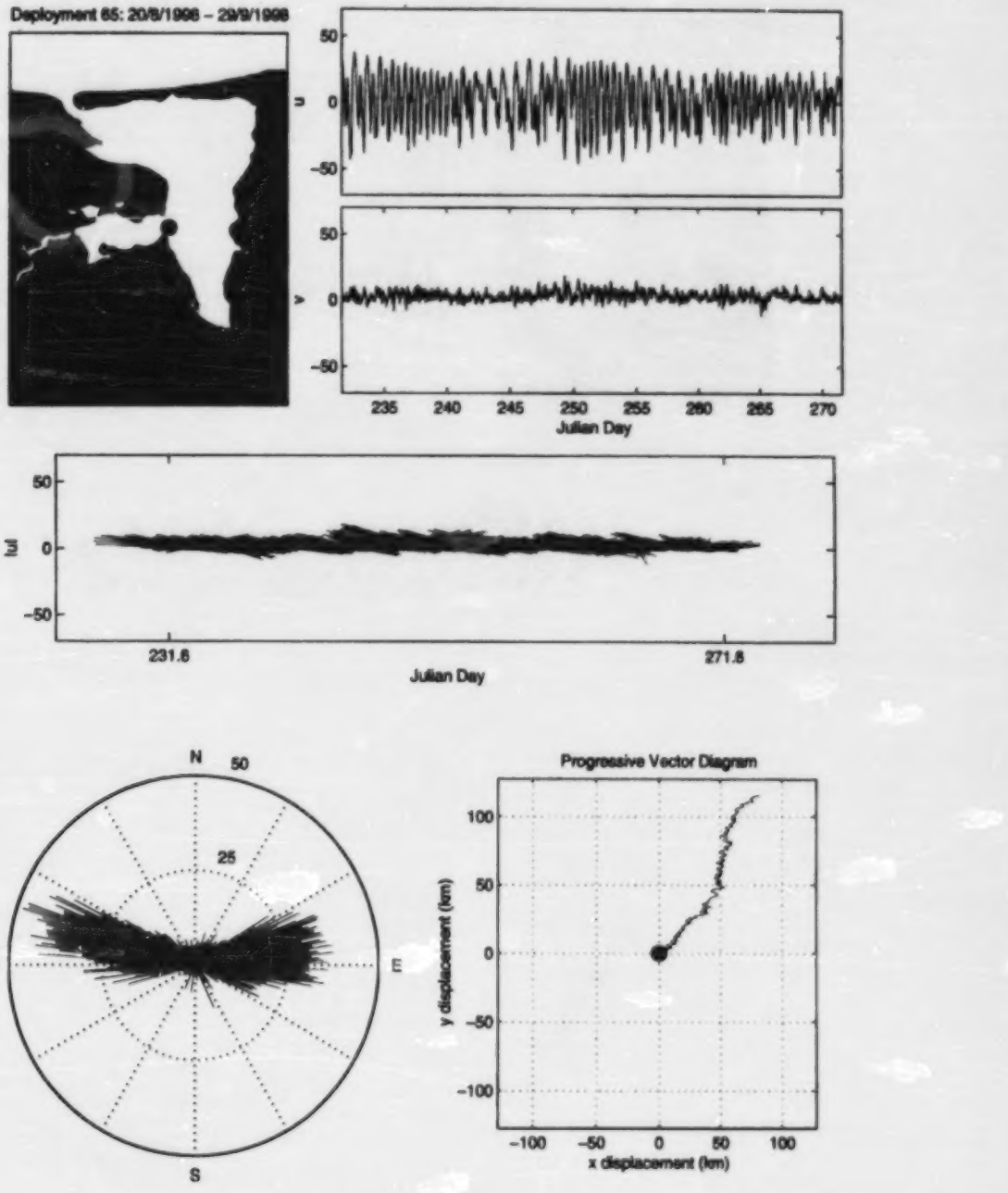

Fig. A.11. Current data for deployment 65.

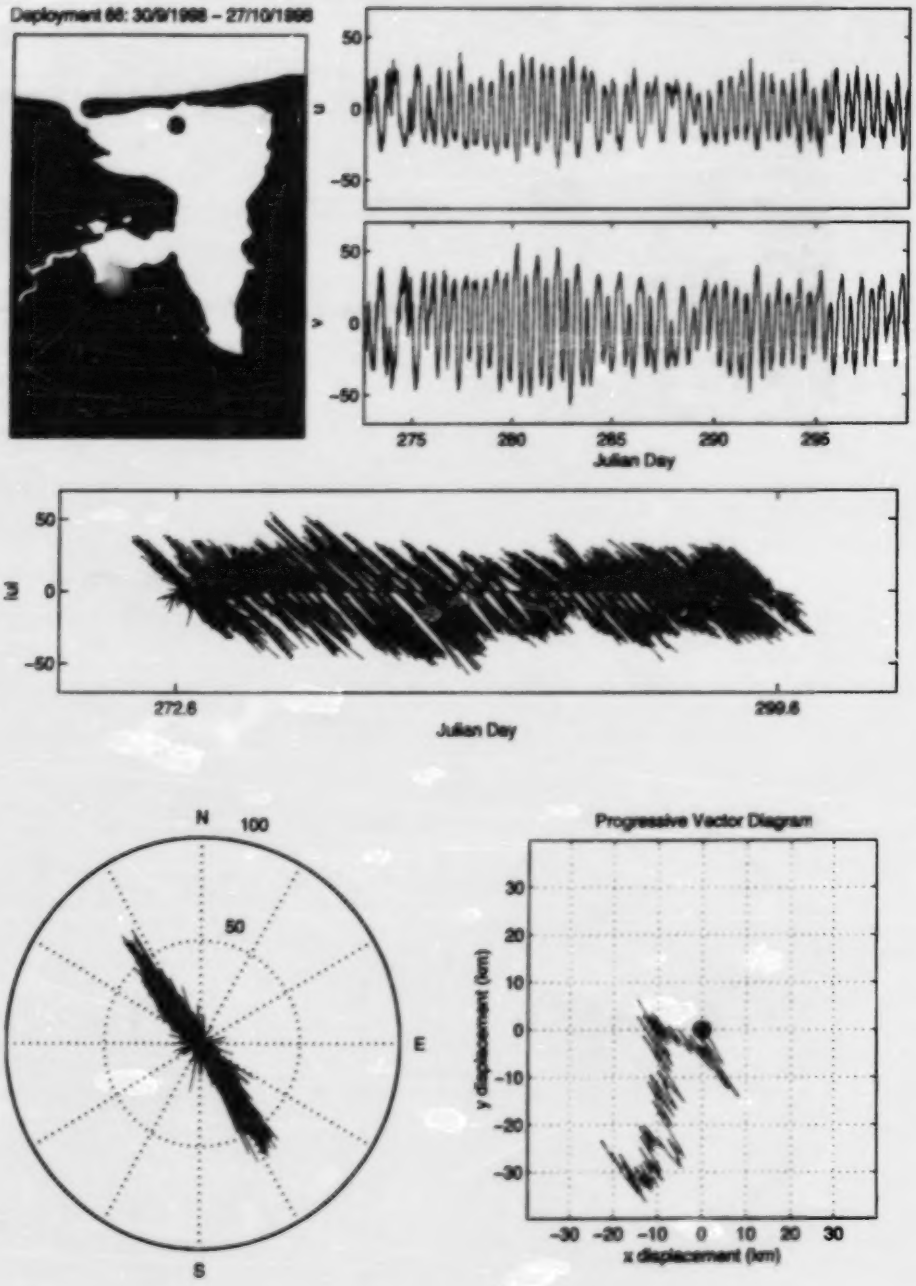

Fig. A.12. Current data for deployment 66.

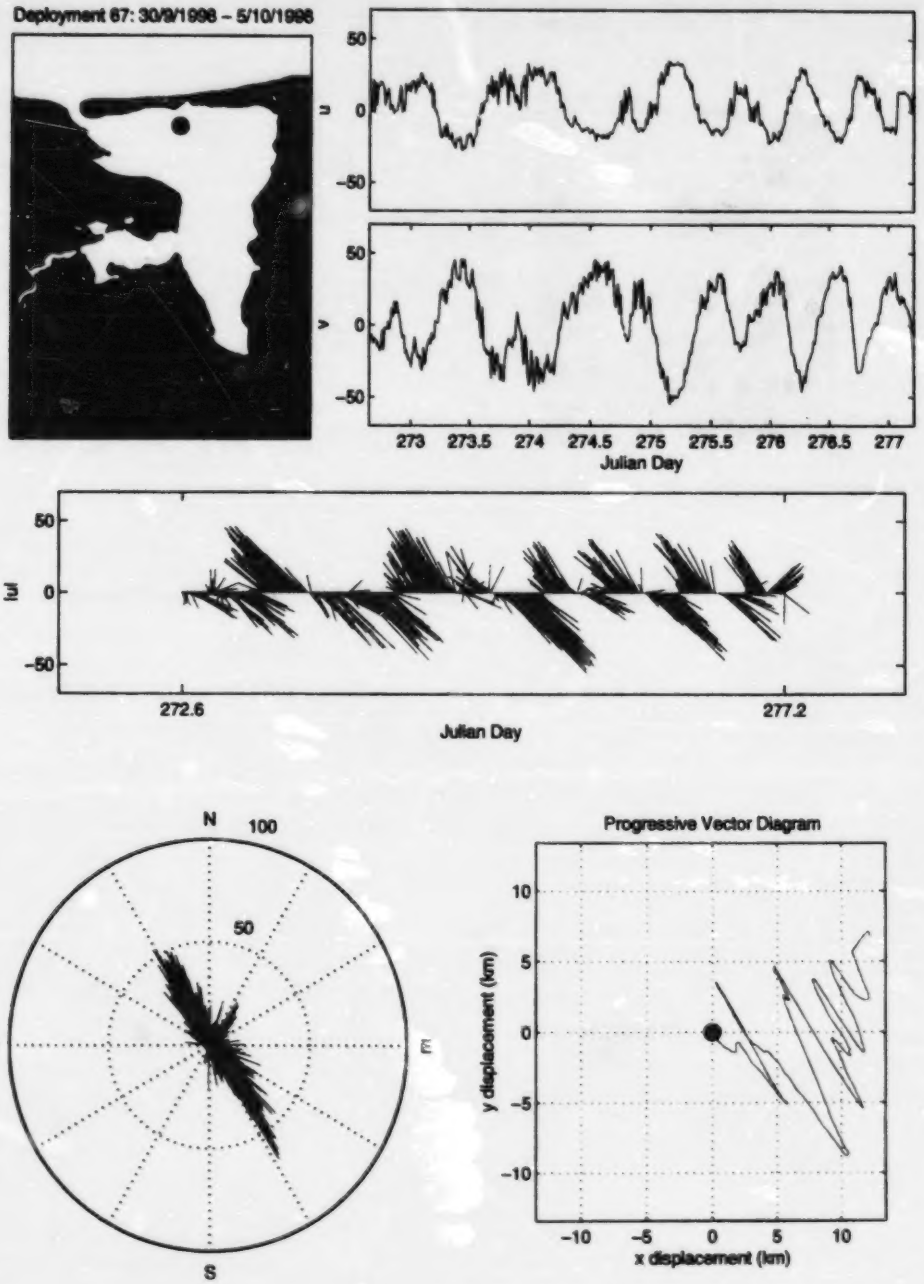

Fig. A.13. Current data for deployment 67.

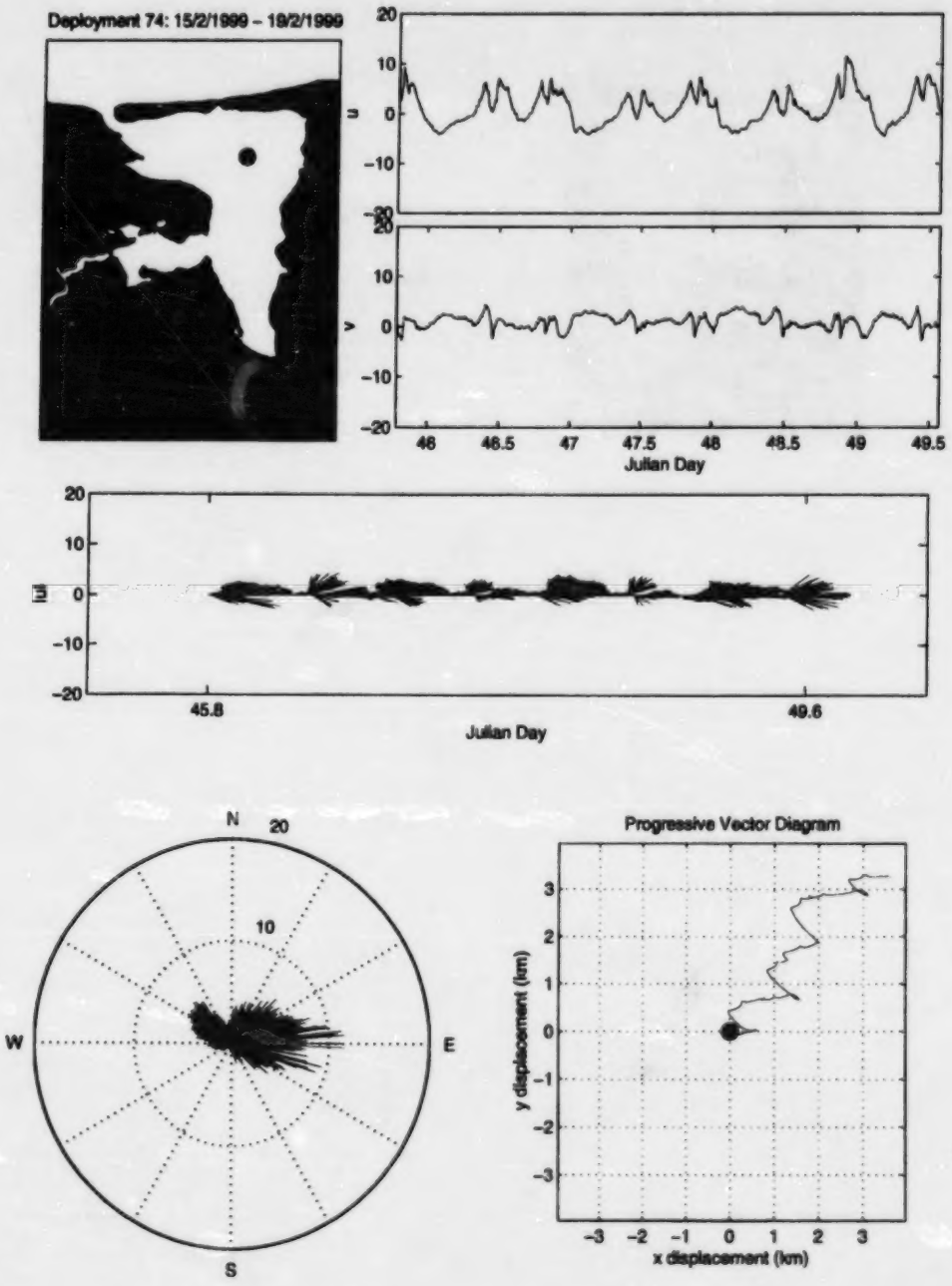

Fig. A.14. Current data for deployment 74.

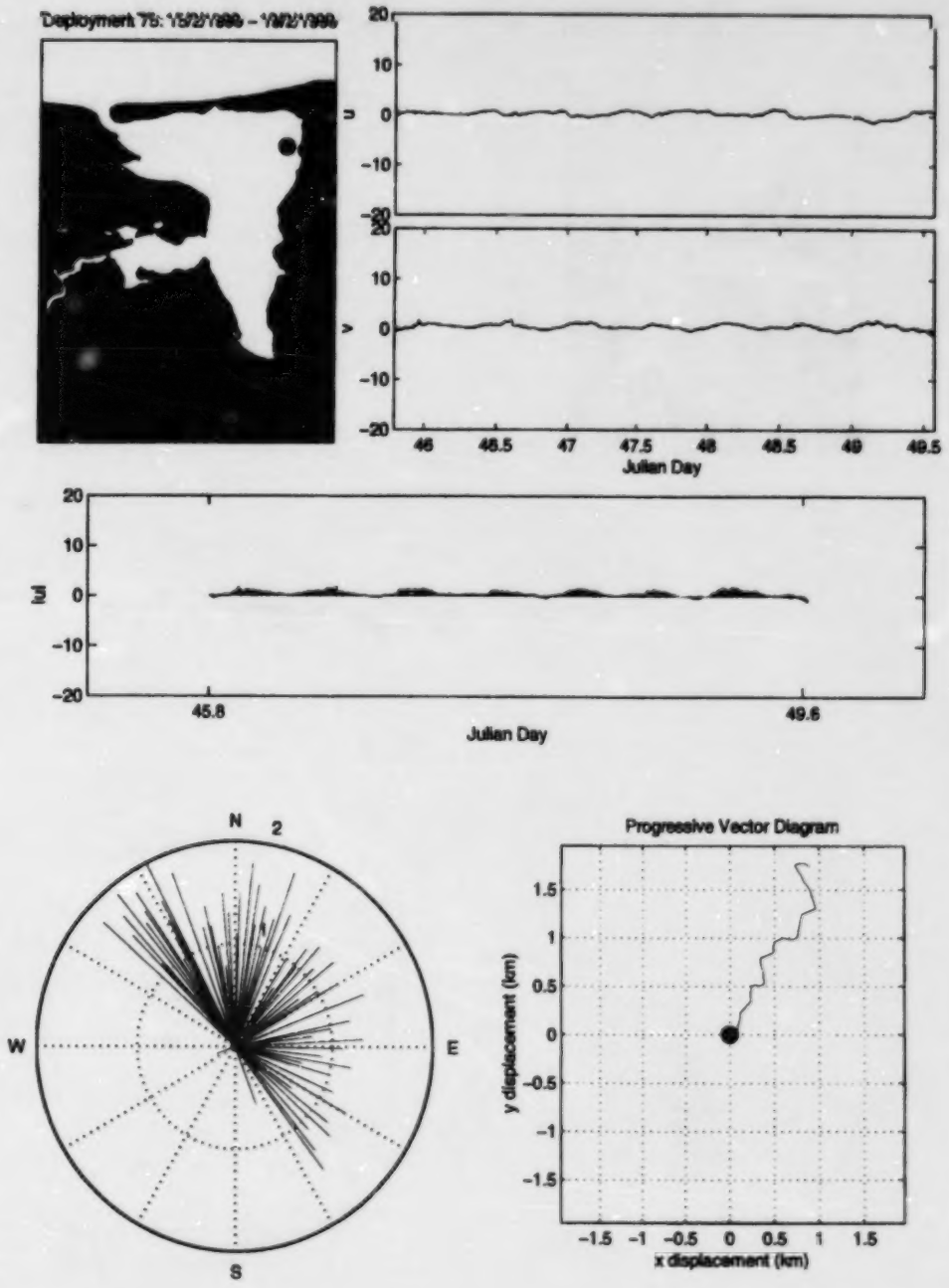

Fig. A.15. Current data for deployment 75.

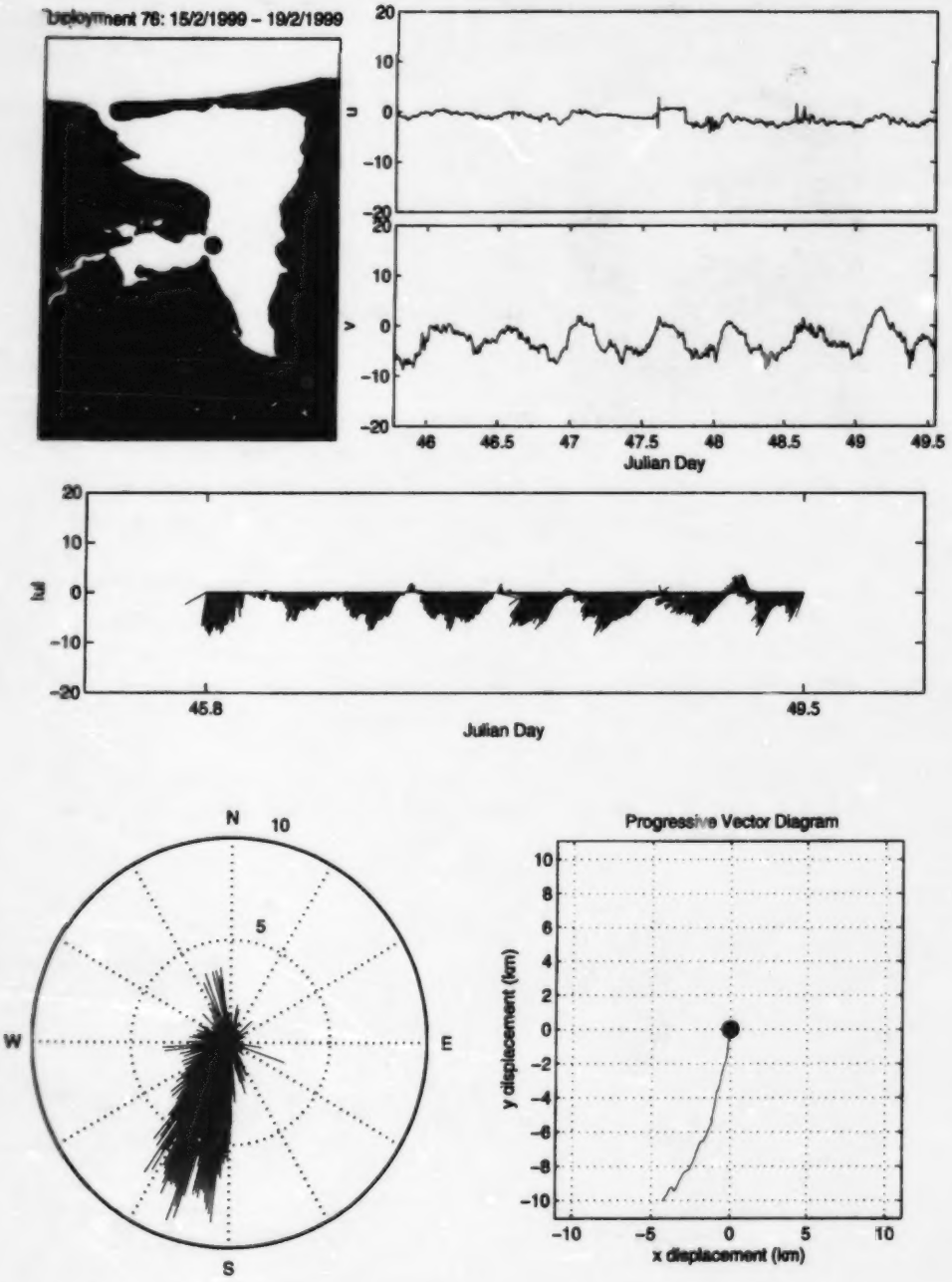

Fig. A.16. Current data for deployment 76.

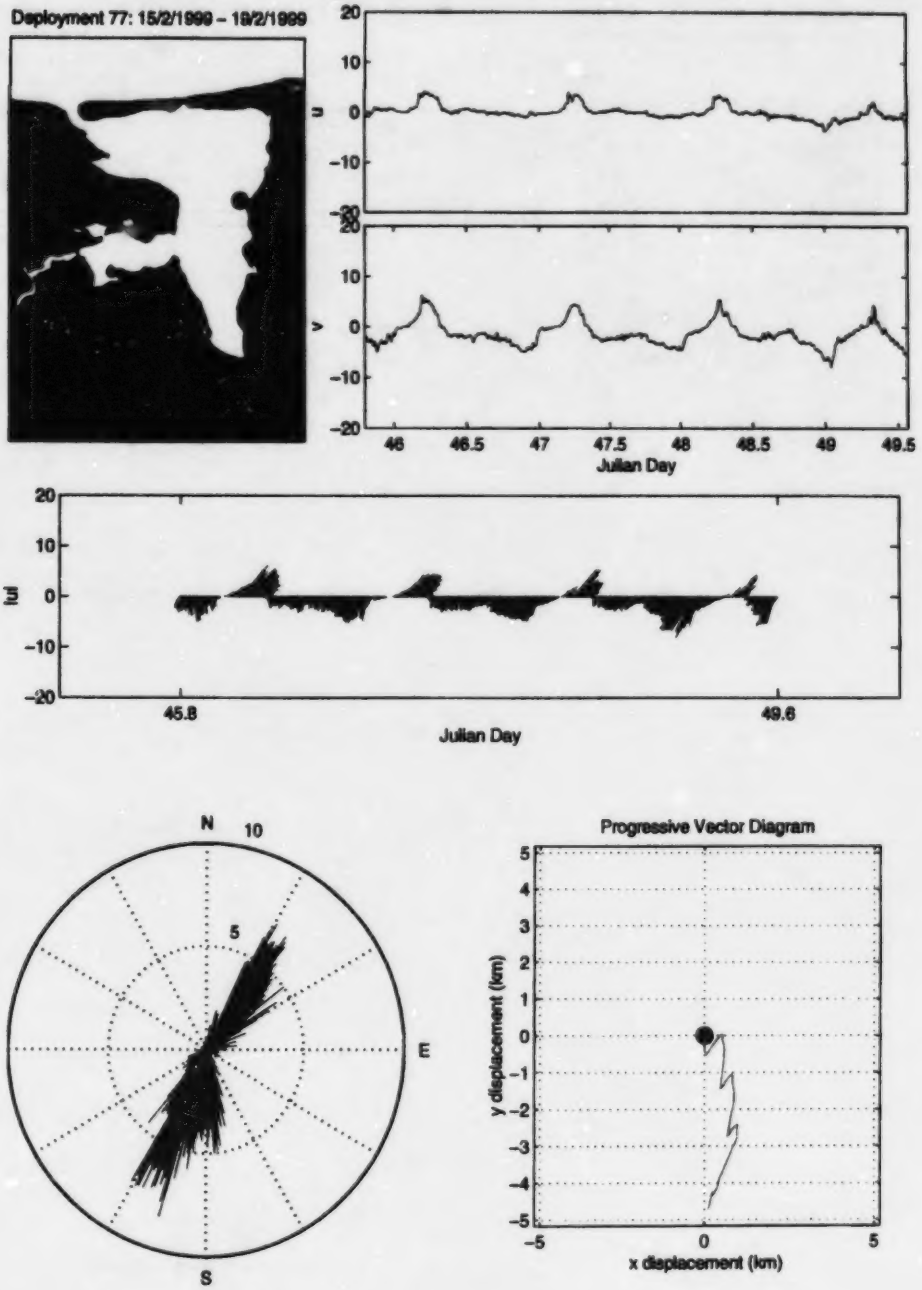

Fig. A.17. Current data for deployment 77.

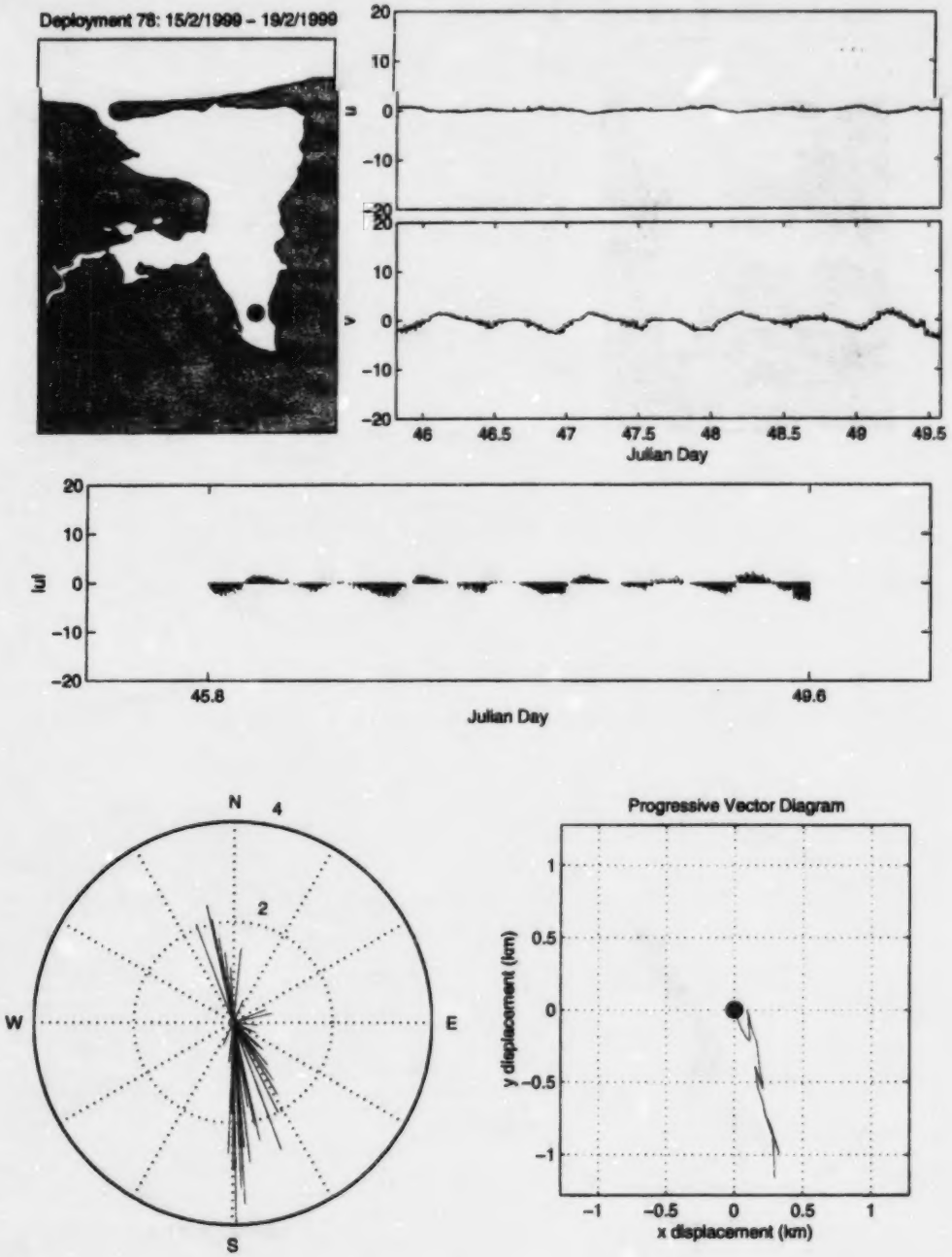

Fig. A.18. Current data for deployment 78.

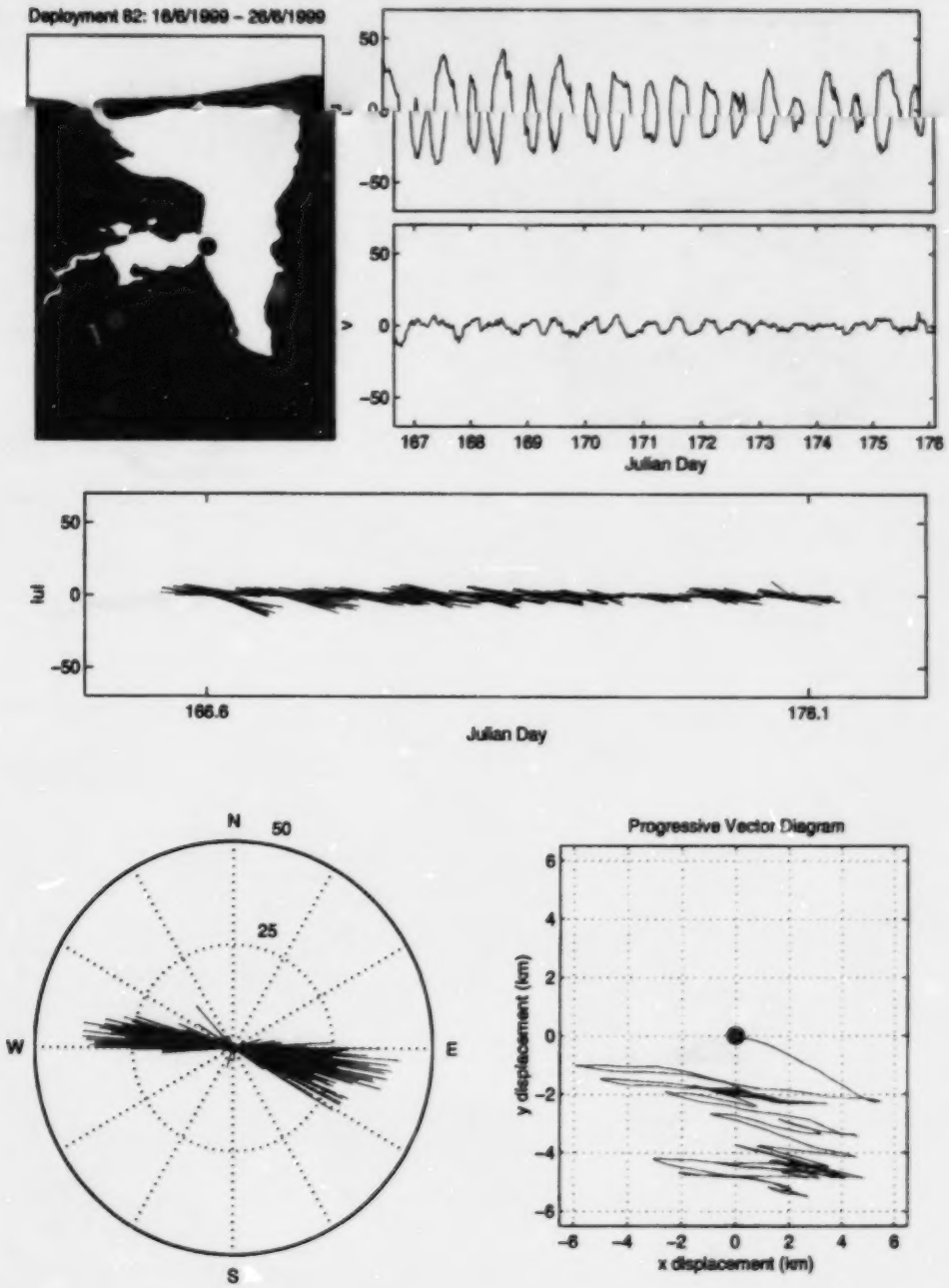

Fig. A.19. Current data for deployment 82.

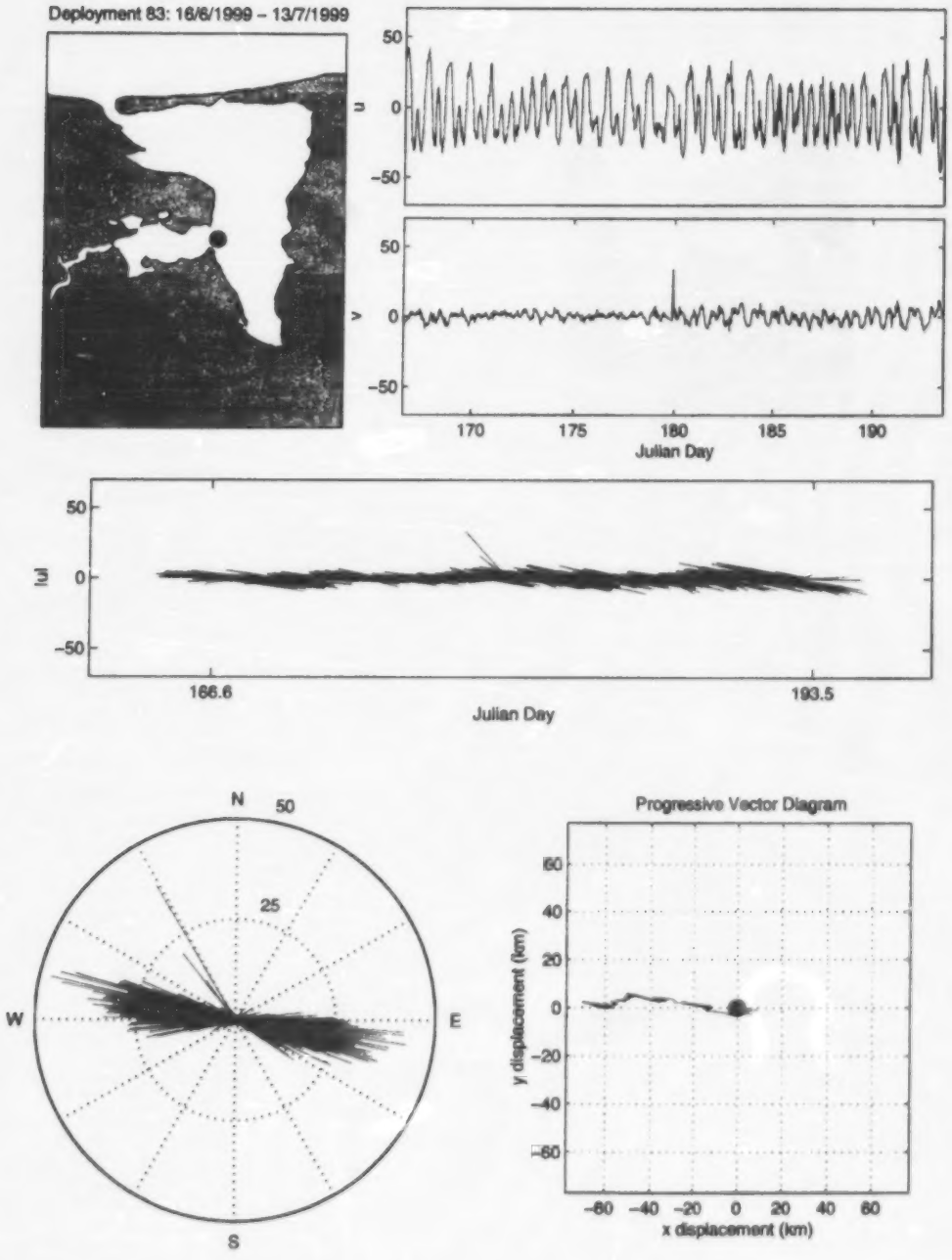

Fig. A.20. Current data for deployment 83.

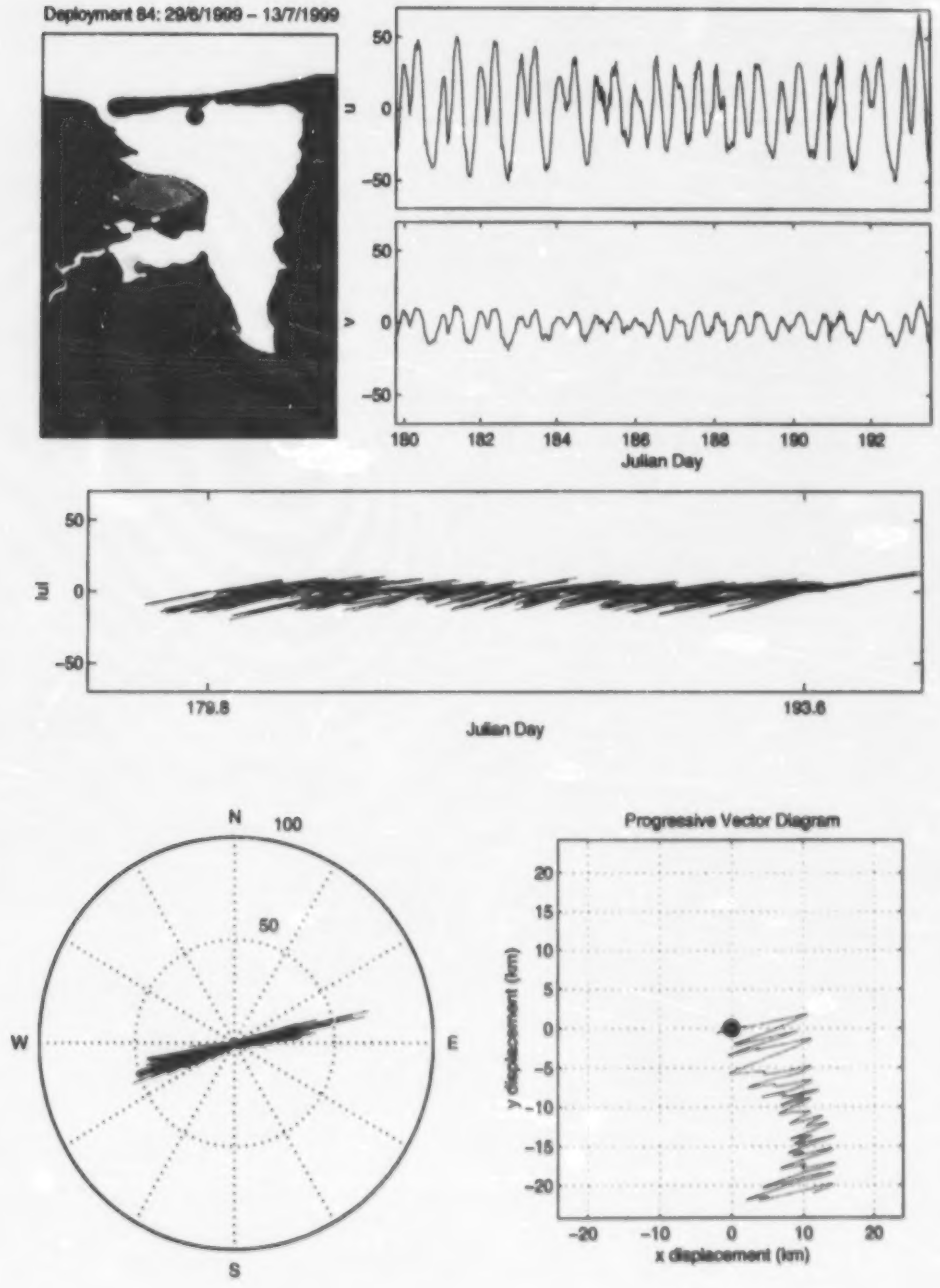

Fig. A.21. Current data for deployment 84.

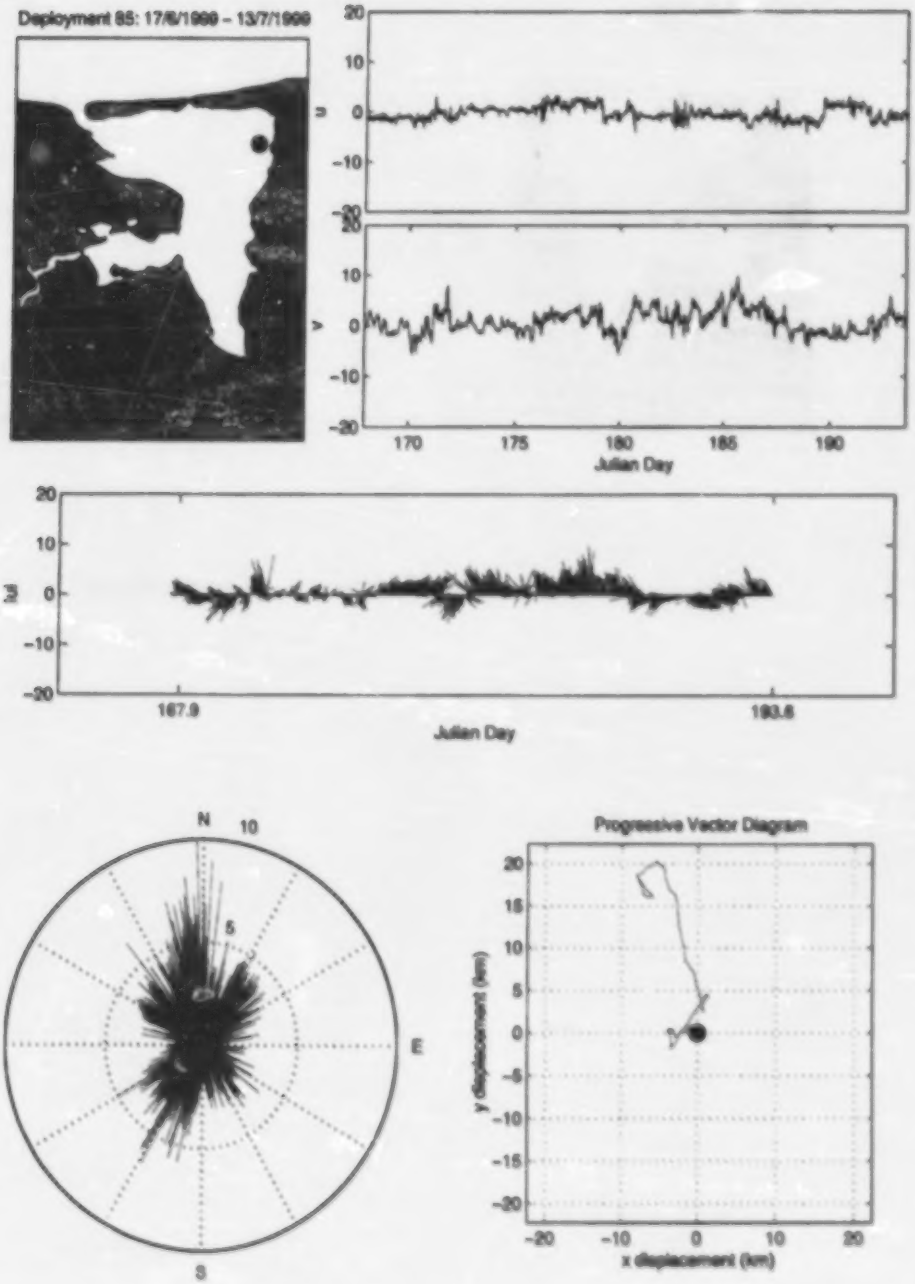

Fig. A.22. Current data for deployment 85.

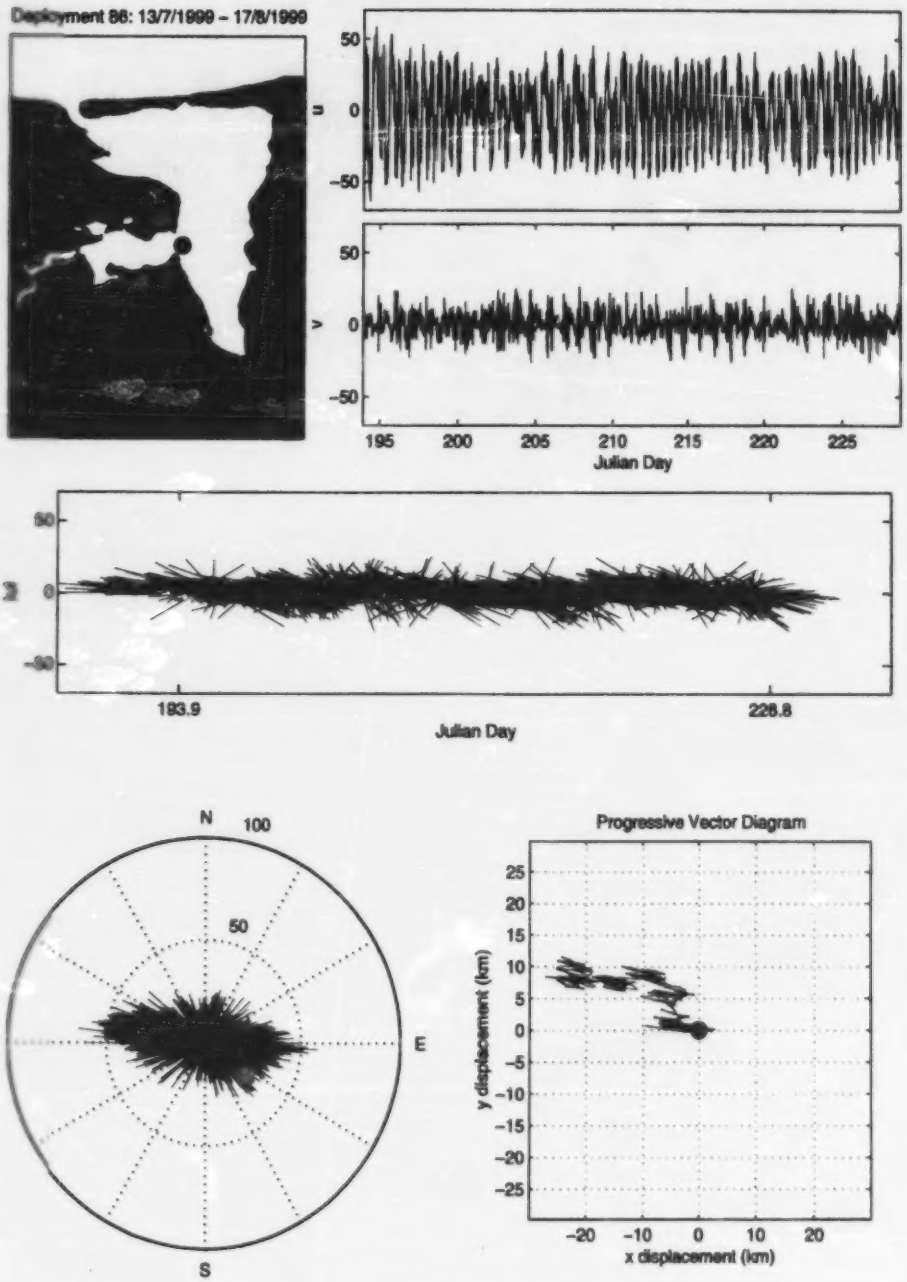

Fig. A.23. Current data for deployment 86.

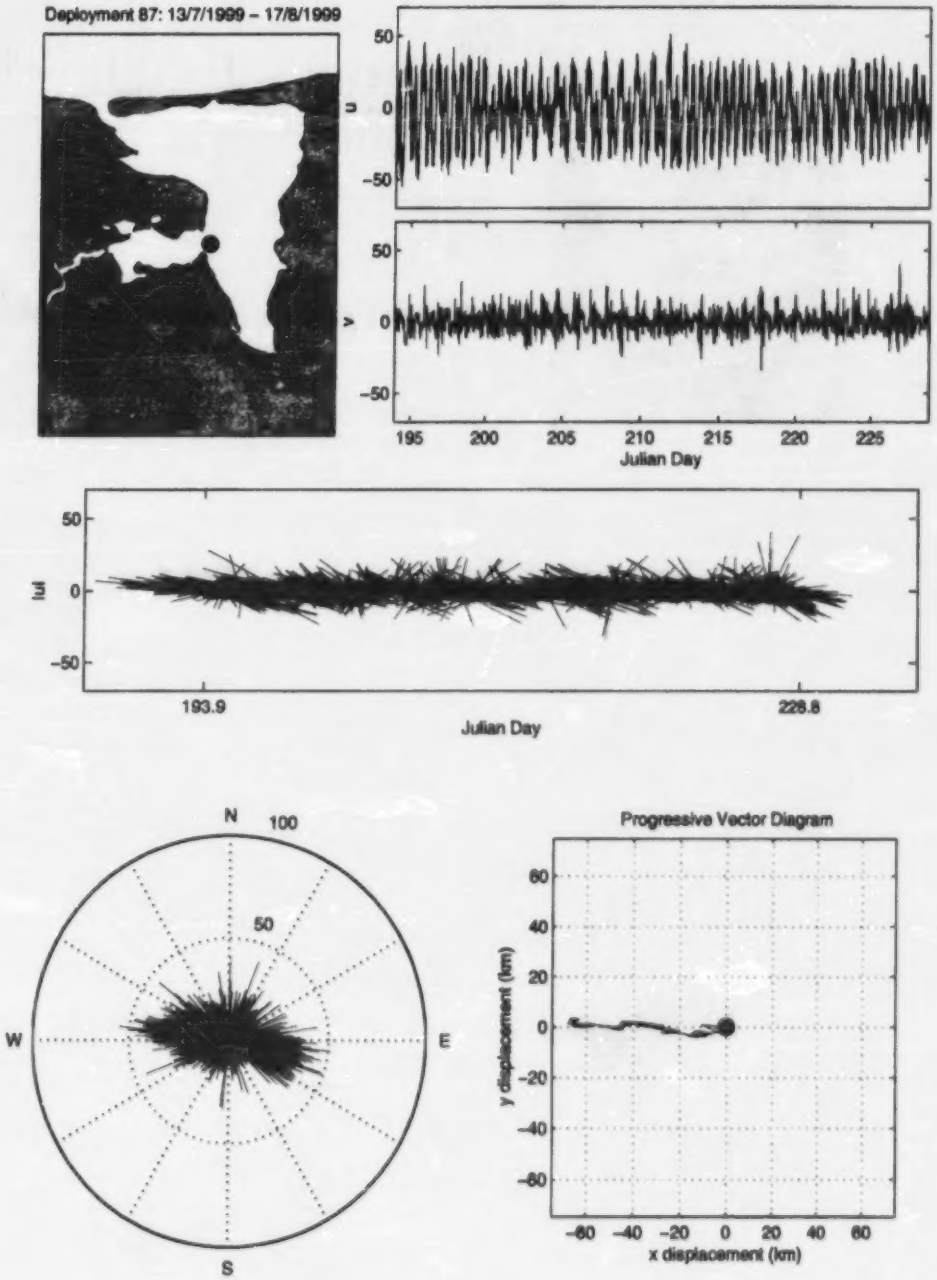

Fig. A.24. Current data for deployment 87.

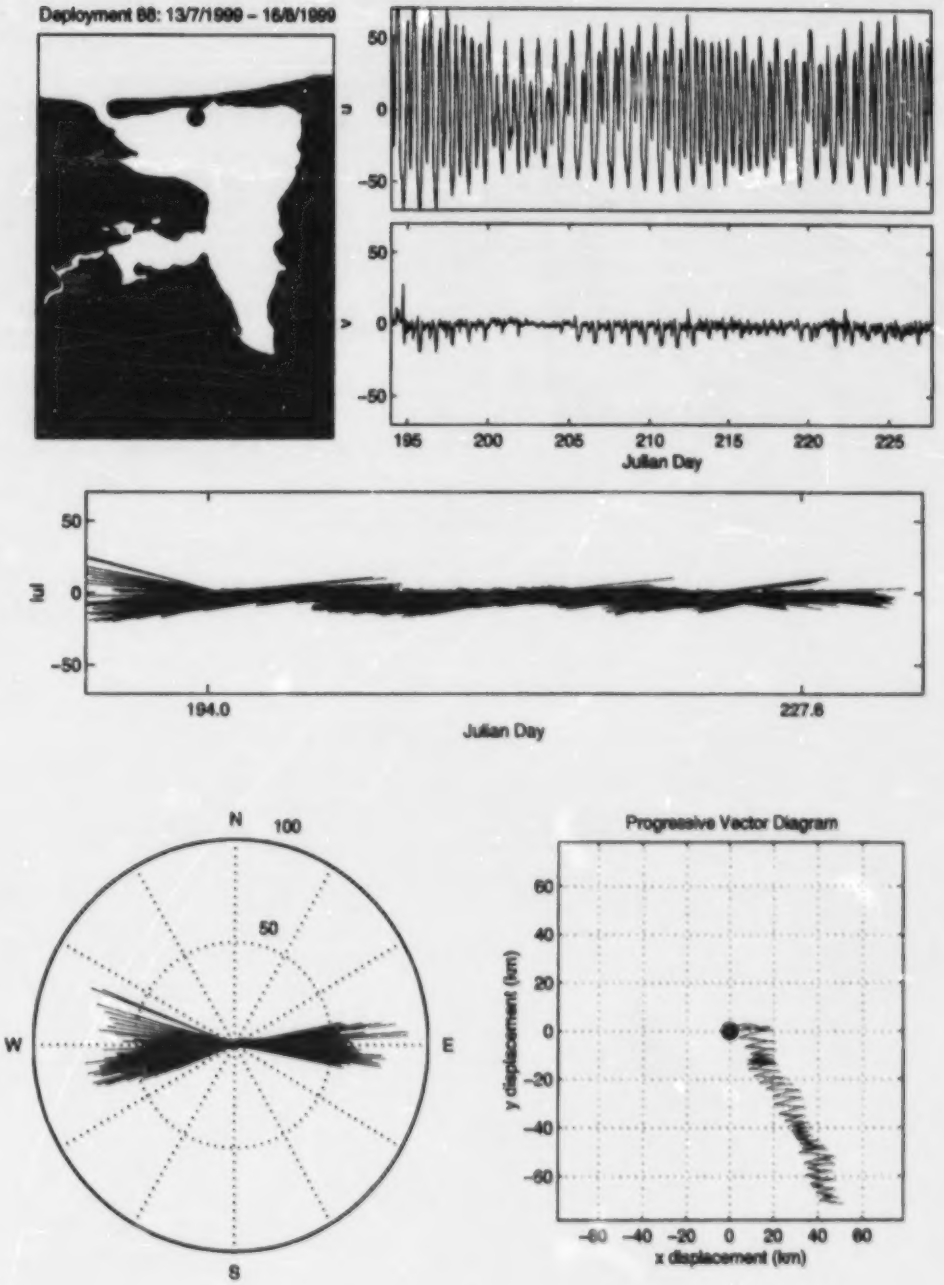

Fig. A.25. Current data for deployment 88.

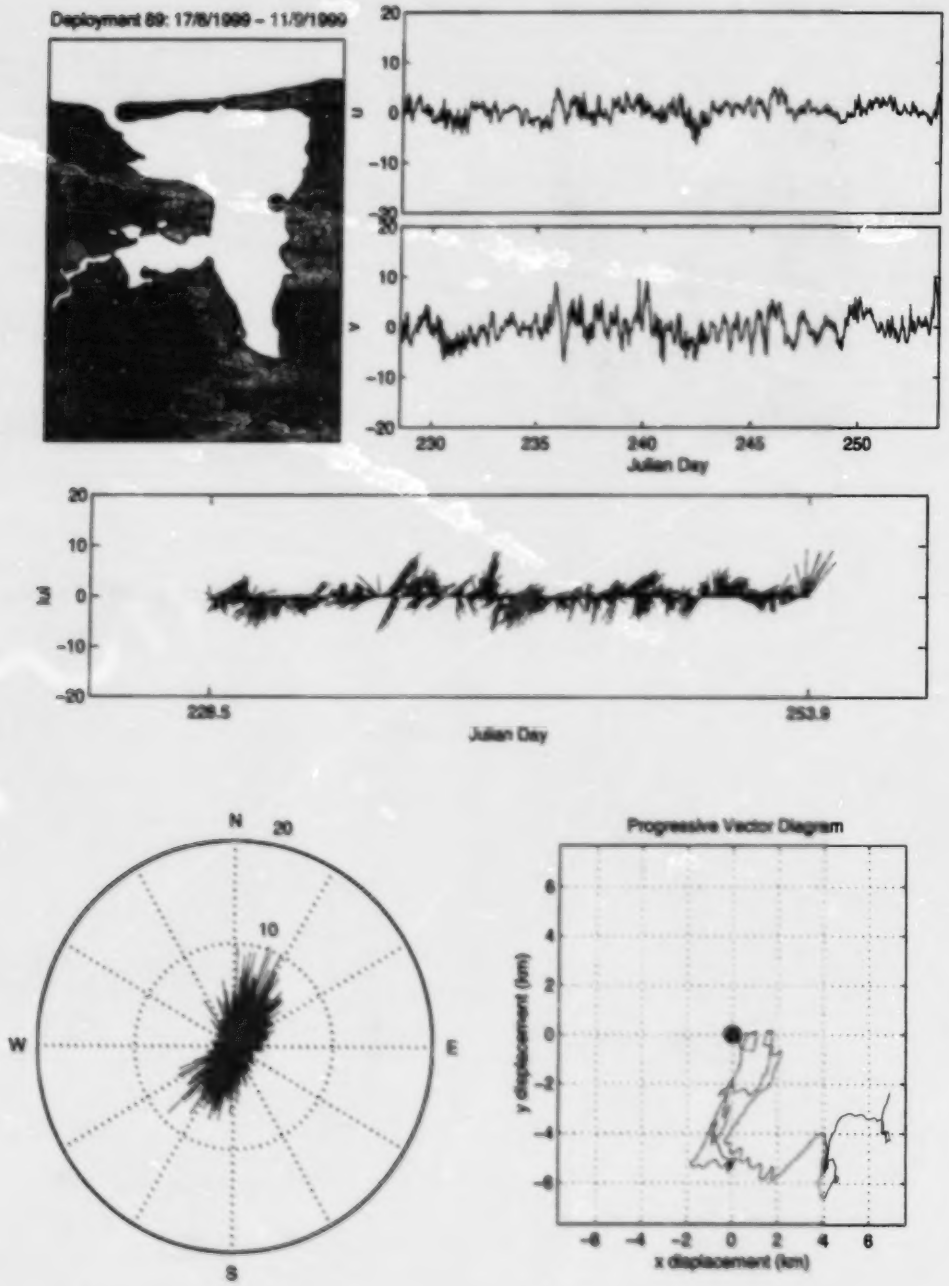

Fig. A.26. Current data for deployment 89.

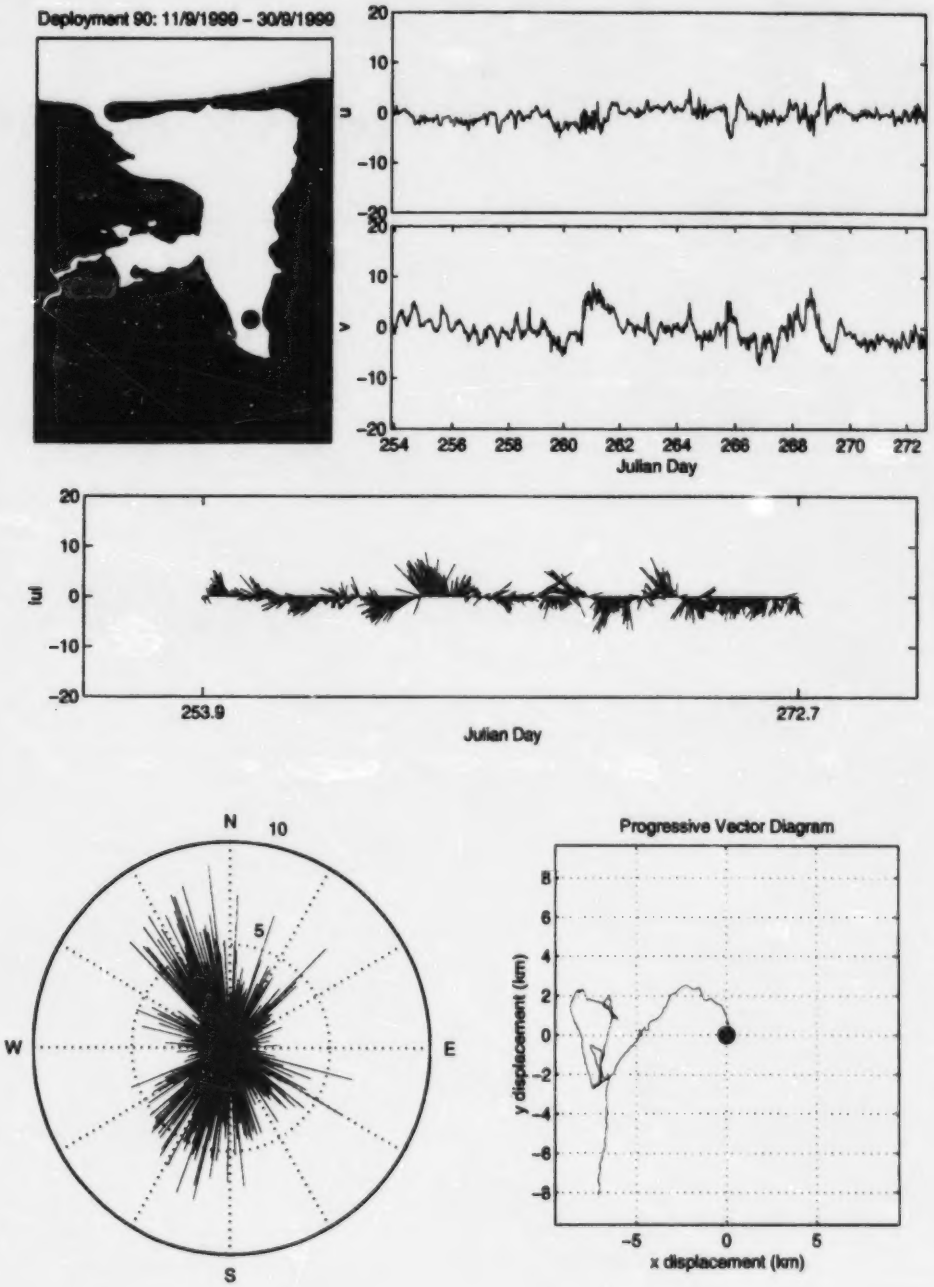

Fig. A.27. Current data for deployment 90.

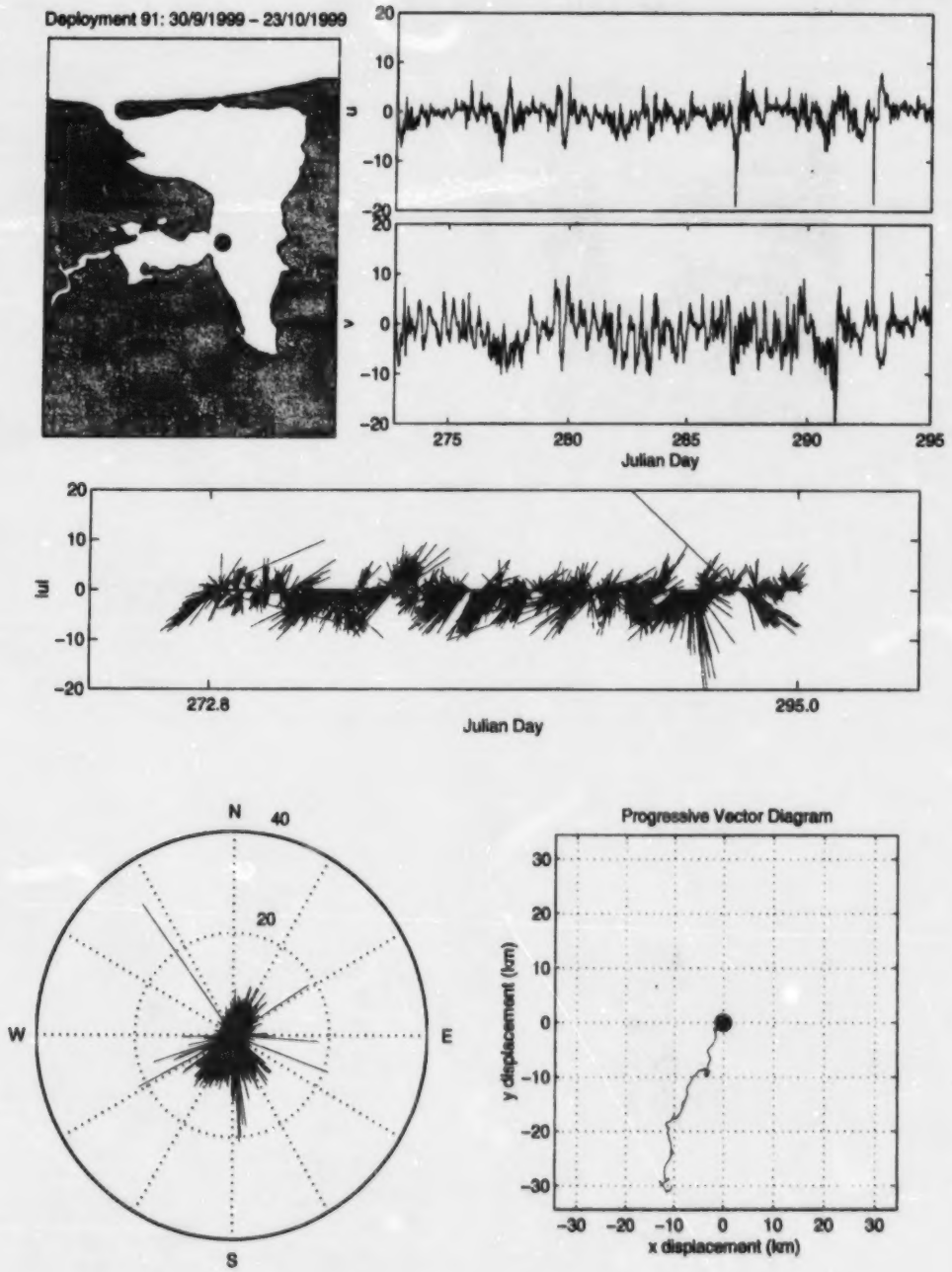

Fig. A.28. Current data for deployment 91.

Appendix B

Vector Wind Data

This appendix contains plots of wind data obtained from meteorological station deployed at Tracadie Bay in 1998 and 1999. Note that the height of the anemometer above ground level is about 3m. For each of the 1998 and 1999 deployments the following information is displayed (left to right, top to bottom):

- Map of Tracadie Bay showing the location of the meteorological station,
- Rose plot showing the distribution of the speed and direction of the wind (independent of time),
- East-west (u) component of the wind velocity vector. This is in meteorological convention (i.e. the direction that the wind is coming from),
- North-south (v) component of the wind velocity vector. This is in meteorological convention (i.e. the direction that the wind is coming from),
- Stick plot of the velocity vector time series in meteorological convention.

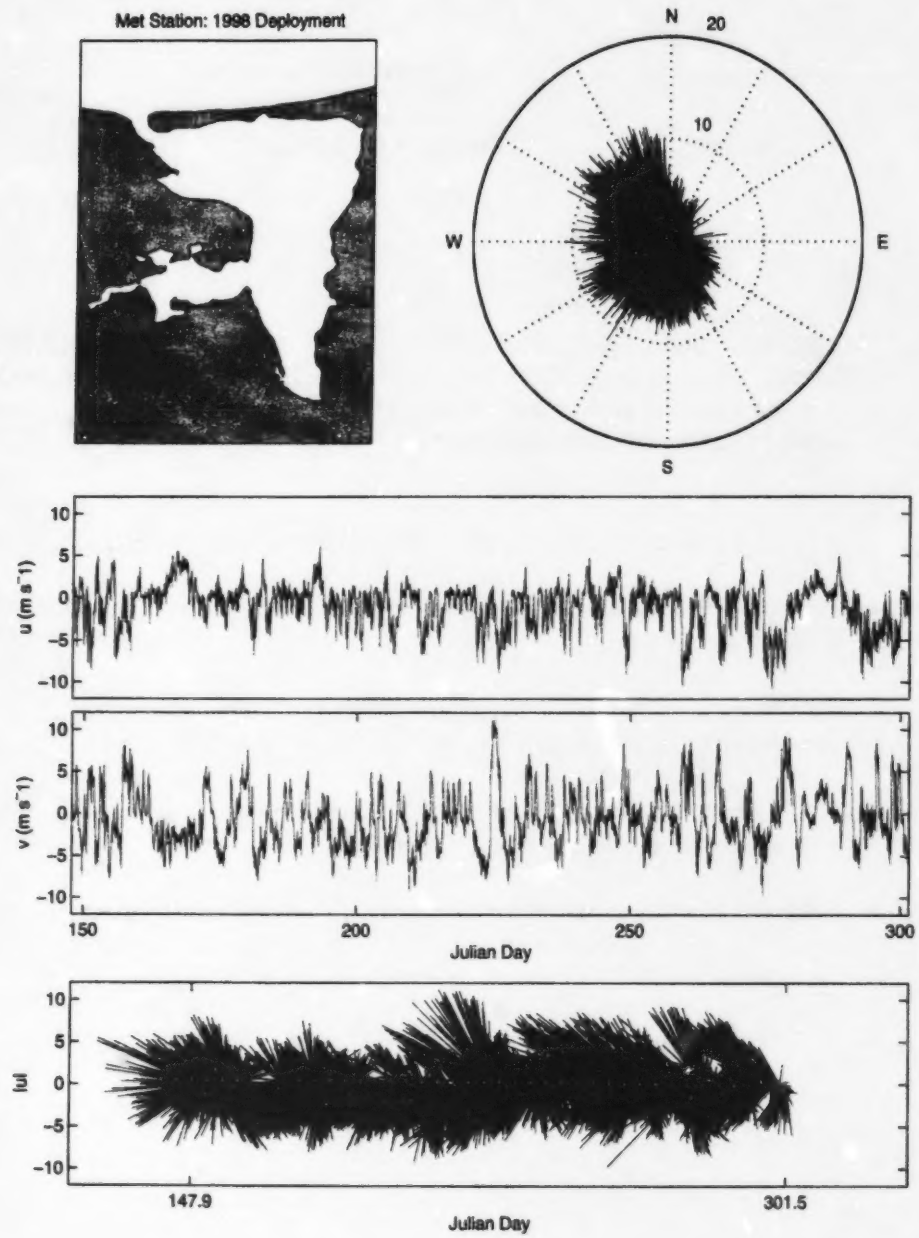

Fig. B.1. Wind observations from 1998.

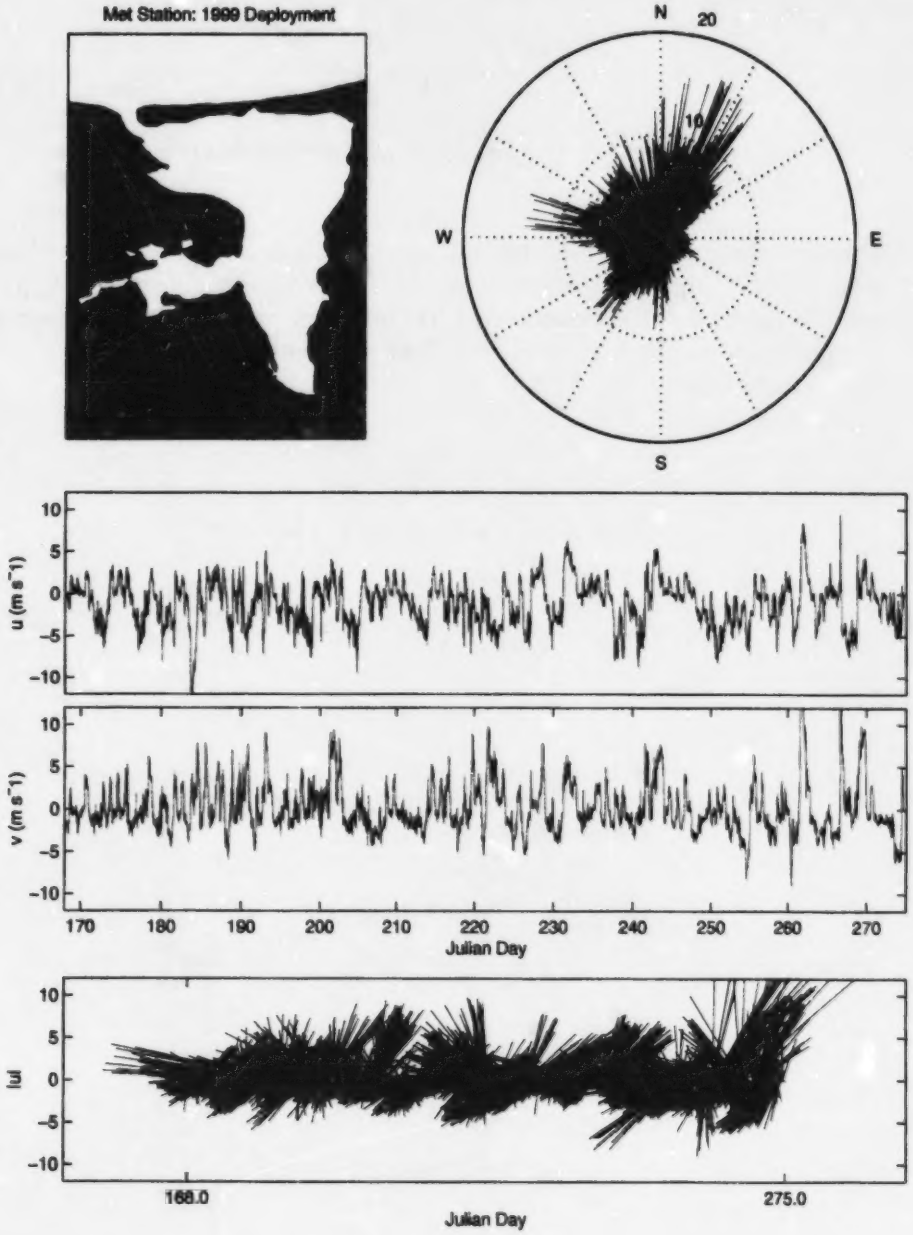

Fig. B.2. Wind observations from 1999.

Appendix C

Under-Ice Deployment of Current Meter Array

This appendix shows data recorded by a current meter array deployed under the ice in the winter of 1999. Fig. C.1 shows the locations of the five current meters and a plot of the sea level during the deployment period. The remaining pages show a time sequence of hourly snapshots of the current vectors. These snapshots are referenced to the sea level time series as indicated by the dot.

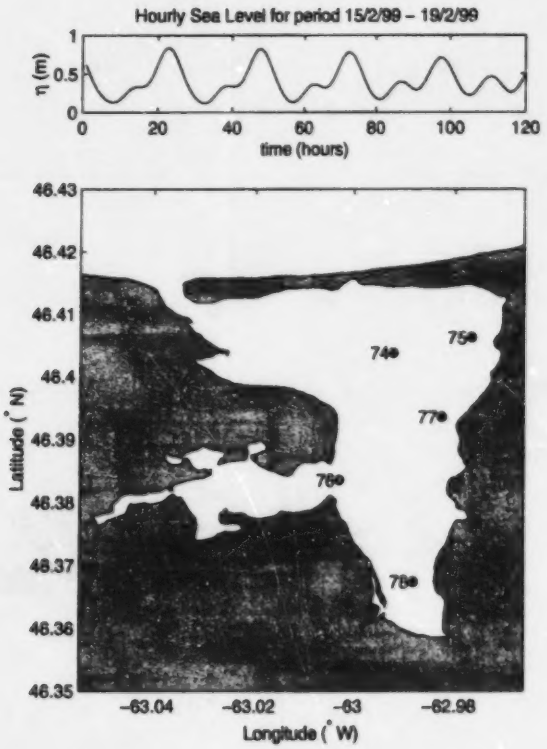

Fig. C.1. The under-ice current meter array. The lower panel shows locations of the 5 current meters in Tracadie Bay. The upper panel shows the predicted hourly sea for the deployment period 15/2/99 - 19/2/99.

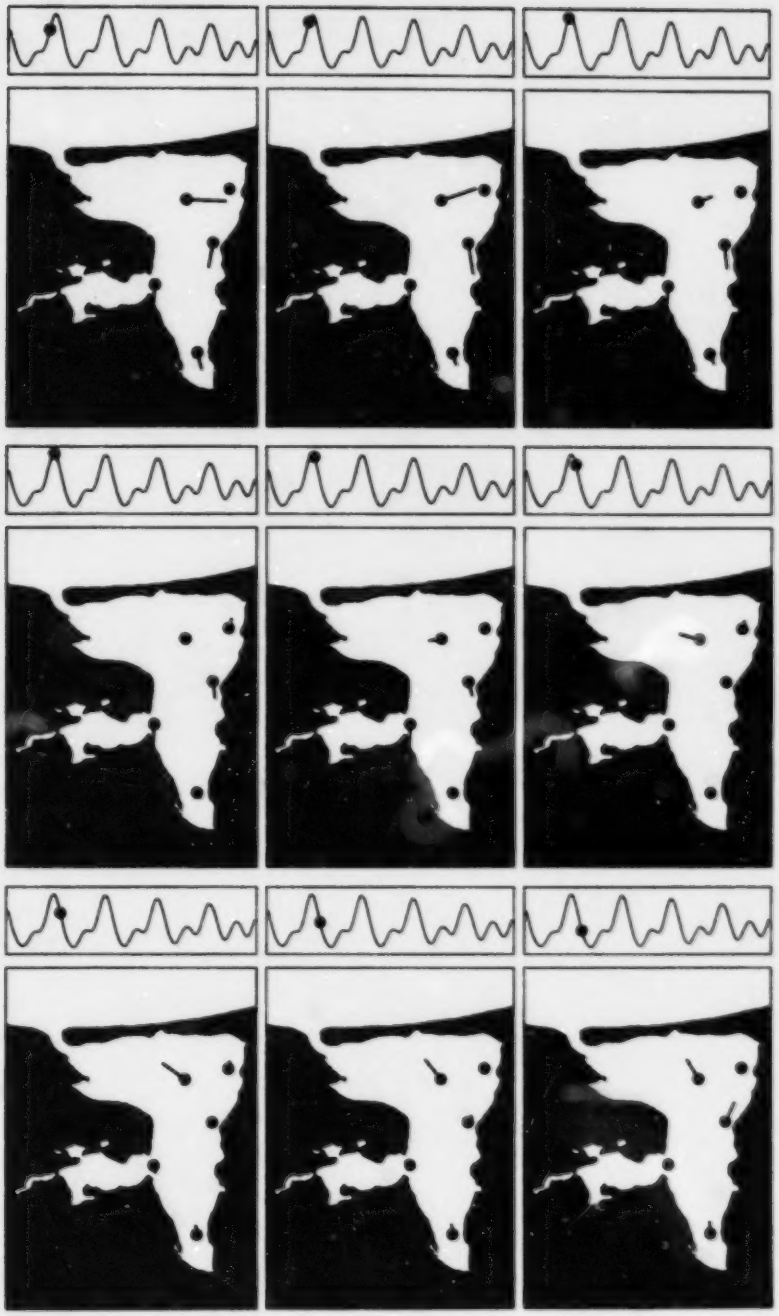

Fig. C.2. Hourly snapshots of current vector from under-ice array.

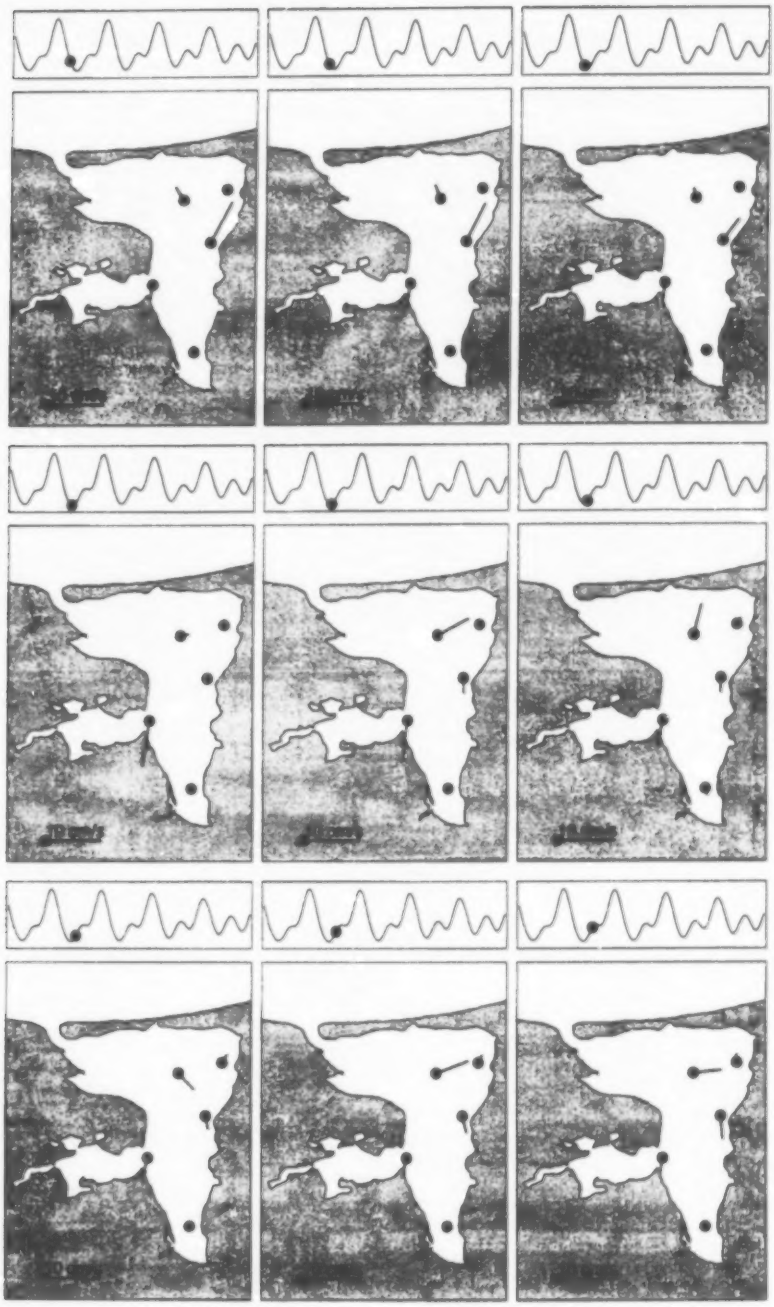

Fig. C.2. continued

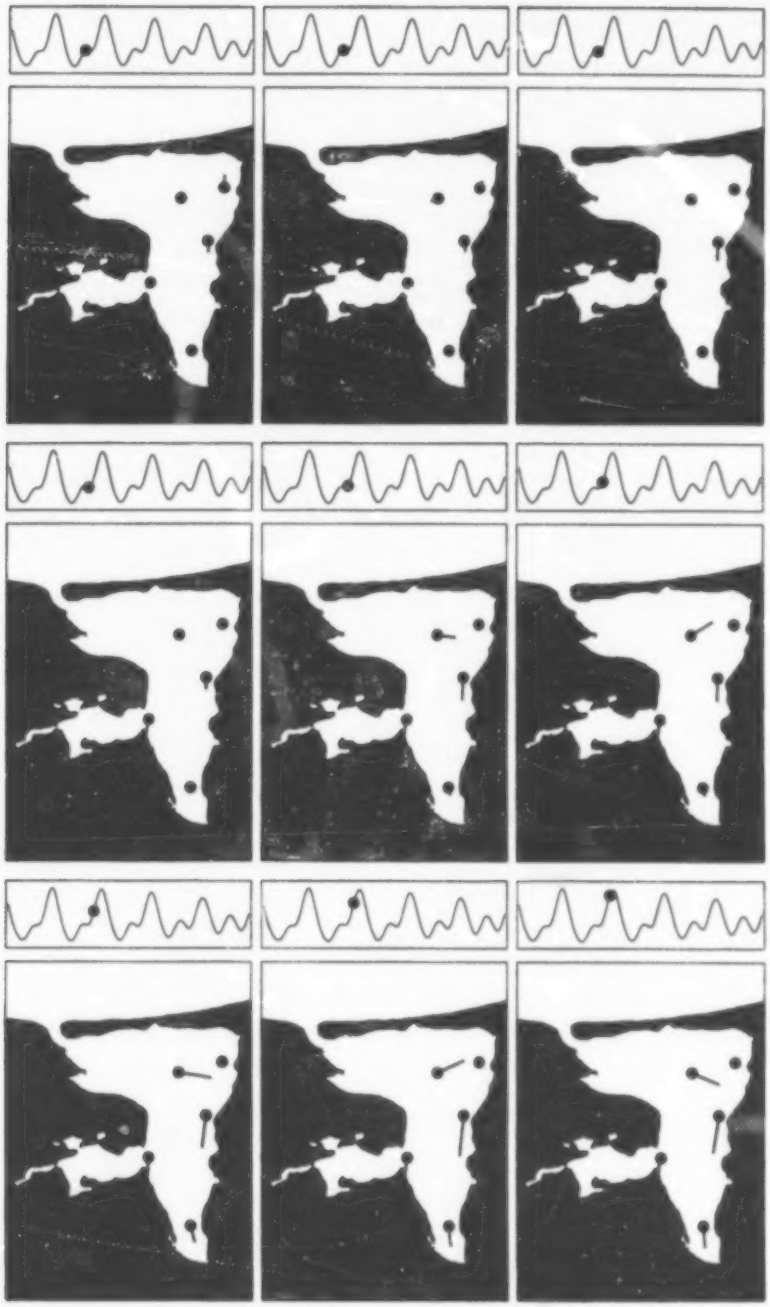

Fig. C.2. continued

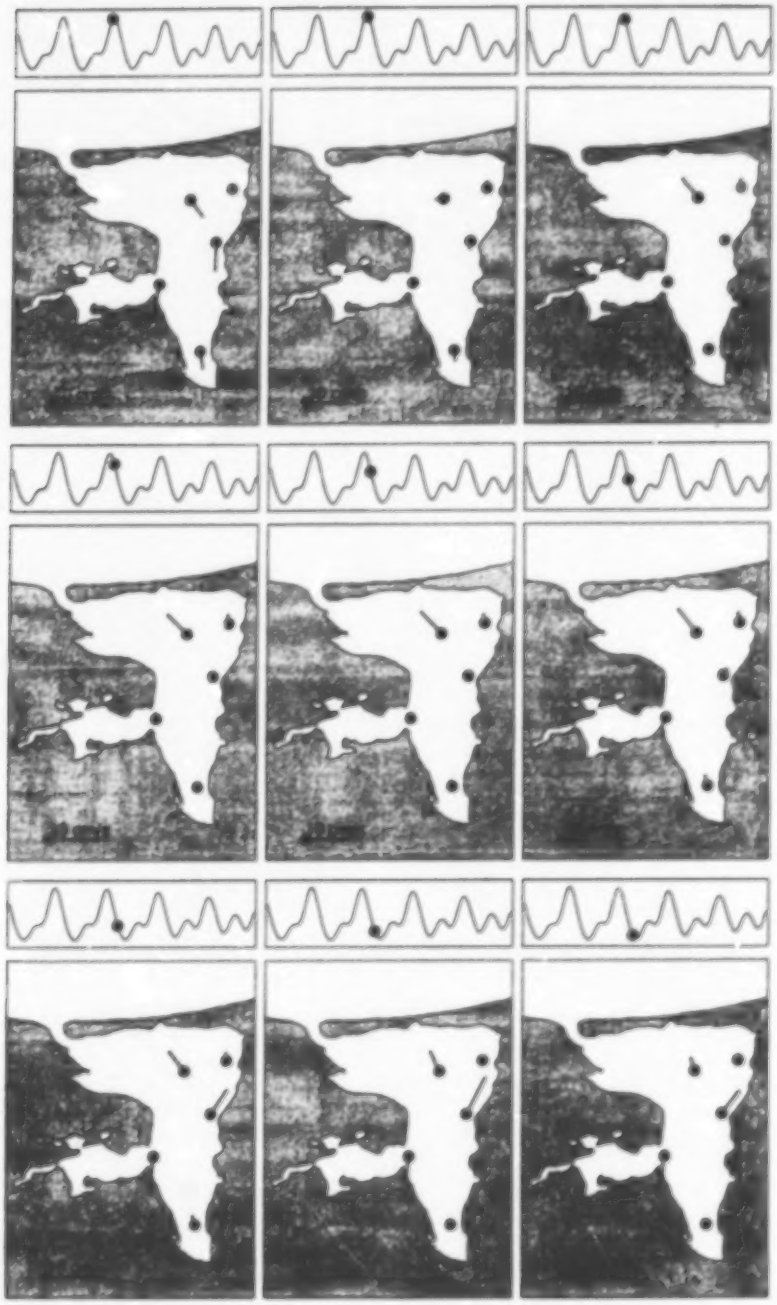

Fig. C.2. continued

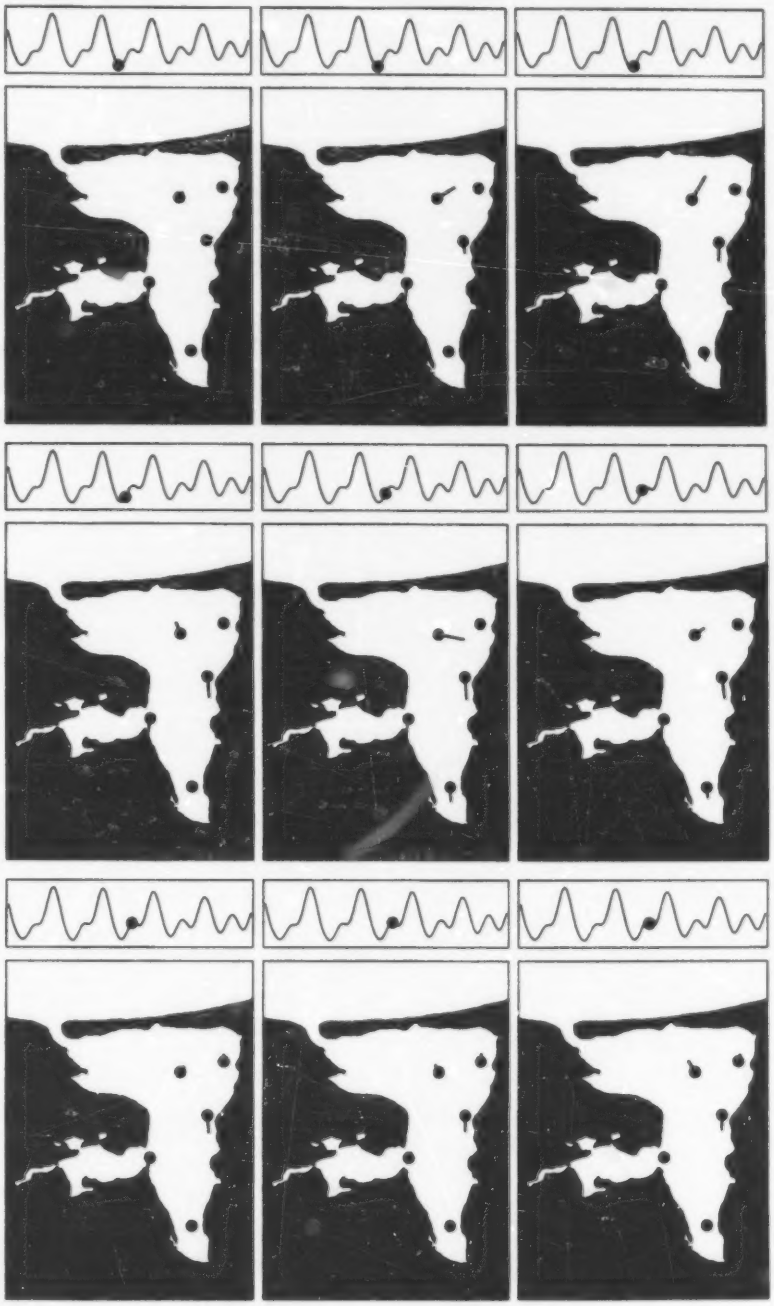

Fig. C.2. continued

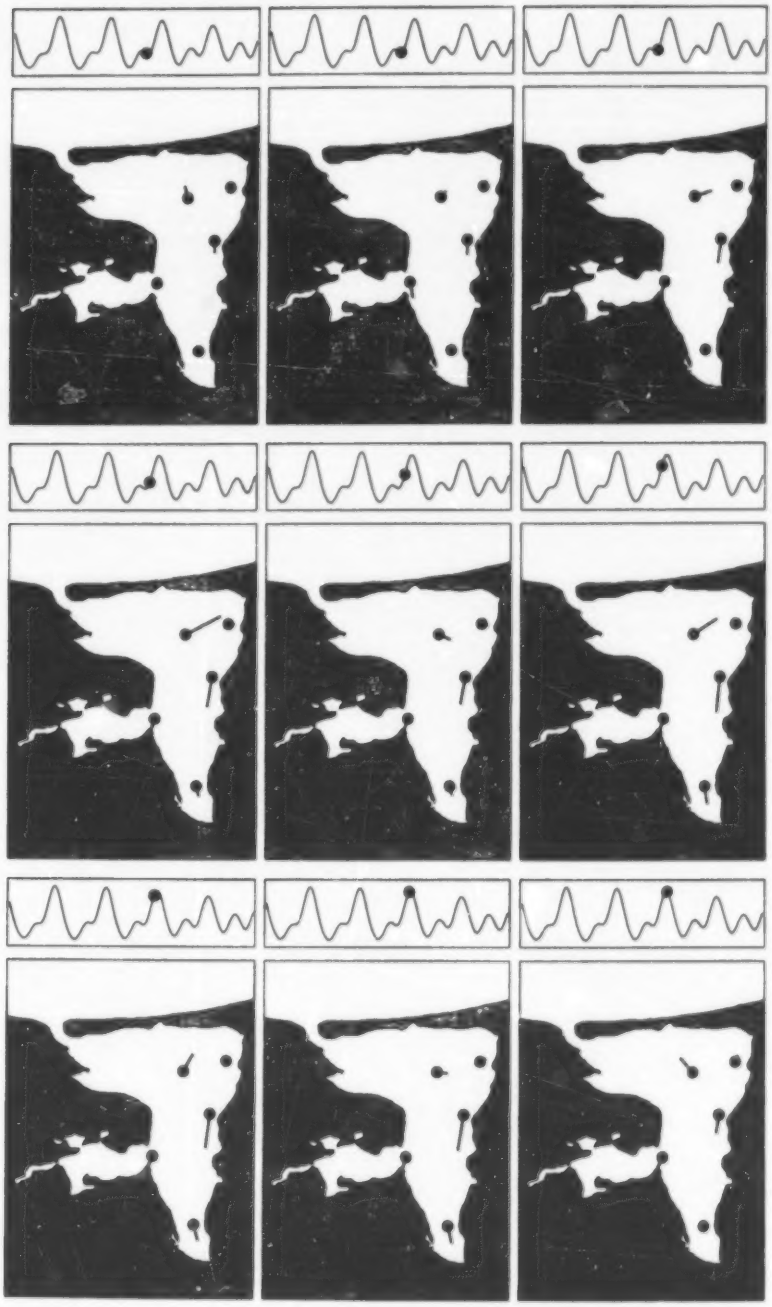

Fig. C.2. continued

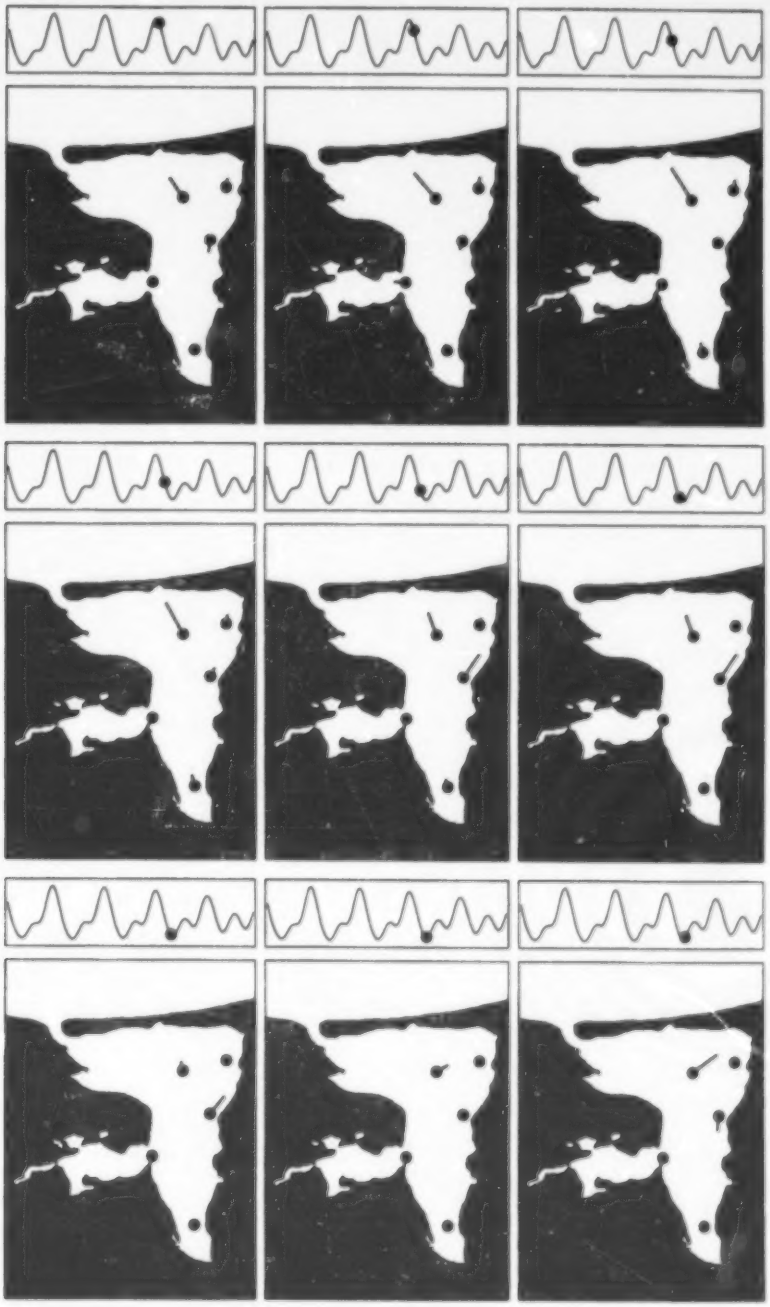

Fig. C.2. continued

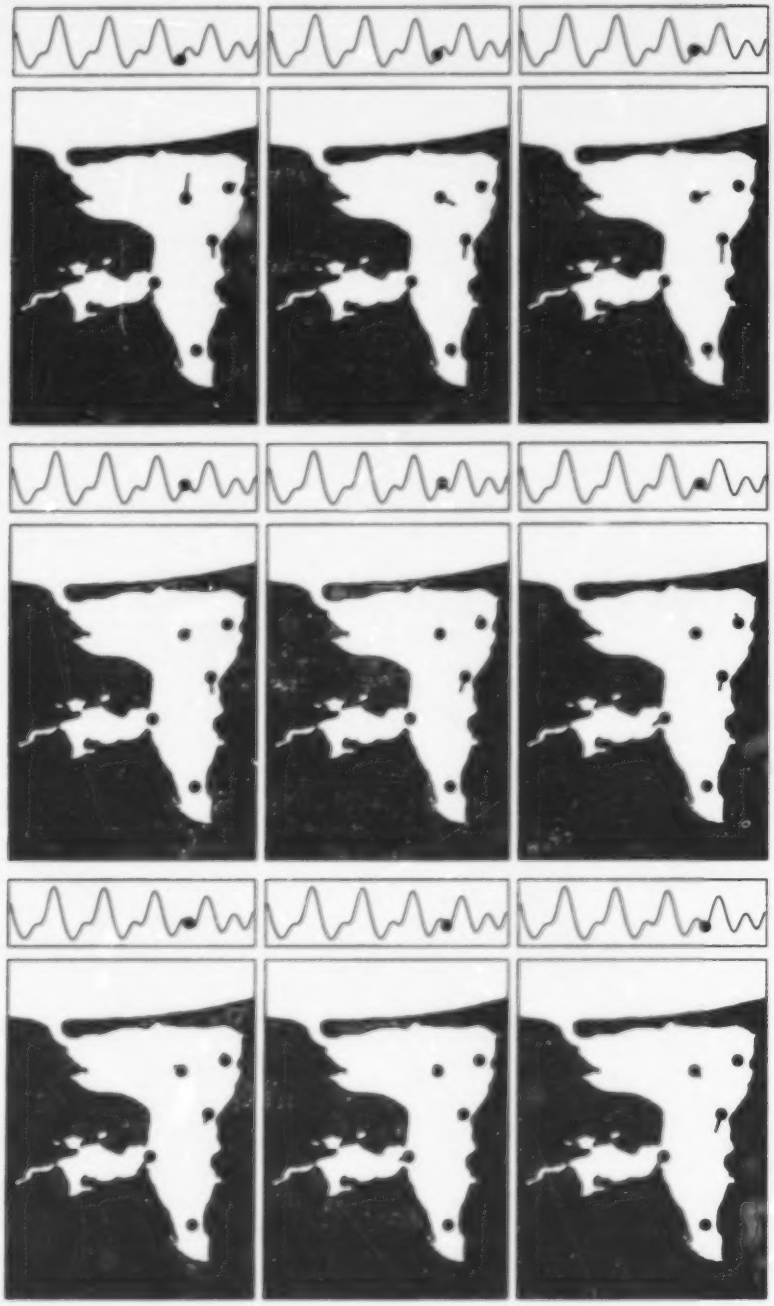

Fig. C.2. continued

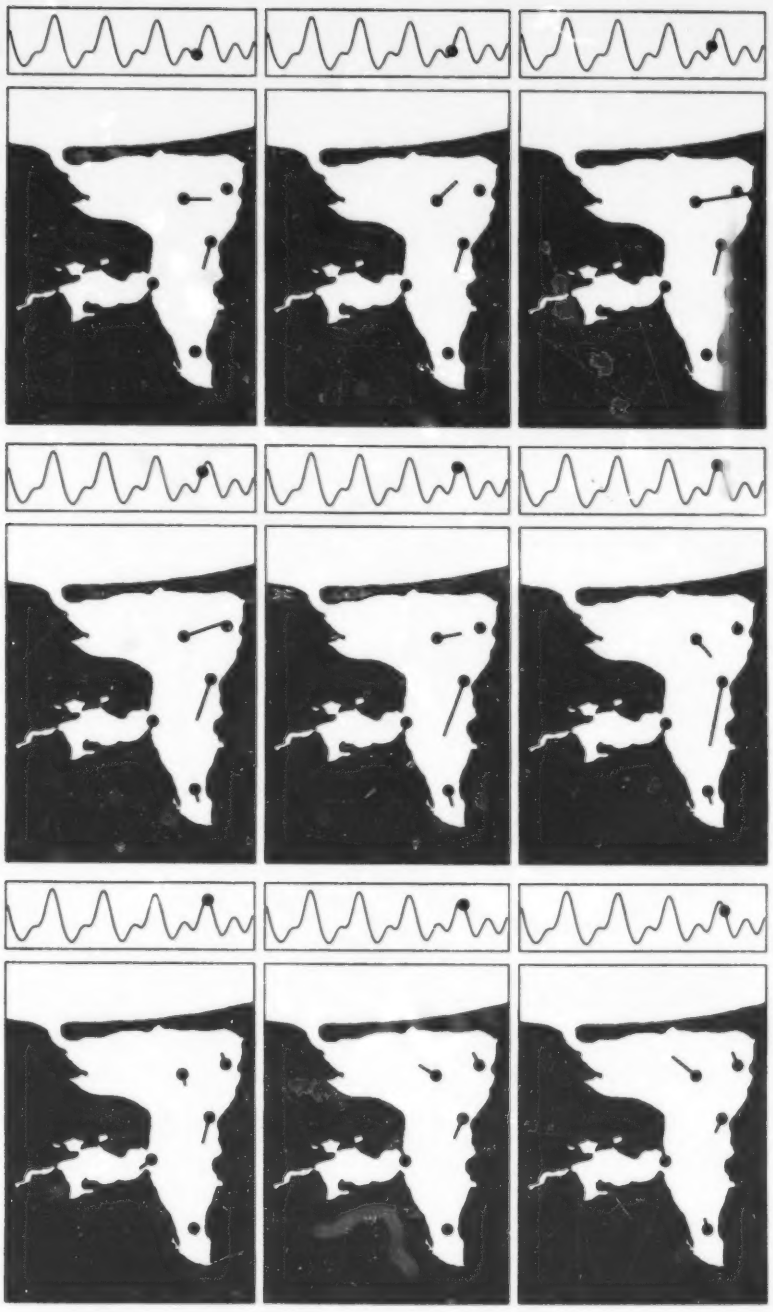

Fig. C.2. continued

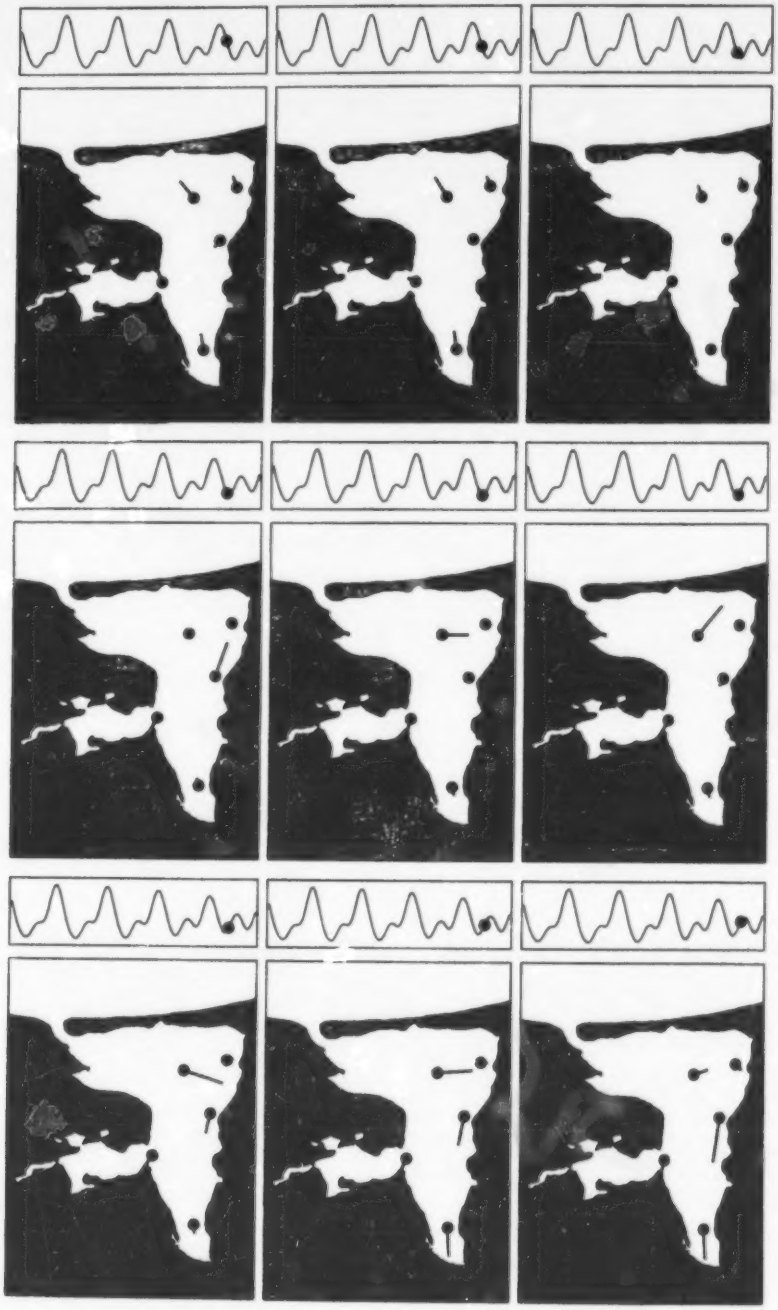

Fig. C.2. continued

Appendix D

Depth-Averaged Currents from ADCP Transects

This appendix shows the depth-averaged currents recorded by a boat-mounted acoustic Doppler current profiler. These data have been quality controlled by de-spiking and removing gross positional errors. They have also been (mildly) smoothed. Refer to the text for details of this processing. Each of the following panels corresponds to a single quasi-continuous deployment period. For each panel, the following information is displayed:

- Time and date of the deployment period,
- Sea level time series with the deployment period highlighted by a thick line,
- A map of Tracadie Bay with superimposed depth averaged currents. The location of the current measurement is given by the dot. The line emanating from that dot represents the current speed and direction. The scaling for the current vector is given in the lower left part of the panel.
- The mean wind speed and direction for the deployment period are given by u_w and θ_w

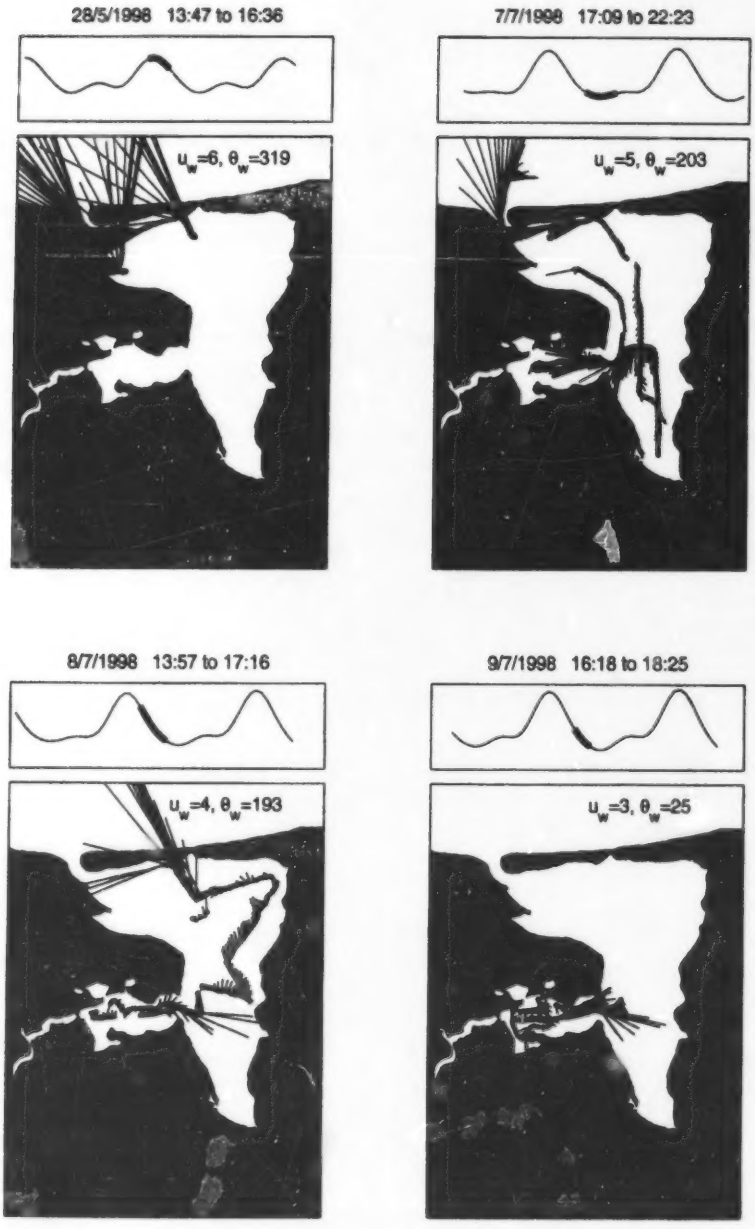

Fig. D.1. Depth-averaged currents from the boat-mounted ADCP.

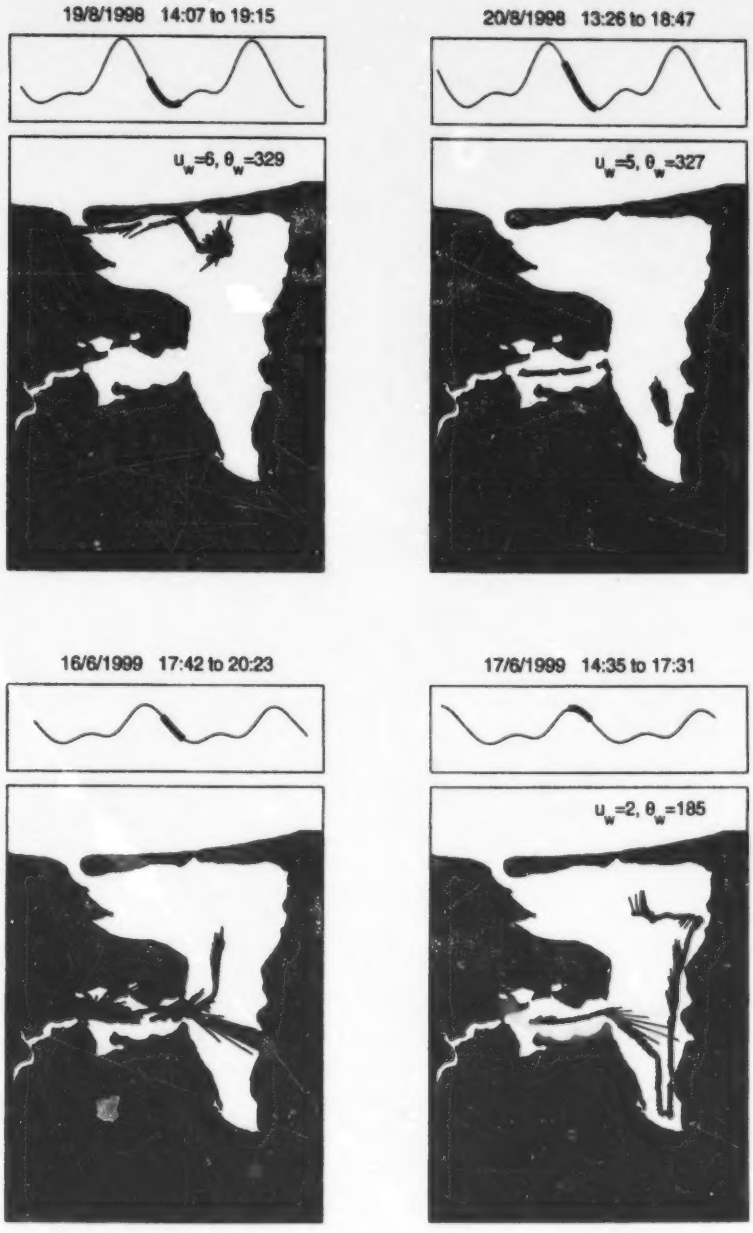

Fig. D.1. continued

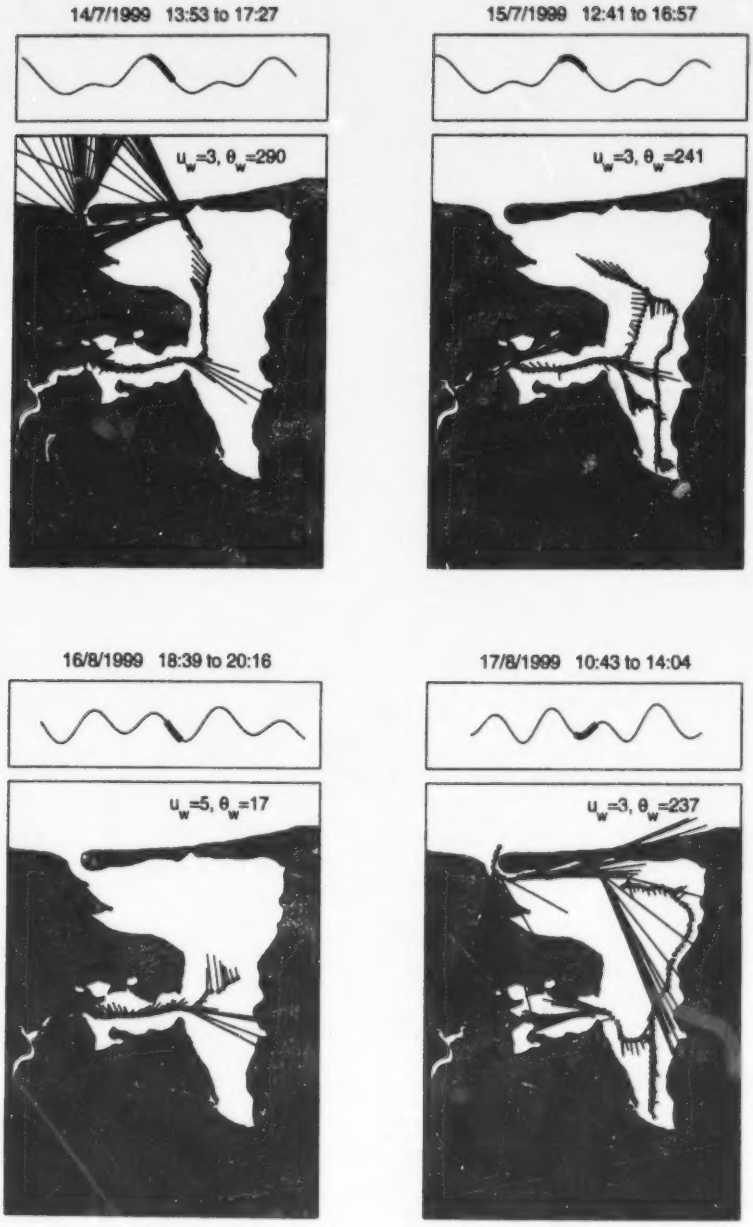

Fig. D.1. continued

Appendix E

Drifter Trajectories

This appendix shows the drifter trajectories from the 4 deployments periods in Tracadie Bay (see text for details). The following information is displayed on each panel:

- Deployment date and time.
- The sea level time series with the deployment period highlighted by the thick line.
- A map of Tracadie Bay with superimposed drifter trajectories. The dot shows the starting point of each drifter and the solid line designates its subsequent path.
- Mean wind speed and direction for the deployment period are given by u_w and θ_w.

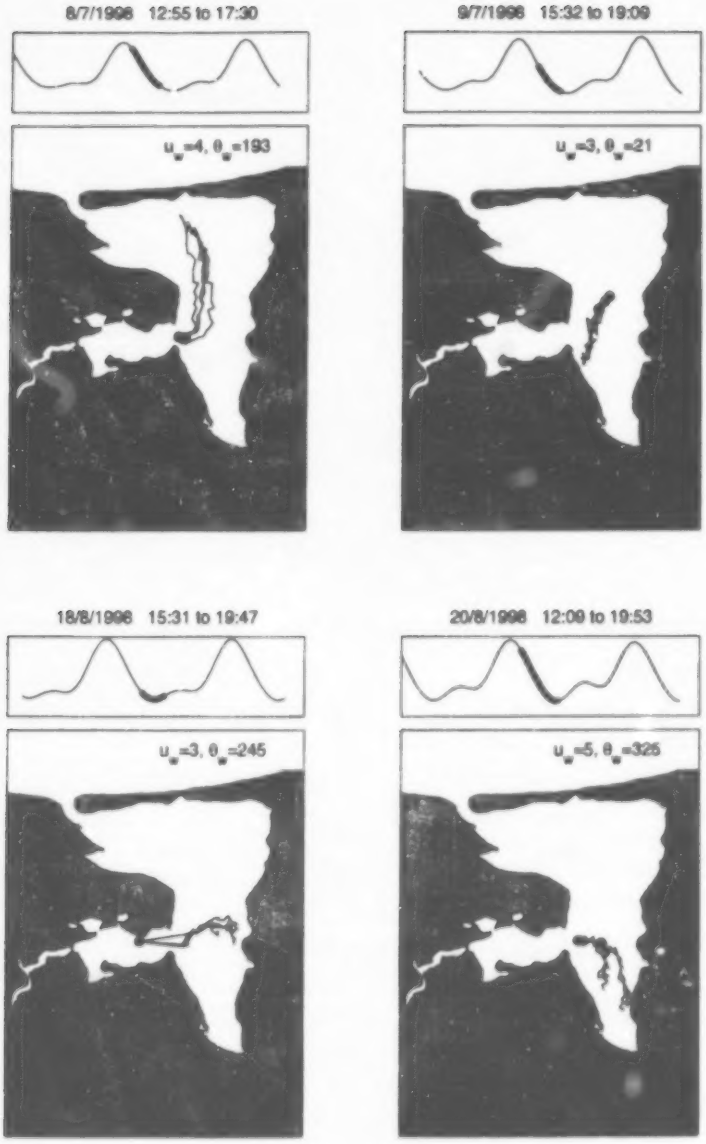

Fig. E.1. Drifter trajectories in Tracadie Bay.